OPTIMAL MARKET MAKING MODELS IN HIGH-FREQUENCY TRADING

A THESIS SUBMITTED TO
THE GRADUATE SCHOOL OF APPLIED MATHEMATICS
OF
MIDDLE EAST TECHNICAL UNIVERSITY

BY

BURCU AYDOĞAN

IN PARTIAL FULFILLMENT OF THE REQUIREMENTS
FOR
THE DEGREE OF DOCTOR OF PHILOSOPHY
IN
FINANCIAL MATHEMATICS

MARCH 2021

Approval of the thesis:

OPTIMAL MARKET MAKING MODELS IN HIGH-FREQUENCY TRADING

submitted by **BURCU AYDOĞAN** in partial fulfillment of the requirements for the degree of **Doctor of Philosophy in Financial Mathematics Department, Middle East Technical University** by,

Prof. Dr. A. Sevtap Selçuk-Kestel
Director, Graduate School of **Applied Mathematics** ________________

Prof. Dr. A. Sevtap Selçuk-Kestel
Head of Department, **Financial Mathematics** ________________

Prof. Dr. Ömür Uğur
Supervisor, **Scientific Computing, METU** ________________

Assoc. Prof. Dr. Ümit Aksoy
Co-supervisor, **Mathematics Dept., Atılım Uni.** ________________

Examining Committee Members:

Prof. Dr. A. Sevtap Selçuk-Kestel
Actuarial Sciences, METU ________________

Prof. Dr. Ömür Uğur
Scientific Computing, METU ________________

Assoc. Prof. Dr. Hamdullah Yücel
Scientific Computing, METU ________________

Assoc. Prof. Dr. Özge Sezgin Alp
Accounting and Financial Management, Başkent Uni. ________________

Prof. Dr. Kasırga Yıldırak
Actuarial Science, Hacettepe University ________________

Date: ________________

I hereby declare that all information in this document has been obtained and presented in accordance with academic rules and ethical conduct. I also declare that, as required by these rules and conduct, I have fully cited and referenced all material and results that are not original to this work.

Name, Last Name: BURCU AYDOĞAN

Signature :

ABSTRACT

OPTIMAL MARKET MAKING MODELS IN HIGH-FREQUENCY TRADING

Aydoğan, Burcu
Ph.D., Department of Financial Mathematics
Supervisor : Prof. Dr. Ömür Uğur
Co-Supervisor : Assoc. Prof. Dr. Ümit Aksoy

March 2021, 152 pages

In this thesis, we aim to develop optimal trading strategies in a limit order book for high-frequency trading by stochastic control theory. First, we address for evolving optimal prices where the underlying asset follows the Heston stochastic volatility model including jump components to explore the effect of the arrival of the orders. The goal of the market maker is to maximize her expected return while controlling the inventories where the remaining is charged with a liquidation cost. Two types of utility functions are considered: quadratic and exponential with a risk averse degree. Then, we study on a model considering an underlying asset with jumps in stochastic volatility. We derive the optimal quotes for both models under the assumptions. For numerical simulations, we apply finite differences and linear interpolation as well as extrapolation methods to obtain a solution of the related Hamilton-Jacobi-Bellman (HJB) equation. We demonstrate the risk metrics of the models including profit and loss distribution (PnL), standard deviation of PnL and Sharpe ratio which play important roles for the trader to make decisions on the strategies in high-frequency trading. Moreover, we provide the comparisons of the strategies with the existing ones. As a real data application, we conduct our simulations for the developed strategies in this thesis on a high-frequency data of Borsa Istanbul (BIST). For this purpose, we first estimate the parameters of each model and then perform the numerical experiments on the optimal quotes. Furthermore, we provide the applications on global stocks in order to see that the models are applicable, reasonable, and profitable also for the developed markets. Lastly, we take into account of the optimal market making models with stochastic latency impact. We contribute to this study by providing the numerical experiments with an artificial data. Finally, the thesis ends up with a conclusion and future research directions.

Keywords: Market making, Limit order book, High-frequency trading, Stochastic control, Hamilton-Jacobi-Bellman equation, Emerging market

ÖZ

YÜKSEK FREKANSLI İŞLEMLERDE OPTİMAL PİYASA YAPICILIĞI MODELLERİ

Aydoğan, Burcu
Doktora, Finansal Matematik Bölümü
Tez Yöneticisi : Prof. Dr. Ömür Uğur
Ortak Tez Yöneticisi : Doç. Dr. Ümit Aksoy

Mart 2021, 152 sayfa

Bu tezde, stokastik kontrol teorisi ile, yüksek frekanslı işlemler için bir limit emir defterinde optimal alım-satım stratejilerinin geliştirilmesi amaçlanmıştır. İlk olarak, dayanak varlığın gelen emirlerin etkisini keşfetmek için atlama bileşenlerini de içeren Heston stokastik volatilite modelini takip ettiği durumda, optimal fiyatların geliştirilmesi ele alınmıştır. Piyasa yapıcının amacı; kalan envanterlerin likidite maliyeti ile ücretlendirildiği durumda envanterleri kontrol ederken, beklenen getirisini maksimize etmektir. İki tür fayda fonksiyonu düşünülmüştür; bunlar sırayla, kuadratik ve riskten kaçınma derecesine sahip üstel fonksiyonlardır. Daha sonra, atlamaların stokastik volatilitede olduğu bir dayanak varlığın modeli çalışılmıştır. İki model için de varsayımlar altında optimal teklifler geliştirilmiştir. Nümerik simülasyonlarda, ilgili Hamilton-Jacobi-Bellman (HJB) denkleminin çözümünü bulmak için sonlu farklar yöntemi ve lineer interpolasyon ile ekstrapolasyon metodları uygulanmıştır. Modellerin kâr ve zarar dağılımı, kâr ve zararın standart sapması, Sharpe oranı gibi yüksek frekanslı işlemlerde stratejiler üzerine karar vermede yatırımcı için önemli olan risk metrikleri gösterilmiştir. Ayrıca, stratejilerin var olanlar ile karşılaştırılması da yapılmıştır. Gerçek veri uygulaması olarak, bu tezde geliştirdiğimiz stratejilerin simülasyonları Borsa İstanbul yüksek frekanslı verisi üzerinde yapılmıştır. Bu amaçla, önce her modelin parametreleri tahmin edilmiş ve daha sonra optimal teklifler üzerine nümerik simülasyonlar gerçekleştirilmiştir. Ayrıca, modellerin gelişmiş piyasalarda da

uygulanabilir, makul ve kâr getirdiğini görmek için global hisse senetleri üzerine uygulamalar gerçekleştirilmiştir. Daha sonra, stokastik gecikme etkili optimal piyasa yapıcılığı modelleri incelenmiştir. Bu çalışmaya yapay bir veri ile yapılmış simülasyonlar ile katkı sağlanmıştır. Son olarak, bu tez bir değerlendirme ve gelecek çalışma yönleri ile sonlandırılmıştır.

Anahtar Kelimeler: Piyasa yapıcılığı, Limit emir defteri, Yüksek frekanslı işlemler, Stokastik kontrol, Hamilton-Jacobi-Bellman denklemi, Gelişmekte olan piyasa

To My Mother

ACKNOWLEDGMENTS

I would like to express my very great gratitude to my thesis supervisor Prof. Dr. Ömür Uğur for his patient and kind guidance, enthusiastic encouragement and valuable suggestions during the development and preparation of this thesis. His willingness to give his time and to share his experiences has brightened my path.

Besides, I would like to express my deepest appreciation to my co-supervisor Assoc. Prof. Dr. Ümit Aksoy for her valuable advices, feedbacks, guidance and kindness during my Ph.D. education.

I also would like to thank my Ph.D. thesis monitoring committee members, Prof. Dr. A. Sevtap Selçuk-Kestel, and Assoc. Prof. Dr. Hamdullah Yücel, for their precious advices, comments, and feedbacks to improve my studies.

I appreciate Atılım University for giving me the opportunity of working as a research assistant during my Ph.D. education. My special thanks should go to the all members of Department of Mathematics for their great working motivation, support and help.

Also, I want to express my thanks to all members of the Institute for Applied Mathematics of METU for their kindness and limitless friendship.

Furthermore, I would like to express my thanks to my very brilliant friend Volkan Kumtepeli for his support.

I am very thankful to my dearest forever friend Nazlı Çiloğlu, always standing by my side with her love during my Ph.D. education as in life.

I wish to express my greatest thanks to my lovely friend Merve Efsun Özkan Sevinir for her warmly support and friendship.

My special thanks go to my lovely friend and roommate at work, Eda Yılmaz, for her endless support and encouragement. I am very grateful to her since she always tries to keep me positive and motivated not just for my thesis and also for life.

Finally, I wish to express my warmest thanks to my lovely family, Güler, Nihat, Aytaç, Ömer, from my heart for their continuous support to make me feel always stronger. I wouldn’t imagine this long journey without their unfailing encouragement. I should thank to my dearest mother Güler seperately as she is the best mother and friend to me with her lovely heart and unconditional love. Without her constant support, it would be impossible for me to finish this thesis. I dedicate this dissertation to her.

TABLE OF CONTENTS

LIST OF TABLES

LIST OF FIGURES

LIST OF ABBREVIATIONS

OU	Ornstein-Uhlenbeck
HFT	High-Frequency Trading
HJB	Hamilton-Jacobi-Bellman
LOB	Limit Order Book
DPP	Dynamic Programming Principle
PDE	Partial Differential Equation
PnL	Profit and Loss
BIST	Borsa Istanbul Stock Exchange

CHAPTER 1

INTRODUCTION

Recently, there have been crucial developments in quantitative financial strategies to execute the orders driven in stock markets by computer programs with a very high speed (in microseconds). In particular, high-frequency trading (HFT) is one of the major topics that attracts the attention excessively due to its benefits on market microstructure, being an interdisciplinary field including the topics stochastic optimization, finance, economics, and statistics. The market microstructure, which can be stated as the research area on the strong trading mechanisms managed for the financial securities, is equipped with the contributions by [33] and [46]. A significant number of algorithmic trading strategies in the markets has also been commenced with the appearance of HFT which is characterized as a less narrow set of trading strategies in the algorithmic trading class and a growing need for the quantitative approaches on the analysis and optimization techniques to develop the trading strategies.

In electronic markets, the aim is to match the traders who desire to sell the assets with the traders who desire to buy those assets. Therefore, the participants submit the orders on both buying and selling sides in the market. The orders may be in two types: market orders and limit orders. Market orders are implemented immediately, however, limit orders do not have this priority. The participants can be market makers who supply the liquidity to the market in a limit order book (LOB) by quoting bid and ask prices.

HFT in a LOB and the related trading strategies in developed markets have been highly popular in recent times. It is also used in emerging markets for few years with the purpose of rising trade volumes and liquidity. Thus, the concept of the LOB is extremely used in financial markets worldwide to permit the traders for buying or selling assets easily through the orders. The interaction between the orders leads a complex dynamics which can be solved by constructing it as a stochastic control problem to obtain the best bid and ask prices. Not surprisingly, the practioners and theorists are so interested in evolving and applying newly discovered optimal market making approaches to trade in miliseconds with the purpose of achieving maximum expected utility.

There are mainly a plenty number of articles on the HFT strategies in a LOB starting with the early study of Ho and Stoll [35]. By the inspiration of this work, many extensions on this topic have been conducted, see, for example, Avellaneda and Stoikov [3], Guilbaud and Pham [32], Guéant, Lehalle and Fernandez-Tapia [31], Cartea and Jaimungal [12] and Ching et al. [15]. Avellaneda and Stoikov [3] develops optimal prices for a single stock around the market price considering the inventory impact. This paper is the seminal work of our studies which we follow in this thesis.

This thesis mainly aims to derive the optimal prices for HFT to execute the limit buy and sell orders by constructing optimal market making models using different stock price processes. We first consider a model where the price is followed by Heston stochastic volatility model [34] plus the jump components to measure the effect of the arrival orders in the price dynamics. The case of the constant volatility has been studied by Cartea and Jaimungal [12] without drift. They studied on a strategy where the asset price follows a Brownian motion plus jump components which are random variables and the inventory is restricted in an interval. We extend their study considering the volatility as stochastic adding jump components and drift coefficient in the price dynamics. An optimal market making model with Heston model is considered in [15] with different assumptions and they solved the associated Hamilton-Jacobi-Bellman (HJB) equation of the stochastic control problem by the quadratic approximations of the inventory. They also took into account of the problem of a price impact model including jumps in the midprice process with a constant and single jump size. In this thesis, we consider the volatility as stochastic which is followed by Heston model consisting jumps either in price or volatility by combining and extending these two works and then generate the optimal bid and ask prices. For the numerical solution of the related HJB equation, we propose a solution by the final condition and then, we apply finite differences and interpolation/extrapolation methods. For other price impacted optimal market making models, one can also refer to Almgren [2] and, Zabaljauregui and Campi [53]. After obtaining a solution for the stochastic optimal control problem, the findings are performed on Borsa Istanbul Stock Exchange Market (BIST) high-frequency data by calibrating the models. The existence and level of the HFT in BIST have been studied by Ersan and Ekinci [21] in the first instance. As the HFT has been widely studied for developed markets, it is expected that more researches will be also performed for emerging markets. Since the usage of electronic submissions have rapidly increased, the statistical properties and modeling of a high-frequency data are provided in some applications, see for instance Cont [16]. Besides, since there is a lack of stochastic latency models on optimal market making in the literature, we try to express the strategy and behaviour of the trader when there is a time difference between submission and execution of the orders which is explained by latency.

The motivation of this thesis is to generate optimal high-frequency trading strategies by deciding for the best bid and ask prices with price impact models where the true price of an asset is processed by a stochastic volatility model with jumps for the arriving orders. Because of the fact that a high-frequency data exhibits the properties of excess kurtosis and skewness values with fluctuating volatility, explaining the price process of a financial instrument with these features attempts to define the price dynamics better in real markets. Hence, we intend to obtain HFT strategies for optimal market making with stock price dynamics having these characteristics. In addition, we aim to generate the optimal prices for trading when the jumps occur in the volatility, since this situation causes the variance to increase more rapidly. When gathering all these, we try to obtain more realistic trading strategies with more realistic stock price dynamics. Specifically, the goal is to maximize the investor's expected utility at the end of the trading with constrained inventories by the proposed strategies. The wealth and inventory processes of the market maker during the trading are changing with respect to the arrived and filled orders as discussed in [12]. By this development, a practioner in a market can trade with optimal prices when the underlying asset of the instrument is followed by the provided price dynamics in this thesis. The formulas can be applied for HFT even in an emerging market. Also, the optimal prices can be derived and applied in markets when the degree of the risk aversion of the investor is settled. Moreover, the trader can define her behaviour on the optimal trading in case of the stochastic latency is paid attention.

The major contribution of the thesis is to extend the model in [12] where the price is followed by Heston stochastic volatility model and solve the nonlinear HJB equation with numerical methods. We take this model into consideration in several cases. First, we consider the problem as whether the suggested solution includes the stochastic volatility effect explicitly or not. However, we aim to maximize the profit of the trader with quadratic and exponential utility functions. As a next contribution, the effect of the arrived orders is examined either in the price or volatility process as the jump components. In numerical experiments, we compare our strategies with the ones which already exist in the literature in terms of the statistics of profit and loss, and inventory processes. We develop the theory of a strategy where the midprice of the asset follows a mean-reverting process with stochastic volatility, but we leave its numerical solution as a further study. After all, we apply our findings for each case on a high-frequency data of an emerging market as a novel application. The thesis also looks at price impacted optimal market making models which are introduced by us when there is a latency between submission and execution of the orders. Numerical results with artificial data are provided for these strategies, as well.

The thesis starts with some definitions and illustrations on a limit order book in Chapter 2. Then, we provide a brief introduction on stochastic control theory and the derivation of the HJB equation of a related control problem. Next, a preview of some referenced optimal market making models in the literature is presented. Chapter 3 is dedicated to the theory and applications of the proposed optimal market making models where the true price of an asset is followed by a stochastic volatility model. We handle the applications with artificial data and a large range of experiments is provided to figure out the contributions of the strategies. Lastly, we theoretically propose a strategy with a mean-reverting process with stochastic volatility for the midprice process in this chapter. In Chapter 4, we include the real data application of the models to see that they work well and provide reasonable results on the high-frequency data of an emerging market. In this part, we additionally employ the outcomes of the models on some stocks of global markets. In Chapter 5, we define the latency for an order as a mean-reverting stochastic process and assume that it is considered in the midprice process of the asset. Then, we develop optimal market making models with the same assumptions given in Chapter 3 with the applications. Finally, Chapter 6 concludes the thesis with an outlook to further studies.

CHAPTER 2

PRELIMINARIES

In this chapter, we provide some necessary definitions and results in the literature that we use for the studies in this thesis. For more details, we refer to [13, 30, 48, 52] and references therein.

2.1 Limit Order Books

In this section, we describe some key concepts in a limit order book (LOB) and high-frequency trading (HFT).

In the concept of HFT, one of the most important fields is the limit order book which is extremely used in financial markets worldwide to permit the traders for buying or selling assets easily through the orders. The limit order book can be described as a list of all orders in a market at any time t for a given asset.

There are two types of orders in a LOB:

- *Limit order*: an order to buy or sell a certain amount of shares for an identified price that is not resulted in an immediate execution.
- *Market order*: an order to buy or sell a certain amount of shares for the best available price that is usually executed immediately.

A market is said to be liquid whereby the numerous participants are instantly able to trade an asset at any time with a low transaction cost. The limit and market orders are continuously sent by liquidity providers and takers who make the market where they can be the same trader during a trading session. Following the crucial developments in trading strategies to execute the orders driven in markets by computer programs with a very high speed (in microseconds), the high-frequency traders take positions on both buying and selling sides of the market that leads a market impact because of the price fluctuations arised by the executions [16].

Correspondingly, we have the following definitions for a limit order book.

Definition 1. The best bid price p_t^- available at time t is defined as the highest bid price within the buy limit orders in the limit order book.

Definition 2. The best ask price p_t^+ available at time t is defined as the lowest ask price within the sell limit orders in the limit order book.

Definition 3. The difference between the best ask and bid prices at time t, that is, $p_t^+ - p_t^-$ which is called as the bid-ask spread.

Definition 4. The midprice in a limit order book at time t is

$$S_t = \frac{1}{2}\left(p_t^+ + p_t^-\right).$$

Once a limit order is submitted, it may either executed immediately or get in a queue of still existing orders that may cause to be cancelled. Hence, another types of operations for both buying and selling can be defined as the cancellations of limit orders which reduce the queue size by the amount of the cancelled orders. The cancellation of limit orders can be easily realized as it ensures the liquidity to the market.

When a limit order arrives, there is a probability that it may not be filled and in this case, the order should be cancelled or converted to a market order. The limit orders are executed first with the priority of the price and then with the time. For instance, if two limit buy (sell) orders are sent to the queue, the one with the highest (lowest) price gets the priority for the exchange. Hence, the orders in a limit order book are lined up from top to the down with the precedence of high buy prices and low sell prices [37]. The state of a trading day is characterized by a sequence of limit orders (b_t, S_t, v_t), where b_t demonstrates the type of the limit order, while S_t denotes the limit order price and v_t states the required quantity of the shares.

2.1.1 Representation of Limit Order Books

In this part, some illustrations for a historical intraday equity data in Turkish stock market, Borsa Istanbul (BIST), are displayed.

Table 2.1 demonstrates a snapshot of THYAO limit order book in Turkish stock market, BIST, with the desired prices and quantities. It can be seen that the best bid price is 14.53 and the best ask price is 14.54. If a market maker who is the liquidity provider wants to sell a number of shares, then she needs to send a market order which will be matched with a limit buy order with the price and time priority principle. For instance, if the amount of the market order is less than 8500, then the order is matched with enough amount on the limit buy order book to fill the desired quantity and the remainings will carry on as the new top of the limit buy order book. Nonetheless, if the market order is sent for 10000 shares, then the first 8500 shares are executed with the price of 14.53 Turkish Lira (TL) and the rest 1500 shares are executed by the price 14.52 TL.

Table 2.1: Sample order books for THYAO

Limit Buy Orders		Limit Sell Orders	
Amount	Price	Amount	Price
4500	14.53	884	14.54
4000	14.53	720	14.54
8351	14.52	1000	14.54
500	14.52	2000	14.54
1000	14.52	100	14.55
4000	14.52	1844	14.56
5700	14.51	500	14.56
4800	14.5	4000	14.57
10000	14.5	6912	14.58
4600	14.49	4000	14.58

The histograms in Figure 2.1 represent a limit order book scheme of two stocks traded in BIST on the day of Jan 2, 2020. Figure 2.1a is an illustration of the available orders with prices and total quantities for an illiquid and rarely traded stock, while Figure 2.1b displays a representative scheme for a liquid and frequently traded stock.

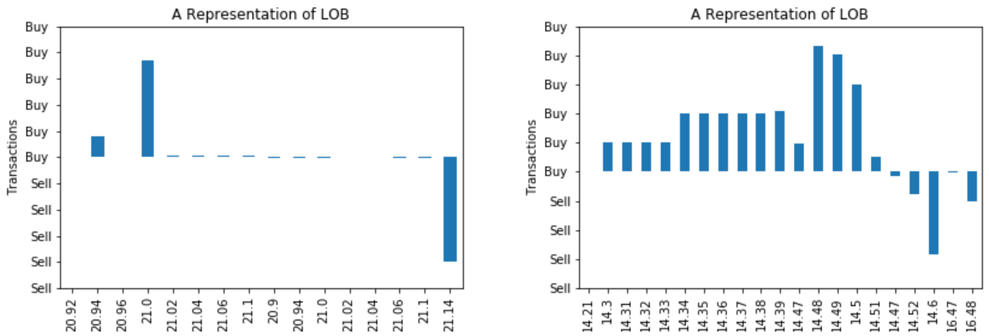

(a) (b)

Figure 2.1: A screenshot of a LOB for an illiquid stock ARCLK (in the left figure) and a liquid stock FENER (in the right figure) which are traded in BIST.

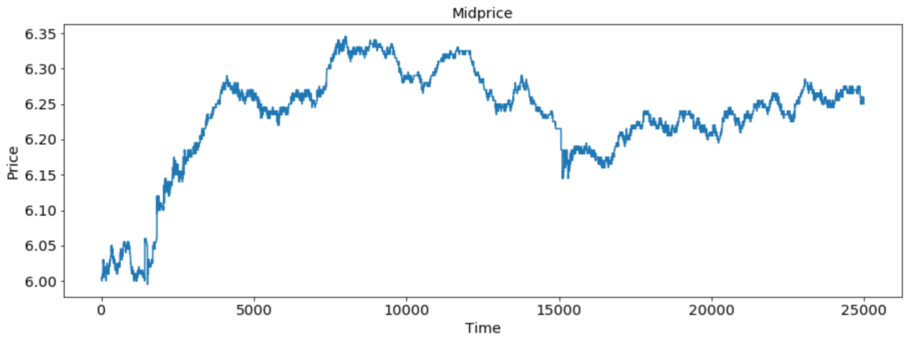

Figure 2.2: Midprice of the stock AFYON in BIST.

Moreover, Figure 2.2 shows the daily midprice of stock AFYON in BIST on Jan 8, 2020 for each trade observed in miliseconds between 10.15 am and 14.30 pm. The next figures have been also plotted for the same time slot.

The weighted price which is called as microprice and calculated by the formula

$$\frac{p_t^- \times v_t^+ + p_t^+ \times v_t^-}{v_t^- + v_t^+},$$

where p_t^- and p_t^+ are the best bid and ask prices, v_t^- and v_t^+ are the relevant quantities at the best prices which is shown in Figure 2.3 for the stock AFYON on the day of Jan 8, 2020. The difference between the microprice and midprice for the same trading day for this stock can be observed in Figure 2.4. We can easily notice that it usually lies in the range of $[-0.05, 0.05]$ while it is a bit more at the beginnings of the trading day.

The difference between the best ask and bid prices where the distance between these prices and the midprice gives the the optimal spreads can be seen in Figure 2.5 for the

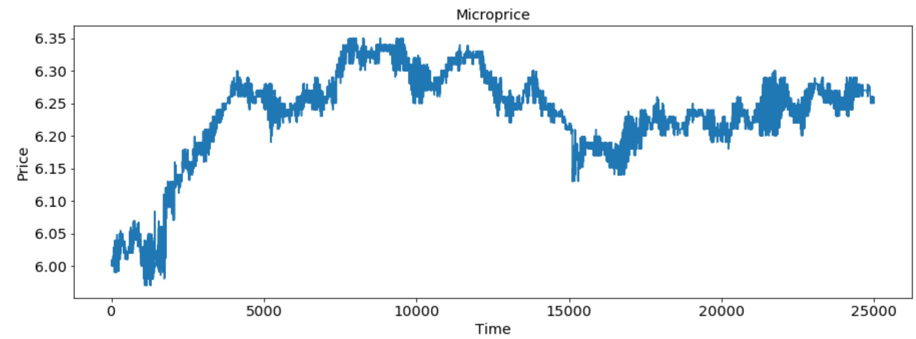

Figure 2.3: Microprice of the stock AFYON in BIST.

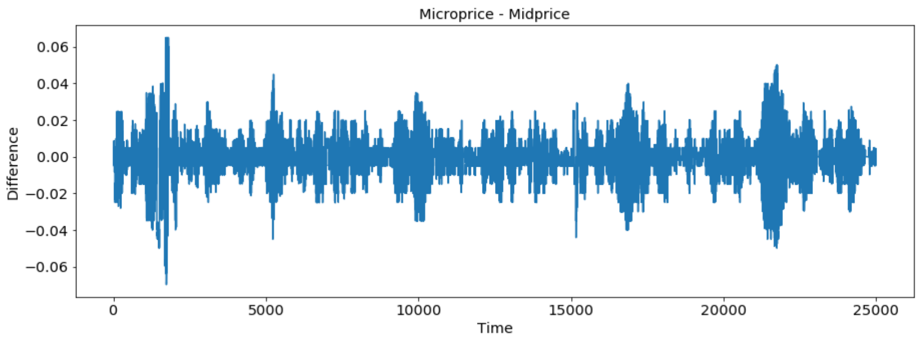

Figure 2.4: Difference between the microprice and midprice of the stock AFYON in BIST.

stock AFYON.

Another concept in a limit order book is the order imbalance that directs the price towards the bid or ask side and can be evaluated for a trading day by the formula

$$\rho_t = v_t^- - v_t^+ v_t^- + v_t^+ \in (-1, 1).$$

For a Turkish stock market case, Figure 2.6 and Figure 2.7 show that how the volume imbalance effects the order type and quantities where Figure 2.6 is plotted for a time

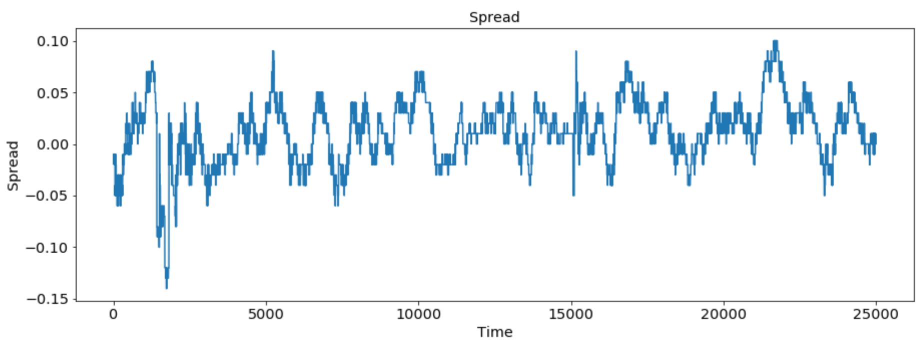

Figure 2.5: Spread for the stock AFYON in BIST.

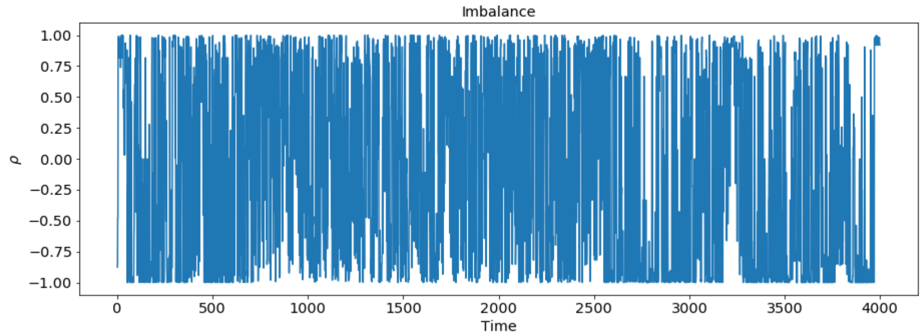

Figure 2.6: Order imbalance for the stock AFYON in BIST.

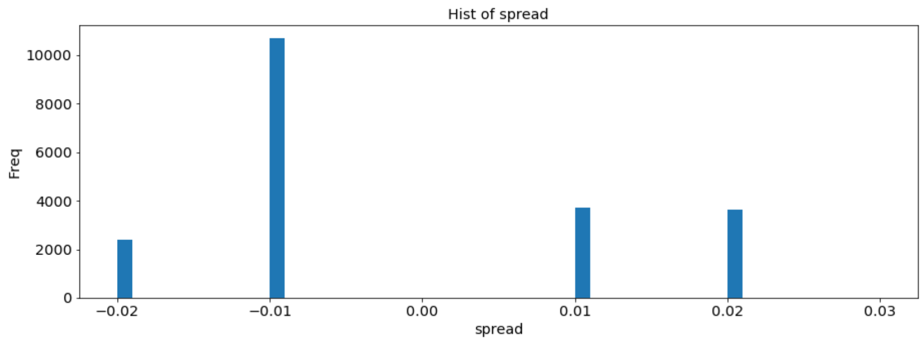

Figure 2.7: Order imbalance histogram representation for the stock AFYON in BIST.

slot of 10.25 am and 10.40 am in miliseconds.

As a next illustration, we show the plot of the market volume curves for each trade between 10.10 am 10.40 am in miliseconds which are influenced by the particular events in the market for the stock AFYON in Figure 2.8 and observe a more intense number of buy orders which is related to the order imbalance.

2.2 Theoretical Remarks

In this section, we provide some basic and important definitions on stochastic processes. For more details, see [7], [38], and [40].

We first introduce the filtration as in the following definition.

Definition 5 (Filtration)**.** Let $(\Omega, \mathcal{F}, \mathbb{P})$ be a probability space where Ω is the sample space, $\mathcal{F}$ is the σ-algebra of events, and $\mathbb{P}$ is the probability measure. A filtration $(\mathcal{F}_t)_{t\geq 0}$ on this probability space is an increasing family of σ-algebras included in $\mathcal{F}$.

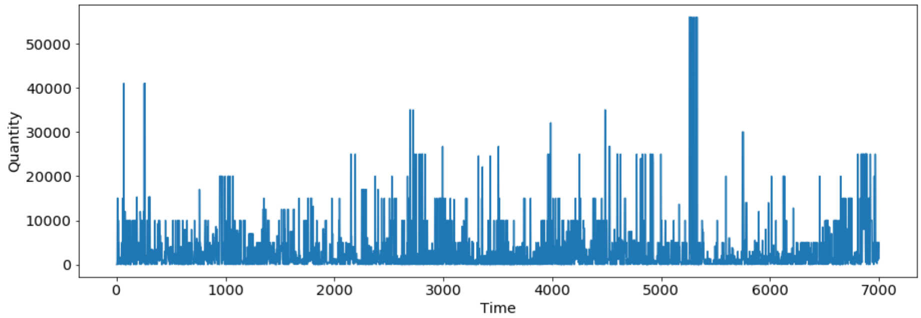

(a)

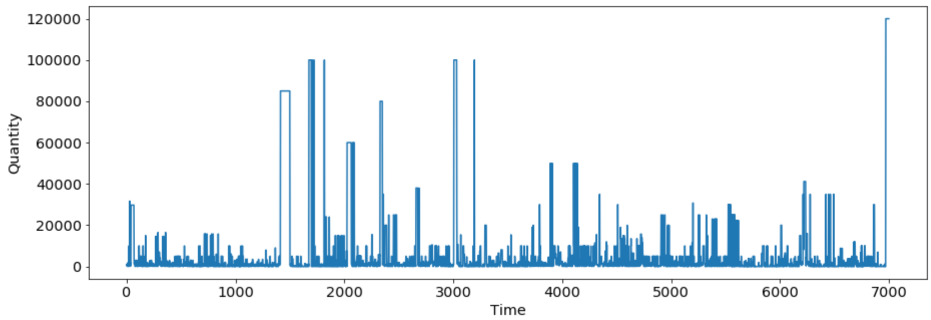

(b)

Figure 2.8: Market volume curve for (a) the sell and (b) the buy orders for the stock AFYON in BIST.

This definition allows us to define a stochastic process that is always adjusted to a filtration.

Definition 6 (Stochastic process)**.** A stochastic process $(X_t)_{t\geq}$ is adapted to a filtration $\mathcal{F}_t$ if X_t is $\mathcal{F}_t$-measurable for every $t \geq 0$.

One of the stochastic processes is the Brownian motion as we define in the next definition.

Definition 7 (Brownian motion)**.** A stochastic process $(W_t)_{t\geq 0}$ is called as a Brownian motion if it satisfies the following properties:

1. $W_0 = 0$,
2. $(W_t)_{t\geq 0}$ is a continuous function of t,
3. $W_t - W_s$ has the normal distribution with mean 0 and variance $t-s$ for $t > s$,
4. The process has independent increments, i.e.,

$$W_{t_n} - W_{t_{n-1}}, W_{t_{n-1}} - W_{t_{n-2}}, \ldots, W_{t_2} - W_{t_1}$$

are independent random variables for $0 \leq t_1 \leq t_2 \leq \cdots \leq t_n$.

In order to study on Brownian motion and stochastic differential equations, the martingale theory is needed to be worked.

Definition 8 (Martingale)**.** A stochastic process X_t is a martingale with respect to the filtration $(\mathcal{F}_t)_{t\geq 0}$ if the following holds:

1. $\mathbb{E}|X_t| < \infty$,
2. X_t is $\mathcal{F}_t$-measurable $\forall t \geq 0$,
3. $\mathbb{E}[X_t|\mathcal{F}_s] = X_s$ a.s. for any $s \leq t$.

Brownian motion is addressed as an example of diffusion processes which are solutions to the stochastic differential equations. In the concept of jump-diffusion processes where a stochastic component and jump process are included, Brownian motion refers to the diffusion part. For the jump parts, Poisson processes are generated as the basic jump processes.

Definition 9 (Poisson process)**.** A random variable $(N_t)_{t\geq 0}$ is called as the Poisson process with intensity λ if

$$\mathbb{P}(N_t = k) = \frac{(\lambda t)^k}{k!} e^{-\lambda t}$$

for $k = 0, 1, 2, \ldots$.

While working with the diffusion processes, a very useful application for the computation of the stochastic integrals which is Itô's formula [40] is a necessity to know. Here, we provide Itô's formula for the jump-diffusion models.

Theorem 1 ([49], Theorem 11.5.1, Itô's formula for jump-diffusion processes)**.** *Let X_t be a jump-diffusion process and $f \in \mathcal{C}^2(\mathbb{R})$. Then,*

$$\begin{aligned} f(X_t) = f(X_0) + \int_0^t f^{'}(X_s) dX_s^c + \frac{1}{2}\int_0^t f^{''}(X_s) d[X^c, X^c]_s \\ + \sum_{0<s\leq t} [f(X_s) - f(X_{s^-})] \end{aligned}$$

where dX_s^c represents the continuous part and $d[X^c, X^c]_s$ denotes the quadratic variation of the process.

Theorem 2 ([39], Theorem 7.4.1, Dynkin's formula)**.** *Let $X_t \in \mathbb{R}^n$ be a jump-diffusion process and let $f : \mathbb{R}^n \to \mathbb{R}$. Let τ be a stopping time with $\mathbb{E}^x[\tau] < \infty$. Then,*

$$\mathbb{E}^x[f(X_\tau)] = f(x) + \mathbb{E}^x\left[\int_0^\tau Af(X_s) ds\right],$$

where x is the initial state variable and A is the infinitesimal generator of the process.

2.3 Stochastic Optimal Control

In this section, we briefly review the dynamic programming principle (DPP) which is initiated in 1958 by Bellman [9] and some connected terms in stochastic calculus that allow to study a stochastic control problem with a related nonlinear partial differential equation (PDE) which is known as the Hamilton-Jacobi-Bellman (HJB) equation.

Stochastic control theory is a mathematical field which tackles the controlled variables performing the behaviour of a dynamical system to achieve a required objective and usually occurs in financial modeling problems. The optimal investment problem discovered by Merton [44] is a well-known and classical example of continuous-time stochastic control problems. The common goal is to maximize an expected profit function or minimize a cost function of a trader. For the purpose of solving the stochastic control problems, a corresponding nonlinear PDE which is known as the Hamilton-Jacobi-Bellman (HJB) equation should be obtained and can be solved as backwards starting from the terminal time.

Let $(\Omega, \mathcal{F}, \mathbb{P})$ be a probability space where Ω is a sample space, $\mathcal{F}$ is a filtration and $\mathbb{P}$ is a probability measure satisfying the usual conditions with a controlled process $X^u = (X_t)_{0 \le t \le T}$ in $\mathbb{R}^n$ which is assumed to be an Itô diffusion process satisfying

$$dX_t^u = \mu(t, X_t^u, u_t)dt + \sigma(t, X_t^u, u_t)dW_t, \quad X_0^u = x, \tag{2.1}$$

where $(W_t)_{0 \le t \le T}$ is a d-dimensional Brownian motion and $u = (u_t)_{0 \le t \le T}$ is the vector valued admissible control process which is defined in $A \subset \mathbb{R}^n$. The measurable functions μ, σ on $[0,T] \times \mathbb{R}^n \times A$ where μ is the drift coefficient and σ is the volatility of the diffusion process satisfy the Lipschitz condition in A in order to assure the existence of a solution to (2.1) [48], that is, there exists $K \ge 0$, $\forall x, y \in \mathbb{R}^n$, $\forall a \in A$,

$$|\mu(x,a) - \mu(y,a)| + |\sigma(x,a) - \sigma(y,a)| \le K|x - y|.$$

We consider given two Borelian real-valued functions F and G on $[0,T] \times \mathbb{R}^n \times A$ and $\mathbb{R}^n$ where F is the running penalty while G is the terminal wealth.

Now, we define the gain function as

$$J^u(x) = \mathbb{E}\left[\int_0^T F(s, X_s^u, u_s)ds + G(X_T^u)\right]$$

where $\mathbb{E}$ stands for the conditional expectation on X_t^u.

Since the objective is to maximize the gain function, therefore the corresponding value function is typically introduced as

$$V(t,x) = \sup_{u \in \mathcal{A}} J^u(x),$$

where $\mathcal{A}$ is the set of all admissible control processes.

By the Dynamic Programming Principle (DPP) [9], a stochastic optimization problem can be represented as

$$V(t,x) = \sup_{u\in\mathcal{A}} \mathbb{E}\left[\int_t^T F(s, X_s^u, u_s)ds + G(X_T^u)\right] \tag{2.2}$$

given the dynamics (2.1) where the value function is attained at the best control $\hat{u}$ among all the controls.

See for instance [10], [13] and [48] to discover that how DPP applies to stochastic control problems.

2.3.1 Hamilton-Jacobi-Bellman Equation

In the value function (2.2), we divide the functional into two parts for any sufficiently small value h and consider

$$\begin{aligned} V(t,x) &= \sup_{u\in\mathcal{A}} \mathbb{E}\left[\int_t^{t+h} F(s, X_s^u, u_s)ds + \int_{t+h}^T F(s, X_s^u, u_s)ds + G(X_T^u)\right] \\ &= \sup_{u\in\mathcal{A}} \mathbb{E}\left[\int_t^{t+h} F(s, X_s^u, u_s)ds + V(t+h, x)\right]. \end{aligned} \tag{2.3}$$

Using Itô's formula for $V(t+h,x)$, we have

$$\begin{aligned} V(t+h,x) = V(t,x) + \int_t^{t+h} &\left(\frac{\partial V(s,x)}{\partial s} + \mu(s,x,u)\frac{\partial V(s,x)}{\partial x}\right. \\ &\left. + \frac{1}{2} tr\left\{\frac{\partial^2 V(s,x)}{\partial x^2}\sigma^2(s,x,u)\right\}\right)ds \\ &+ \int_t^{t+h} \frac{\partial V(s,x)}{\partial x}\sigma(s,x,u)dW. \end{aligned} \tag{2.4}$$

Here,

$$tr\left\{\frac{\partial^2 V(s,x)}{\partial x^2}\sigma^2(s,x,u)\right\}$$

denotes the trace of the matrix

$$\frac{\partial^2 V(s,x)}{\partial x^2}\sigma^2(s,x,u).$$

Placing (2.4) into (2.3), we have

$$\begin{aligned}
V(t,x) = \sup_{u\in\mathcal{A}} \mathbb{E}\Bigg[\int_t^{t+h} & F(s, X_s^u, u_s)ds + V(t,x) \\
& + \int_t^{t+h} \left(\frac{\partial V(s,x)}{\partial s} + \mu(s,x,u)\frac{\partial V(s,x)}{\partial x} \right. \\
& \left. + \frac{1}{2} tr\left\{ \frac{\partial^2 V(s,x)}{\partial x^2}\sigma^2(s,x,u) \right\} \right) ds \\
& + \int_t^{t+h} \frac{\partial V(s,x)}{\partial x}\sigma(s,x,u)dW \Bigg] \\
= \sup_{u\in\mathcal{A}} \mathbb{E}\Bigg[\int_t^{t+h} & F(s, X_s^u, u_s)ds + V(t,x) \\
& + \int_t^{t+h} \left(\frac{\partial V(s,x)}{\partial s} + \mu(s,x,u)\frac{\partial V(s,x)}{\partial x} \right. \\
& \left. + \frac{1}{2} tr\left\{ \frac{\partial^2 V(s,x)}{\partial x^2}\sigma^2(s,x,u) \right\} \right) ds \Bigg].
\end{aligned}$$

It follows that

$$\begin{aligned}
\sup_{u\in\mathcal{A}} \mathbb{E}\Bigg[\int_t^{t+h} & \left(F(s, X_s^u, u_s) + \frac{\partial V(s,x)}{\partial s} + \mu(s,x,u)\frac{\partial V(s,x)}{\partial x} \right. \\
& \left. + \frac{1}{2} tr\left\{ \frac{\partial^2 V(s,x)}{\partial x^2}\sigma^2(s,x,u) \right\} \right) ds \Bigg] = 0.
\end{aligned}$$

Then, we get

$$\sup_{u\in\mathcal{A}} \mathbb{E}\left[\int_t^{t+h} \Big(F(s, X_s^u, u_s) + (\partial_s + \mathcal{L}_s^u)V(s,x) \Big) ds \right] = 0$$

where

$$\mathcal{L}_t^u V(t,x) = \mu(t,x,u)\partial_x V(t,x) + \frac{1}{2} tr\left\{ \sigma^2(t,x,u)\partial_{xx}V(t,x) \right\}$$

is the infinitesimal operator associated to (2.1).

Now, dividing each side by h and taking $h \to 0$, we reach to the following Hamilton-Jacobi-Bellman (HJB) equation:

$$\begin{aligned}
\partial_t V(t,x) + \sup_{u\in\mathcal{A}} \{\mathcal{L}_t^u V(t,x) + F(t,x,u)\} = 0 \\
V(T,x) = G(x).
\end{aligned}$$

Theorem 3 ([48], Theorem 3.5.2, Verification theorem)**.** *Let $v \in \mathcal{C}^{1,2}([0,T] \times \mathbb{R}^n)$ be a function satisfying the growth condition, that is, there exists a constant C such that*

$$|v(t,x)| \leq C(1+|x|^2), \quad \forall (t,x) \in [0,T] \times \mathbb{R}^n.$$

Assume that

$$\partial_t v(t,x) + \sup_{u \in \mathcal{A}} \{\mathcal{L}_t^u v(t,x) + F(t,x,u)\} \leq 0, \quad \forall (t,x) \in [0,T] \times \mathbb{R}^n,$$

$$G(x) - v(T,x) \leq 0, \quad x \in \mathbb{R}^n.$$

Then,

$$v \geq V \quad \text{on} \quad [0,T] \times \mathbb{R}^n$$

for all Markovian controls $u \in \mathcal{A}$. Further, there exists a measurable function $u^*(t,x)$ $\forall (t, x \in [0,T] \times \mathbb{R}^n)$ such that

$$\begin{aligned} &\partial_t v(t,x) + \sup_{u \in \mathcal{A}} \{\mathcal{L}_t^u v(t,x) + F(t,x,u)\} \\ &= \partial_t v(t,x) + \mathcal{L}_t^{u^*(t,x)} v(t,x) + F(t,x,u^*(t,x)) = 0 \end{aligned}$$

with final condition

$$v(T,x) = G(x),$$

and the stochastic differential equation

$$dX_s = \mu(s, X_s, u^*(s,X_s))ds + \sigma(s, X_s, u^*(s,X_s))dW_s, \quad X_s = x,$$

admits a unique solution represented by X_s^* and $\{u^*(s, X_s^*)_{t \leq s \leq T}\} \in \mathcal{A}$. Hence,

$$v(t,x) = V(t,x) \quad \forall (t,x) \in [0,T] \times \mathbb{R}^n,$$

and u^* is an optimal Markovian control.

2.3.2 Stochastic Control for Counting Processes

Now, we consider the case where the state variable is integrated with a compound Poisson process $(N_t^u)_{0 \leq t \leq T}$. Since the trader's target is to maximize the gain function in this situation, the stochastic optimization problem is proposed by the value function

$$V(t,n) = \sup_{u \in \mathcal{A}} \mathbb{E}\left[\int_t^T F(s, N_s^u, u_s)ds + G(N_T^u)\right],$$

where $\mathcal{A}$ is the set of all admissible strategies, $u = (u_t)_{0 \le t \le T}$ is the vector valued control process, and $(N_t^u)_{0 \le t \le T}$ is a controlled compound Poisson process with intensity $\lambda_t^u = \lambda(t, N_{t^-}^u, u_t)$ and $N_{0^-} = n$, and $\hat{N}_t^u = N_t - \int_0^t \lambda_s^u ds$ is a martingale.

We have

$$\begin{aligned} V(t,n) &= \sup_{u \in \mathcal{A}} \mathbb{E}\left[\int_t^{t+h} F(s, N_s^u, u_s) ds + \int_{t+h}^T F(s, N_s^u, u_s) ds + G(N_T^u)\right] \\ &= \sup_{u \in \mathcal{A}} \mathbb{E}\left[\int_t^{t+h} F(s, N_s^u, u_s) ds + V(t+h, n)\right] \end{aligned} \tag{2.5}$$

for any sufficiently small number h.

By the Itô's formula for $V(t+h,n)$, we have

$$\begin{aligned} V(t+h,n) = V(t,n) &+ \int_t^{t+h} (\partial_t + \mathcal{L}_s^u) V(s, N_s^u) ds \\ &+ \int_t^{t+h} [V(s, N_{s^-}^u + 1) - V(s, N_{s^-}^u)] d\hat{N}_s^u, \end{aligned} \tag{2.6}$$

where

$$\mathcal{L}_t^u V(t,n) = \lambda(t,n,u)[V(t,n+1) - V(t,n)].$$

Now, putting (2.6) into (2.5) implies

$$\begin{aligned} V(t,n) = \sup_{u \in \mathcal{A}} \mathbb{E}\Bigg[V(t,n) &+ \int_t^{t+h} \Big(F(s, N_s^u, u_s) + (\partial_t + \mathcal{L}_s^u) V(s, N_s^u) \Big) ds \\ &+ \int_t^{t+h} [V(s, N_{s^-}^u + 1) - V(s, N_{s^-}^u)] d\hat{N}_s^u \Bigg]. \end{aligned}$$

Since the expectation of martingales is zero, we obtain

$$\sup_{u \in \mathcal{A}} \mathbb{E}\left[\int_t^{t+h} \Big(F(s, N_s^u, u_s) + (\partial_t + \mathcal{L}_s^u) V(s, N_s^u) \Big) ds \right] = 0.$$

Afterward, we divide each side by h and take the limit $h \to 0$ to obtain the related HJB equation:

$$\begin{aligned} \partial_t V(t,n) + \sup_{u \in \mathcal{A}} \Big\{ \lambda(t,n,u)[V(t,n+1) - V(t,n)] + F(t,n,u) \Big\} &= 0, \\ V(T,n) &= G(n). \end{aligned}$$

Remark 1. Assume that we have the stochastic differential equation with the dynamics

$$dX_t^u = \mu(t, X_t^u, N_t^u, u_t)dt + \sigma(t, X_{t^-}^u, N_{t^-}^u, u_t)dN_t^u \tag{2.7}$$

and so the value function

$$V(t, x, n) = \sup_{u\in\mathcal{A}} \mathbb{E}\left[\int_t^T F(s, X_s^u, N_s^u, u_s)ds + G(X_T^u, N_T^u)\right]$$

with $N_{t^-} = n$ and $X_{t^-} = x$.

Adapting the same structure in Section 2.3.2, the HJB equation in this case can be derived as

$$\partial_t V(t, x, n) + \sup_{u\in\mathcal{A}} \left\{ \mathcal{L}_t^u V(t, x, n) + F(t, x, n, u) \right\} = 0,$$

$$V(T, x, n) = G(x, n),$$

where the infinitesimal operator $\mathcal{L}_t^u$ of (2.7) is

$$\begin{aligned} \mathcal{L}_t^u V(t, x, n) &= \mu(t, x, n, u)\partial_x V(t, x, n) \\ &\quad + \lambda(t, x, n, u)[V(t, x + \sigma(t, x, n, u), n + 1) - V(t, x, n)]. \end{aligned}$$

Remark 2. Now, suppose that we deal with the control problem with a stock price dynamics having the stochastic differential equation which includes both diffusion and jump parts as follows:

$$dX_t^u = \mu_t^u dt + \sigma_t^u dW_t + \varepsilon_t^u dN_t^u,$$

where ε_t^u represents the jump size of the counting process $(N_t^u)_{0\leq t\leq T}$ with intensity λ_t^u. The value function of the trader is

$$V(t, x) = \sup_{u\in\mathcal{A}} \mathbb{E}\left[\int_t^T F(s, X_s^u, u_s)ds + G(X_T^u)\right].$$

In this case, the corresponding HJB equation can be obtained as

$$\partial_t V(t, x) + \sup_{u\in\mathcal{A}} \left\{ \mathcal{L}_t^u V(t, x) + F(t, x, u) \right\} = 0,$$

$$V(T, x) = G(x),$$

where the infinitesimal generator $\mathcal{L}_t^u$ is

$$\begin{aligned} \mathcal{L}_t^u V(t, x) &= \mu(t, x, u)\partial_x V(t, x) + \frac{1}{2} tr \left\{\sigma^2(s, x, u)\partial_{xx} V(t, x)\right\} \\ &\quad + \lambda(t, x, u)[V(t, x + \varepsilon) - V(t, x)]. \end{aligned}$$

2.4 Optimal Market Making Problem

In electronic markets, any trader can become a market maker who provides the liquidity to the markets in a LOB; and market makers are permitted to submit the orders on both buy and sell sides of the market by the trading mechanisms. A limit order book is a platform where the high-frequency traders submit their orders and execute their strategies. Thus, the market makers can make profits executing the orders on both buy and sell sides with a very fast speed that provides small margins for each transaction and repeating this action numerous times in a trading day. In order to supply the liquidity to the markets, the market maker quotes a lower bid price, a higher ask price and expects to gain a profit by the difference of the best offered prices. Deciding for the best bid and ask prices that a market maker sets up is a hard and complex problem in many aspects due to the fact that the problem should be tackled as a combined problem of the modeling the asset price dynamics and the optimal spreads. The other issue while solving this problem is to reduce the risk related to the price changes particularly in a large inventory case.

Fortunately, the stochastic control theory helps to handle such kind of optimization problem by seeking an optimal strategy in order to maximize the trader's objective function and to face a dynamic problem for the high-frequency trading. The theory encourages the study of optimizing activities in financial markets as it allows to accomplish the complex optimization problems involving constraints that are consistent with the price dynamics while managing the inventory risk. Execution risk that may be occured because of the non executing or partially executing limit orders is the other source of risk on market making strategies. The third type of the risks in limit order books is the adverse selection risk that arises with more informed traders. In order to detect the optimal quotes in the market, it is, therefore, necessary to solve the corresponding nonlinear Hamilton-Jacobi-Bellman (HJB) equation for the optimal stochastic control problem. This is generally achieved by applying various root-finding algorithms that can handle the complexity and high-dimensionality of the equation, see, e.g., [4, 6].

In the framework of the optimal trading strategy for high-frequency trading in a LOB, there are many papers following early studies of Ho and Stoll [35] and Grossman and

Miller [29]. Avellaneda and Stoikov [3] revise the study of Ho and Stoll [35] building a practical model that considers a single dealer trading a single stock facing with a stochastic demand modeled by a continuous time Poisson process. The literature on the optimal market making problem has been burgeoning since 2008 with the work of Avellaneda and Stoikov [3], inspiring Guilbaud and Pham [32] to derive a model involving limit and market orders with optimal stochastic spreads. Bayraktar and Ludkovski [8] consider the optimal liquidation problem where they model the order arrivals with intensities depending on the liquidation price. More advanced models have been developed with adverse selection effects and stronger market order dynamics, see for example the paper of Cartea, Jaimungal and Ricci [14]. Guéant, Lehalle and Fernandez-Tapia [31] extend and formalize the results of Avellaneda and Stoikov [3]. Another extended market making model with inventory constraints is provided by Fodra and Labadie [24] who consider a general case of midprice by linear and exponential utility criteria and find closed-form solutions for the optimal spreads. Cartea and Jaimungal [12] propose a solution to deal with the problem of including the market impact on the midprice and have worked on risk metrics for the high-frequency trading strategies they have developed. Moreover, Ching *et al.* [15] improve the existing models with Heston stochastic volatility model, to characterize the volatility of the stock price with price impact and to implement an approximation method to solve the nonlinear HJB equation. They have considered a constant price impact using the same counting processes for both arrival and filled limit orders. More recently, Baldacci *et al.* [5] study the optimal control problem for an option market maker with Heston model in an underlying asset using the vega approximation for the portfolio.

2.4.1 A Brief Review of the Related Literature

In this part, we present a brief background of the early optimal market making models of the market microstructure that exist in the literature.

2.4.1.1 Ho and Stoll Model

The model is an extension of the Garman's model [26] which is considered as one of the first market making models in which the continuous transactions are not allowed and is introduced by Ho and Stoll [35].

They assume that the buy and sell orders follow Poisson processes N_t^a and N_t^b with intensities λ^a and λ^b, respectively. Then, they quote the bid and ask prices as

$$p^b = p - b,$$
$$p^a = p + a,$$

where p is the true price of the asset, b and a are the costs for the selling and buying the asset, respectively.

The inventory process I_t of the dealer follows a jump diffusion process:

$$dI_t = r_I I_t dt + p(dN_t^b - dN_t^a) + I_t dW_t^I,$$

where r_I is the mean return of the inventory account.

The change in the cash account value can be found by the process

$$dF_t = rF_t dt - p^b dN_t^b + p^a dN_t^a,$$

where r is the risk-free rate.

The wealth process Y_t of the market maker is defined by

$$dY_t = r_Y Y_t dt + Y_t dW_t^Y$$

with mean return r_Y per unit time.

The aim of the market maker is to maximize her expected utility of her final wealth at the final time T, that is,

$$W_T = F_T + I_T + Y_T.$$

Thence, the optimal control problem for the market maker is simply constituted by

$$\sup_{p^b, p^a} [U(F_T + I_T + Y_T)]$$

and the dynamic programming approach can be represented for the solution which helps to find the optimal costs of selling and buying the asset.

2.4.1.2 Avellaneda and Stoikov Model

Now, we demonstrate the seminal work on market making problem introduced by Avellaneda and Stoikov [3].

The framework is operated on a single stock which follows a standard Brownian motion price dynamics

$$dS_u = \sigma dW_u,$$

where $S_t = s$ is the initial value, W_t is a standard one-dimensional Brownian motion and σ is the volatility.

The market maker can continuously quote the bid price p^b and the ask price p^a to buy and sell the assets. It is assumed that there is no cost for updating the bid and ask prices, respectively, p^b and p^a. The differences

$$\delta^b = s - p^b,$$
$$\delta^a = p^a - s$$

are so-called the spreads. The bid-ask spread is denoted by

$$\delta^b + \delta^a.$$

The amount of cash jumps whensoever a buy or sell order is executed and hence is modeled by

$$dX_t = p^a dN_t^a - p^b dN_t^b,$$

where N_t^b is the number of stocks bought and N_t^a is the amount of stocks sold by the dealer. They are assumed to follow Poisson processes with the intensities $\lambda^b(\delta^b) = Ae^{-k\delta^b}$ and $\lambda^a(\delta^a) = Ae^{-k\delta^a}$ where A characterizes the liquidity of the asset and k is the exponential decay factor. The inventory of the market maker at time t, that is, the number of stocks held is

$$q_t = N_t^b - N_t^a.$$

The aim is to maximize the expected utility function of the dealer at the maturity time T for the optimal feedback controls δ^a and δ^b. Thus, we have the value function

$$v(x, s, q, t) = \mathbb{E}[-\exp(-\gamma(x + qS_T))],$$

where x is the initial wealth, γ is the risk aversion parameter, and q is the current inventory of the dealer.

Here, we have

$$\begin{aligned} v(x,s,q,t) =& \mathbb{E}[-\exp(-\gamma(x+qS_T))] \\ =& \mathbb{E}[-\exp(-\gamma x)\cdot\exp(-\gamma q S_T)] \\ =& -\exp(-\gamma x)\cdot\mathbb{E}[\exp(-\gamma q S_T)]. \end{aligned}$$

Let $Y = \exp(-\gamma q S_T)$. Then,

$$\ln Y = -\gamma q S_T \sim N(-s\gamma q, \gamma^2 q^2 \sigma^2 (T-t))$$

since $\mathbb{E}[S_u] = S_t = s$ and $\mathrm{Var}(S_u) = \sigma^2(u-t)$, and so that

$$S(u) \sim N(s, \sigma^2(u-t))$$

indicates

$$S_T \sim N(s, \sigma^2(T-t)).$$

Hence, we obtain that Y has a log-normal distribution with parameters $-s\gamma q$ and $\gamma^2 q^2 \sigma^2 (T-t)$. Therefore,

$$\mathbb{E}(Y) = \exp(-s\gamma q + \frac{1}{2}\gamma^2 q^2 \sigma^2 (T-t)).$$

This result implies that the value function can be written in other form as

$$v(x,s,q,t) = -\exp(-\gamma x)\exp(-\gamma q s)\exp\left(\frac{\gamma^2 q^2 \sigma^2 (T-t)}{2}\right). \tag{2.8}$$

Now, they define the reservation bid price r^b as the highest price that the buyer is willing to pay for a stock and the reservation ask price r^a as the lowest price that the seller is willing to accept for a stock which are implicitly introduced by the relations

$$v(x - r^b(s,q,t), s, q+1, t) = v(x,s,q,t), \tag{2.9}$$

$$v(x + r^a(s,q,t), s, q-1, t) = v(x,s,q,t). \tag{2.10}$$

When (2.9) and (2.10) are used in the value function equation (2.8), the following closed-form formulas for the reservation prices are obtained:

$$\begin{aligned} r^a(s,q,t) &= s + (1-2q)\frac{\gamma\sigma^2(T-t)}{2}, \\ r^b(s,q,t) &= s - (1+2q)\frac{\gamma\sigma^2(T-t)}{2}. \end{aligned}$$

Then, the reservation or indifference price that is the average of the reservation bid and ask prices is given by

$$r(s,q,t) = \frac{r^a(s,q,t) + r^b(s,q,t)}{2} = s - q\gamma\sigma^2(T-t).$$

The intention of the market maker is to maximize the expected utility function for the optimal controls δ^a and δ^b, i.e.,

$$u(s,x,q,t) = \sup_{\delta^a,\delta^b \in \mathcal{A}} \mathbb{E}[-\exp(-\gamma(X_T + q_T S_T))],$$

where $\mathcal{A}$ is the set of admissible strategies, X_T and q_T are the final wealth and inventory of the dealer, respectively.

The function u solves the following Hamilton-Jacobi-Bellman (HJB) equation:

$$\begin{aligned} u_t + \frac{1}{2}\sigma^2 u_{ss} + \sup_{\delta^b} \lambda^b(\delta^b)[u(s, x - s + \delta^b, q+1, t) - u(s,x,q,t)] \\ + \sup_{\delta^a} \lambda^a(\delta^a)[u(s, x + s + \delta^a, q-1, t) - u(s,x,q,t)] = 0, \\ u(s,x,q,T) = -\exp(-\gamma(x+qs)). \end{aligned} \tag{2.11}$$

To solve the HJB equation, the authors consider the guess

$$u(s,x,q,t) = -\exp(-\gamma x)\exp(-\gamma\theta(s,q,t)), \tag{2.12}$$

where $\theta(s,q,t)$ is approximated by a Taylor expansion about the inventory value q.

Plugging (2.12) into (2.11), the equation turns out to

$$\begin{aligned} \theta_t + \frac{1}{2}\sigma^2\theta_{ss} - \frac{1}{2}\sigma^2\gamma\theta_s^2 + \sup_{\delta^b}\left[\frac{\lambda^b(\delta^b)}{\gamma}[1 - e^{\gamma(s-\delta^b-r^b)}]\right] \\ + \sup_{\delta^a}\left[\frac{\lambda^a(\delta^a)}{\gamma}[1 - e^{-\gamma(s+\delta^a-r^a)}]\right] = 0, \\ \theta(s,q,T) = qs. \end{aligned} \tag{2.13}$$

Using the first order optimality condition, the optimal spreads can then be obtained as

$$\begin{aligned} \delta^b =& s - r^b(s,q,t) + \frac{1}{\gamma}\ln\left(1 - \gamma\frac{\lambda^b(\delta^b)}{\frac{\partial\lambda^b}{\partial\delta^b}(\delta^b)}\right), \\ \delta^a =& r^a(s,q,t) - s + \frac{1}{\gamma}\ln\left(1 - \gamma\frac{\lambda^a(\delta^a)}{\frac{\partial\lambda^a}{\partial\delta^a}(\delta^a)}\right). \end{aligned} \tag{2.14}$$

Afterwards, by the definitions of the reservation prices, they can also be written depending on θ:

$$\begin{aligned} r^b(s,q,t) &= \theta(s,q+1,t) - \theta(s,q,t), \\ r^a(s,q,t) &= \theta(s,q,t) - \theta(s,q-1,t). \end{aligned} \tag{2.15}$$

The asymptotic expansion of θ in the inventory variable q is given by

$$\theta(s,q,t) = \theta^{(0)}(s,t) + \theta^{(1)}(s,t)q + \theta^{(2)}(s,t)q^2 + \theta^{(3)}(s,t)q^3 + \cdots .$$

Substituting θ into the reservation prices given by (2.15) yields

$$\begin{aligned} r^b(s,q,t) &= \theta^{(1)}(s,t) + (1+2q)\theta^{(2)}(s,t) + \cdots , \\ r^a(s,q,t) &= \theta^{(1)}(s,t) + (-1+2q)\theta^{(2)}(s,t) + \cdots . \end{aligned} \tag{2.16}$$

Hence, the reservation price can be obtained as

$$r(s,q,t) = \frac{r^a + r^b}{2} = \theta^{(1)}(s,t) + 2q\theta^{(2)}(s,t).$$

By (2.14) and (2.16), the bid-ask spread given in [3] can be found as

$$\delta^a + \delta^b = -2\theta^{(2)}(s,t) + \frac{2}{\gamma}\ln\left(1 + \frac{\gamma}{k}\right).$$

Substituting (2.14) into (2.13) and using the definitions of the intensity functions, the following equation is derived:

$$\begin{aligned} \theta_t + \frac{1}{2}\sigma^2\theta_{ss} - \frac{1}{2}\sigma^2\gamma\theta_s^2 + \frac{A}{k+\gamma}(e^{-k\delta^a} + e^{-k\delta^b}) &= 0, \\ \theta(s,q,T) &= qs. \end{aligned}$$

The authors consider that the higher terms in the asymptotic expansion of θ are small enough to be negligible and take only the coefficients of q and q^2 which results in the equations

$$\begin{aligned} \theta_t^{(1)} + \frac{1}{2}\sigma^2\theta_{ss}^{(1)} &= 0, \\ \theta^{(1)}(s,T) &= s, \end{aligned}$$

and

$$\begin{aligned} \theta_t^{(2)} + \frac{1}{2}\sigma^2\theta_{ss}^{(2)} - \frac{1}{2}\sigma^2\gamma(\theta_s^{(1)})^2 &= 0, \\ \theta^{(2)}(s,T) &= 0, \end{aligned}$$

where the solutions are $\theta^{(1)}(s,t) = s$ and $\theta^{(2)}(s,t) = -\frac{1}{2}\sigma^2\gamma(T-t)$. By the solution of θ, the following results can be obtained:

$$r(S,t) = S - q\gamma\sigma^2(T-t),$$

$$\delta^a + \delta^b = \gamma\sigma^2(T-t) + \frac{2}{\gamma}\ln\left(1+\frac{\gamma}{k}\right).$$

Finally, the optimal bid and ask spreads are found as

$$\delta^b = (1+2q)\frac{\gamma\sigma^2(T-t)}{2} + \frac{1}{\gamma}\ln\left(1+\frac{\gamma}{k}\right),$$
$$\delta^a = (1-2q)\frac{\gamma\sigma^2(T-t)}{2} + \frac{1}{\gamma}\ln\left(1+\frac{\gamma}{k}\right)$$

in this framework.

In the numerical applications, the authors obtain the optimal prices p^b and p^a by the formulas

$$p^b = s - \delta^b,$$
$$p^a = s + \delta^a,$$

and test the strategy by looking at the profit and loss function, and the terminal inventory q_T for different values of the risk aversion degree γ. More details can be found in the related paper [3].

2.4.1.3 Guéant, Lehalle and Fernandez-Tapia Formula

Guéant, Lehalle and Fernandez-Tapia [31] extend the work of Avellaneda and Stoikov [3] by transforming the optimal stochastic control problem into a system of ordinary differential equations and solving the problem with the constraints of the inventory process.

They consider the same price, inventory, and wealth dynamics and the optimization problem as studied in Avellaneda and Stoikov [3]:

$$
\begin{aligned}
dS_t &= \sigma dW_t, \\
q_t &= N_t^b - N_t^a, \\
dX_t &= p^a dN_t^a - p^b dN_t^b, \\
u(s,x,q,t) &= \sup_{\delta^a,\delta^b \in \mathcal{A}} \mathbb{E}[-\exp(-\gamma(X_T + q_T S_T))]
\end{aligned}
$$

with the intensities $\lambda^b(\delta^b) = Ae^{-k\delta^b}$ and $\lambda^a(\delta^a) = Ae^{-k\delta^a}$.

They assume that the inventories are bounded such that $q \in \{-Q, \ldots, Q\}$ and then write the associated HJB equation:

$$
0 = \begin{cases}
\partial_t u(s,x,q,t) + \frac{1}{2}\sigma^2 \partial_{ss}^2 u(s,x,q,t) \\
\quad + \sup_{\delta^b} \lambda^b(\delta^b) \left[u(s, x - s + \delta^b, q+1, t) - u(s,x,q,t)\right] \\
\quad + \sup_{\delta^a} \lambda^a(\delta^a) \left[u(s, x + s + \delta^a, q-1, t) - u(s,x,q,t)\right], \;\; -Q < q < Q, \\
\partial_t u(s,x,Q,t) + \frac{1}{2}\sigma^2 \partial_{ss}^2 u(s,x,Q,t) \\
\quad + \sup_{\delta^a} \lambda^a(\delta^a) \left[u(s, x + s + \delta^a, Q-1, t) - u(s,x,Q,t)\right], \;\; q = Q, \\
\partial_t u(s,x,-Q,t) + \frac{1}{2}\sigma^2 \partial_{ss}^2 u(s,x,-Q,t) \\
\quad + \sup_{\delta^b} \lambda^b(\delta^b) \left[u(s, x - s + \delta^b, -Q+1, t) - u(s,x,-Q,t)\right], \;\; q = -Q
\end{cases}
$$

with the final condition $u(s,x,q,T) = -\exp(-\gamma(x+qs))$.

Next, they consider a family of functions $(v_q)_{|q| \le Q}$ which is a solution of the following linear system of ODEs:

$$
\begin{aligned}
\dot{v}_q(t) &= \alpha q^2 v_q(t) - \eta(v_{q-1}(t) + v_{q+1}(t)), \quad \forall q \in \{-Q+1, \ldots, Q-1\}, \\
\dot{v}_Q(t) &= \alpha Q^2 v_Q(t) - \eta v_{Q-1}(t), \\
\dot{v}_{-Q}(t) &= \alpha Q^2 v_{-Q}(t) - \eta v_{-Q+1}(t)
\end{aligned}
$$

with $\forall q \in \{-Q, \ldots, Q\}$, $v_q(T) = 1$, where

$$\alpha = \frac{k}{2}\gamma\sigma^2,$$
$$\eta = A\left(1 + \frac{\gamma}{k}\right)^{-(1+\frac{k}{\gamma})}.$$

Then, $u(s, x, q, t) = -\exp\{-\gamma(x + qs)\}\, v_q(t)^{-\frac{\gamma}{k}}$ is the value function of the control problem.

By using the change of variables, the authors are able to solve the optimal control problem and they find the optimal prices as

$$\delta^b = \frac{1}{k}\ln\left(\frac{v_q(t)}{v_{q+1}(t)}\right) + \frac{1}{\gamma}\ln\left(1 + \frac{\gamma}{k}\right), \quad q \neq Q,$$
$$\delta^a = \frac{1}{k}\ln\left(\frac{v_q(t)}{v_{q-1}(t)}\right) + \frac{1}{\gamma}\ln\left(1 + \frac{\gamma}{k}\right), \quad q \neq -Q,$$

and the bid-ask spread as

$$\delta^b + \delta^a = -\frac{1}{k}\ln\left(\frac{v_{q+1}(t)v_{q-1}(t)}{(v_q(t))^2}\right) + \frac{2}{\gamma}\ln\left(1 + \frac{\gamma}{k}\right).$$

2.4.1.4 Cartea and Jaimungal Model

The model is developed by Cartea and Jaimungal [12] where they examine the effect of the arrival of the market orders by adding jump components in the midprice model.

The authors assume that the midprice of the stock follows

$$dS_t = \sigma dW_t + \varepsilon^+ dM_t^+ - \varepsilon^+ dM_t^+,$$

where $M_t^- = \int_0^t \int_{\mathbb{R}_+^2} \mu^-(dy, ds)$ and $M_t^+ = \int_0^t \int_{\mathbb{R}_+^2} \mu^+(dy, ds)$ are the counting processes corresponding to the arrival of sell and buy market orders with intensities λ^- and λ^+ and $\varepsilon^\pm$ are the random variables representing jump sizes with $\mathbb{E}[\varepsilon^\pm] = \epsilon^\pm$ having the distribution functions $F^\pm$. Here, $\mu^\pm(dy, dt)$ are Poisson random measures on $\mathbb{R}_+^2 \times [0, T]$ with mean measures $\nu^\pm(dy, dt) = \lambda^\pm F^\pm(dy_1)G^\pm(dy_2)$ where the distribution $F^\pm$ satisfies $\int_0^\infty F(dy_1) = 1$, $\int_0^\infty y_1^2 F(dy_1) < +\infty$, and $G^\pm(dy_2) = \frac{1}{\kappa^\pm}e^{-\kappa^\pm y_2}dy_2$ with $\kappa^\pm > 0$.

The total inventory of the trader at time t is given by

$$q_t = N_t^- - N_t^+,$$

and the trader's wealth X_t satisfies

$$dX_t = (S_t + \delta_t^+)dN_t^+ - (S_t - \delta_t^-)dN_t^-,$$

where

$$N_t^{\pm} = \int_0^t \int_{\mathbb{R}_+ \times [\delta_s^{\pm}, +\infty)} \mu^{\pm}(dy, ds).$$

It is assumed that the limit order at price level $S_t \pm \delta_t^{\pm}$ is filled with the probability $e^{-\kappa \delta_t^{\pm}}$.

In the model, the expected terminal wealth is aimed to maximize while penalizing and constraining inventories that results in the control problem

$$H(t, x, q, S) = \sup_{(\delta_s^{\pm}) \in \mathcal{A}} \mathbb{E}[X_T + q_T(S_T - \alpha q_T) - \phi\sigma^2 \int_t^T q_s^2 ds],$$

where the term $-\alpha q_T^2$ penalizes the deviations of the inventory at maturity time and ϕ penalizes the deviations during the whole trading session.

The related HJB equation of the optimal control problem is written as

$$\begin{aligned}
0 = {} & \partial_t H + \frac{1}{2}\sigma^2 \partial_{SS} H - \phi\sigma^2 q^2 \\
& + \lambda^+ \sup_{\delta^+} \Big[e^{-\kappa^+ \delta^+} \mathbb{E}(H(t, x + (S + \delta^+), q - 1, S + \varepsilon^+) - H(t, x, q, S)) \\
& \qquad + (1 - e^{-\kappa^+ \delta^+}) \mathbb{E}(H(t, x, q, S + \varepsilon^+) - H(t, x, q, S)) \Big] \\
& + \lambda^- \sup_{\delta^-} \Big[e^{-\kappa^- \delta^-} \mathbb{E}(H(t, x - (S - \delta^-), q + 1, S - \varepsilon^-) - H(t, x, q, S)) \\
& \qquad + (1 - e^{-\kappa^- \delta^-}) \mathbb{E}(H(t, x, q, S - \varepsilon^-) - H(t, x, q, S)) \Big]
\end{aligned}$$

with the final condition

$$H(t, x, q, S) = x + q(S - \alpha q).$$

In order to solve the HJB equation,

$$H(t, x, q, S) = x + q(S - \alpha q) + h_q(t),$$

is proposed as a solution that leads to the following equation:

$$\phi\sigma^2 q^2 = \begin{cases} \partial_t h_q + \lambda^+ \sup_{\delta^+}\Big[-\varepsilon^+ q + e^{-\kappa\delta^+}(\delta^+ - \varepsilon^+ - \alpha(1-2q) + h_{q-1} - h_q)\Big] \\ \qquad + \lambda^- \sup_{\delta^-}\Big[-\varepsilon^- q + e^{-\kappa\delta^-}(\delta^- - \varepsilon^- - \alpha(1+2q) + h_{q+1} - h_q)\Big], \\ \hfill q \neq \underline{q}, \overline{q}, \\ \partial_t h_q + \lambda^+ \sup_{\delta^+}\Big[-\varepsilon^+ q + e^{-\kappa\delta^+}(\delta^+ - \varepsilon^+ - \alpha(1-2q) + h_{q-1} - h_q)\Big] \\ \hfill -\varepsilon^-\lambda^- q, \;\; q = \overline{q}, \\ \partial_t h_q + \lambda^- \sup_{\delta^-}\Big[-\varepsilon^- q + e^{-\kappa\delta^-}(\delta^- - \varepsilon^- - \alpha(1+2q) + h_{q+1} - h_q)\Big] \\ \hfill +\varepsilon^+\lambda^+ q, \;\; q = \underline{q}, \end{cases}$$

with the terminal condition $h_q(T) = 0$ and the inventory constraints $q \in [\underline{q}, \overline{q}]$.

Eventually, the optimal controls are derived by applying the first-order optimality conditions to each sup term as follows:

$$\delta^{+*}(t,q) = \frac{1}{\kappa} + \varepsilon^+ + \alpha(1-2q) - h_{q-1}(t) + h_q(t), \quad q \neq \underline{q},$$

and

$$\delta^{-*}(t,q) = \frac{1}{\kappa} + \varepsilon^- + \alpha(1+2q) - h_{q+1}(t) + h_q(t), \quad q \neq \overline{q}.$$

For the applications, one can refer to the related paper [12].

CHAPTER 3

OPTIMAL MARKET MAKING MODELS DRIVEN BY STOCHASTIC VOLATILITY IN THE UNDERLYING ASSET

In this chapter, we extend the existing optimal market making models in a limit order book by assuming the volatility as stochastic in the assets as novel models. We first assume that the stock price is set up as a jump-diffusion model including two independent jump processes to measure the effects of arriving market orders and with a stochastic volatility. As another extension, we suppose that the jump effects of each order occur in the volatility of the asset. It is well known that jumps and stochastic volatility are salient properties of financial instruments and such models of stock price driven by a stochastic volatility including jumps can describe the real market better since the volatility is fluctuating in reality.

Optimal controls of the models proposed here are found by writing the corresponding HJB equation for each of the stochastic optimization problem in order to exploit the numerical results.

3.1 Market Making Optimization Problems in a Limit Order Book

We first define a probability space $(\Omega, \mathcal{F}, \mathbb{P})$ with a sample space Ω, filtration $\mathcal{F}$, and a probability measure $\mathbb{P}$ for all random variables and stochastic processes.

To start, we aim to set up a high-frequency trading model in order to gain from the expected profit by building trading strategies on limit buy and sell orders. The model that we explore in this part is based on a stock price which is generated by two independent Poisson processes with different intensities representing the different jump amounts to employ the adverse selection effects. Besides, the model includes the stochastic volatility dynamics.

3.1.1 Setup of the Model

Assume that the midprice S_t of the stock in the market follows the dynamics:

$$\begin{aligned} dS_t &= \mu dt + \sqrt{\nu_t} dB_t^1 + \varepsilon^+ dM_t^+ - \varepsilon^- dM_t^-, \\ d\nu_t &= k(\theta - \nu_t)dt + \sigma\sqrt{\nu_t} dB_t^2, \\ dB_t^1 dB_t^2 &= \rho dt, \end{aligned} \tag{3.1}$$

which employs the Heston stochastic volatility model [34], where B_t^1 and B_t^2 are Wiener processes and $\rho \in [-1, 1]$ is the instantaneous correlation coefficient between them. Here, μ is the constant drift term, θ is the long-term variance parameter, k is the rate at which the stochastic volatility ν_t reverts to θ, σ is the volatility of the volatility, and $\nu_t \geq 0$ follows a mean-reverting square root process. We should note that if the Feller's condition, $2k\theta \geq \sigma^2$ [22], is satisfied, then the volatility process ν_t becomes always positive. In the model, $M_t^\pm$ are independent Poisson processes with intensities $\lambda^\pm$ which count the number of arrived market orders and $\varepsilon^\pm$ are the jump sizes in the midprice caused by the orders which are i.i.d. random variables with finite second moments having $\mathbb{E}[\varepsilon^\pm] = \epsilon^\pm$.

We construct the model for the case of market making problem. Hence, we assume that there is a market maker who continuously proposes optimal bid and ask quotes at prices $S_t - \delta_t^-$ and $S_t + \delta_t^+$, where $\delta_t^\pm$ are the related optimal depths at which the market maker posts the limit orders.

The inventory of the market maker with an initial inventory $q_0 = 0$ is restricted to be between upper and lower bounds during the trading session at any time t; particularly, $q \in [\underline{q}, \overline{q}]$ and therefore it has the following dynamics:

$$q_t = q_0 + N_t^- - N_t^+, \quad q_t \in \mathbb{Z}, \quad t \in [0, T],$$

with maturity time T, where N_t^- and N_t^+ are the two independent counting processes for the market orders that are filled by the buy and sell orders, respectively. The inventory changes with probability $e^{-\kappa^{\pm}\delta_t^{\pm}}$ for filled limit orders and $\kappa^{\pm}$ represents the liquidity of the stock. Hence, $N_t^{\pm}$ is updated as 1 if the arriving order is a market order and is filled with the probability $e^{-\kappa^{\pm}\delta_t^{\pm}}$; otherwise $N_t^{\pm}$ becomes 0. We should note that the processes $M_t^{\pm}$ jump when the processes $N_t^{\pm}$ jump since $N_t^{\pm}$ are processes for filled orders. On the other hand, in case of $M_t^{\pm}$ jump, the processes $N_t^{\pm}$ jump only if the market order is sufficiently large to fill the limit order and the processes $N_t^{\pm}$ are not Poisson.

Since the market maker trades continuously, the wealth process X_t, the cash of the trader during any time t, has the stochastic dynamics as follows:

$$\begin{aligned} dX_t &= p_t^+ dN_t^+ - p_t^- dN_t^- \\ &= (S_t + \delta_t^+) dN_t^+ - (S_t - \delta_t^-) dN_t^- . \end{aligned}$$

Additionally, based on the current wealth, inventory and price of the stock at any time t, the profit and loss value of the trader can be calculated by $x_t + q_t S_t$.

Supposing that the market orders arrive and are filled by the limit orders, the rate of execution, $\Lambda_t : \mathbb{R} \to \mathbb{R}_+$, can be written as

$$\Lambda_t^{\pm}(\delta_t^{\pm}) = \lambda^{\pm} e^{-\kappa^{\pm}\delta_t^{\pm}}. \tag{3.2}$$

Now, we can define the market maker's problem as a stochastic optimization model. The strategy of the market maker is to maximize the expected cash value at the maturity time T. By using the stochastic control approach as done in (2.3), the value function for this maximization problem can be formalized as follows:

$$W(t,x,S,\nu;q) = \sup_{(\delta_s^{\pm})_{t\le s\le T} \in \mathcal{A}_t} \mathbb{E}\left[U(X_T, S_T; q_T) - \psi\sigma^2 \int_t^T q_s^2 \nu_s ds \right], \tag{3.3}$$

where $U(X_T, S_T; q_T)$ is the utility function, and

$$\mathcal{A}_t = \left\{ (\delta_s^{\pm *})_{t\le s\le T} \ge 0 : \delta_s^{\pm *} \text{ is } \mathcal{F}\text{-predictable} \right\} \tag{3.4}$$

is the set of admissible strategies on $[t,T]$ corresponding to all self-financing strategies. Here, $\mathbb{E}[\cdot]$ denotes the conditional expectation given $X_{t^-} = x$, $q_{t^-} = q$, $S_{t^-} = S$ and $\nu_{t^-} = \nu$ such that the inventories are bounded from above by $\overline{q} > 0$ and from below by $\underline{q} < 0$. In the admissible strategies, we force to have $\lim_{q\to\underline{q}} \delta_t^{+*} = +\infty$ and

$\lim_{q\to\overline{q}} \delta_t^{-*} = +\infty$ for the boundaries of the inventory set. The term ψ in (3.3) represents the constant term to penalize the variations on $[0, T]$ in the value function; and the component $\psi\sigma^2\mathbb{E}\left[\int_t^T q_s^2\nu_s ds\right]$ is the penalty function on the inventories. While the market maker wants to maximize her profit from the transactions over a finite time horizon, she also wants to keep her inventories under control and gets rid of the remaining inventories at the final time T.

3.2 HJB Equation of the Model for the Value Function Defined with Quadratic Utility

Under the assumptions provided in Section 3.1 and assuming that $(S_t, M_t^{\pm}, N_t^{\pm})$ is Markovian, the optimization problem (3.3) can be solved using the stochastic control approach [10, 48, 52]. The solution will be based on two different choices of utility functions, quadratic and exponential, in the sequel. We choose to study on these utility functions to discover the optimal qualitative behaviour of the optimal strategy in cases that the trader is risk neutral and risk averse, respectively.

We first assume that the utility function is of the form

$$U(X_T, S_T; q_T) = X_T + q_T S_T + \eta(q_T),$$

and that the market maker is a risk-neutral investor. This utility function can also be regarded as a linear utility function with only inventory penalty. Indeed, the function $\eta(q_T)$ may be considered as a function that penalizes the left over inventories at maturity time with a constant execution cost parameter $\alpha > 0$ being $\eta(q_T) = -\alpha q_T^2$. Thereby, one has the corresponding value function

$$W(t, x, S, \nu; q) = \sup_{(\delta_s^{\pm})_{t\le s\le T}\in\mathcal{A}_t} \mathbb{E}\left[X_T + q_T S_T + \eta(q_T) - \psi\sigma^2\int_t^T q_s^2\nu_s ds\right], \quad (3.5)$$

which should be satisfied by a HJB equation.

Proposition 1. The value function (3.5) satisfies the HJB equation,

$$
\begin{aligned}
&\partial_t W + \mu \partial_S W + k(\theta - \nu_t)\partial_\nu W + \frac{1}{2}\nu_t \partial_{SS} W + \frac{1}{2}\sigma^2 \nu_t \partial_{\nu\nu} W + \sigma\rho\nu_t \partial_{S\nu} W - \psi \nu_t q^2 \sigma^2 \\
&\quad + \sup_{\delta_t^+} \Big\{ \Lambda_t^+(\delta_t^+) \mathbb{E}\left[W(t, x + (S_t + \delta_t^+), S_t + \varepsilon^+, \nu_t; q-1) - W(t, x, S_t, \nu_t; q) \right] \\
&\qquad + (\lambda^+ - \Lambda_t^+(\delta_t^+)) \mathbb{E}\left[W(t, x, S_t + \varepsilon^+, \nu_t; q) - W(t, x, S_t, \nu_t; q) \right] \Big\} \\
&\quad + \sup_{\delta_t^-} \Big\{ \Lambda_t^-(\delta_t^-) \mathbb{E}\left[W(t, x - (S_t - \delta_t^-), S_t - \varepsilon^-, \nu_t; q+1) - W(t, x, S_t, \nu_t; q) \right] \\
&\qquad + (\lambda^- - \Lambda_t^-(\delta_t^-)) \mathbb{E}\left[W(t, x, S_t - \varepsilon^-, \nu_t; q) - W(t, x, S_t, \nu_t; q) \right] \Big\} = 0, \quad (3.6)
\end{aligned}
$$

with the final condition,

$$W(T, x, S, \nu; q) = x + q(S - \alpha q), \tag{3.7}$$

where Λ_t is given in (3.2) and the expectation is taken over the random variables $\varepsilon^{\pm}$.

Proof. It is clear that the value function (3.5) for $\mathbb{R}_+ \times \mathbb{R}^n \to \mathbb{R}$ is in the form of

$$\sup_{u_t \in \mathcal{A}_t} \mathbb{E}\left[\int_t^T F(s, X_s^u, u_s) ds + G(X_s^u) \right]$$

and that it is optimal when $u_t = u(t, S_t)$ is the admissible control process of the problem, where $\mathcal{A}_t$ is the set of the admissible strategies, F and G are the instantaneous and terminal reward functions, respectively.

We want to derive a partial differential equation (PDE) for the value function (3.5). Further, we fix $(t, x) \in (0, T) \times \mathbb{R}^n$ and choose any stopping time $t + h < T$ where $h > 0$ which is a small enough number. Then, we consider the expected utility function

$$\mathbb{E}_{t,x}\Big[\int_t^{t+h} F(s, X_s^u, u_s) ds \Big].$$

It is trivial to have the inequality

$$W(t, x, S, \nu; q) \geq \mathbb{E}_{t,x}\Big[\int_t^{t+h} F(s, X_s^u, u_s) ds + W(t+h, X_{t+h}^u, S, \nu; q) \Big]. \tag{3.8}$$

By Itô's formula, we also obtain

$$\begin{aligned} W(t+h, X^u_{t+h}, S, \nu; q) = W(t, x, S, \nu; q) \\ &+ \int_t^{t+h} \{\partial_t W(s, X^u_s, S, \nu; q) + \mathcal{L}_t W(s, X^u_s, S, \nu; q)\}\, ds \\ &+ \int_t^{t+h} \partial_x W(s, X^u_s, S, \nu; q) dB^1_s. \end{aligned}$$

Plugging this into (3.8), we get

$$\mathbb{E}_{t,x}\Big[\int_t^{t+h} [F(s, X^u_s, u_s)ds + \partial_t W(s, X^u_s, S, \nu; q) + \mathcal{L}^u_t W(s, X^u_s, S, \nu; q)]\, ds\Big] \leq 0, \tag{3.9}$$

where $\mathcal{L}^u_t$ is the infinitesimal generator for $W(t, X^u_t, S, \nu; q)$, see Section 2.3.2.

Dividing (3.9) by h and taking the limit as $h \to 0$, we obtain

$$F(t, x, u) + \partial_t W(t, x, S, \nu; q) + \mathcal{L}^u_t W(t, x, S, \nu; q) \leq 0. \tag{3.10}$$

Since (3.10) holds for all admissible control processes, finally we obtain the HJB equation which is explicitly given by (3.6):

$$\begin{aligned} \partial_t W + \sup_{u \in \mathcal{A}_t} \{\mathcal{L}^u_t W(t, x, S, \nu; q) + F(t, \nu_t, u)\} = 0, \\ W(T, x, S, \nu; q) = G(x). \end{aligned}$$

This completes the proof. For more details, one can refer to [10, 48, 52]. □

3.2.1 Derivation of the Optimal Quotes

For the case of a quadratic utility function, we derive the optimal spreads for limit orders and observe their behaviours. For this purpose, we should propose an appropriate solution to (3.6) with the final condition (3.7) and show that this solution verifies the value function (3.5).

3.2.1.1 Case 1: The suggested solution includes the effect of the stochastic volatility explicitly

In this case, we assume that the effect of the stochastic volatility can be explicitly seen in the ansatz which is suggested by the final condition. In the following proposition, we provide the optimal spreads for this case.

Proposition 2. Let

$$W(t,x,S,\nu;q) = x + q(S-\alpha q) + u(t,\nu;q) \tag{3.11}$$

be a solution to the HJB equation (3.6) where $u(t,\nu;q)$ is called as the reservation price. Then, the optimal feedback controls of (3.6) are given by

$$\begin{aligned} \delta_1^{+*}(t,\nu;q) &= \tfrac{1}{\kappa^+} + \epsilon^+ + \alpha(1-2q) - u(t,\nu;q-1) + u(t,\nu;q), \quad q \neq \underline{q}, \\ \delta_1^{-*}(t,\nu;q) &= \tfrac{1}{\kappa^-} + \epsilon^- + \alpha(1+2q) - u(t,\nu;q+1) + u(t,\nu;q), \quad q \neq \overline{q}. \end{aligned} \tag{3.12}$$

Proof. We start with inserting the specified proposed solution (3.11) into (3.6) and substituting the intensity functions of the filled orders, which are $\Lambda_t^{\pm}(\delta_t^{\pm}) = \lambda^{\pm} e^{-\kappa^{\pm}\delta_t^{\pm}}$. Then, (3.6) is reduced to

$$\begin{aligned} \psi\nu q^2\sigma^2 - \mu q = \partial_t u &+ k(\theta-\nu)\partial_\nu u + \frac{1}{2}\sigma^2\nu\partial_{\nu\nu}u \\ &+ \sup_{\delta_t^+} \lambda^+ \Big\{ q\epsilon^+ \\ &\quad + e^{-\kappa^+\delta^+}(\delta^+ - \epsilon^+ - \alpha(1-2q) + u(t,\nu;q-1) - u(t,\nu;q)) \Big\} \\ &+ \sup_{\delta_t^-} \lambda^- \Big\{ -q\epsilon^- \\ &\quad + e^{-\kappa^-\delta^-}(\delta^- - \epsilon^- - \alpha(1+2q) + u(t,\nu;q+1) - u(t,\nu;q)) \Big\} \end{aligned} \tag{3.13}$$

for $q \in (\underline{q}, \overline{q})$ with final condition $u(T,\nu;q) = 0$.

Finally, applying the first order optimality conditions to the supremum terms in (3.13), the optimal choices of depths, given by (3.12), can be obtained in order to complete the proof. □

Note that when the function $u(t,\nu;q)$ is independent of ν, the formulas given by (3.12) correspond to the optimal control results in Cartea and Jaimungal [12].

We use the optimal spreads (3.12), derived in this section, to solve the nonlinear HJB equation (3.6). Therefore, inserting them into (3.13) yields the following PDE for the verification:

$$\psi\nu q^2\sigma^2 - \mu q = \partial_t u + k(\theta-\nu)\partial_\nu u + \frac{1}{2}\sigma^2\nu\partial_{\nu\nu}u + \lambda^+\left[q\epsilon^+ + \frac{1}{\kappa^+}e^{-1-\kappa^+(\epsilon^+ + \alpha(1-2q) - u(t,\nu;q-1) + u(t,\nu;q))}\right] + \lambda^-\left[-q\epsilon^- + \frac{1}{\kappa^-}e^{-1-\kappa^-(\epsilon^- + \alpha(1+2q) - u(t,\nu;q+1) + u(t,\nu;q))}\right] \tag{3.14}$$

for $q \in (\underline{q}, \overline{q})$ with the final condition $u(T,\nu;q) = 0$.

We should also note that the behaviour of the equation is changed at the boundary points of the inventory limits. Being $q = \underline{q}$ means that the selling is forbidden for the market maker, since there will be no leftover inventories if the selling action happens. As a result, we have the HJB equation

$$\psi\nu q^2\sigma^2 - \mu q = \partial_t u + k(\theta-\nu)\partial_\nu u + \frac{1}{2}\sigma^2\nu\partial_{\nu\nu}u + \lambda^-\left[-q\epsilon^- + \frac{1}{\kappa^-}e^{-1-\kappa^-(\epsilon^- + \alpha(1+2q) - u(t,\nu;q+1) + u(t,\nu;q))}\right] + \lambda^+ q\epsilon^+. \tag{3.15}$$

Therefore, in this case, we can only find the optimal buy spread δ_t^{-*}.

Similarly, in the case of $q = \overline{q}$, buying is forbidden for the market maker. Thus, we have

$$\psi\nu q^2\sigma^2 - \mu q = \partial_t u + k(\theta-\nu)\partial_\nu u + \frac{1}{2}\sigma^2\nu\partial_{\nu\nu}u + \lambda^+\left[q\epsilon^+ + \frac{1}{\kappa^+}e^{-1-\kappa^+(\epsilon^+ + \alpha(1-2q) - u(t,\nu;q-1) + u(t,\nu;q))}\right] - \lambda^- q\epsilon^-. \tag{3.16}$$

We should recall that we impose the inventory q_t to be in a finite range $[\underline{q}, \overline{q}]$ for the whole trading session.

The computational difficulty to solve the equations (3.14), (3.15) and (3.16) together arises due to the fact that the equations contain a discrete variable q with continuous variables t and ν. Further, u values at level $q-1$, as well as $q+1$, feed the u values at level q. Hence, to overcome this difficulty, we solve the verification equation by applying finite difference discretization scheme backwards in time. For the details, see

Section A.1 in Appendix A. After calculating $u(t,\nu;q)$, we can generate the optimal distances given by the formulas (3.12).

However, $u(t,\nu;q)$ can be also solved by a transformation as given in Remark 3 in the following.

Remark 3. By the transformation $u(t,\nu;q)=\frac{1}{\kappa}\ln\omega(t,\nu;q)$ with $\boldsymbol{\omega}(t,\nu;q)=[\omega(t,\nu;\overline{q}),\omega(t,\nu;\overline{q}-1),\dots,\omega(t,\nu;\underline{q})]'$ where $\kappa^+=\kappa^-=\kappa$, storing all q's into a vector and after some calculations; (3.14), (3.15), and (3.16) can be transformed into the following nonlinear system of PDEs

$$\boldsymbol{\omega_t}+A\boldsymbol{\omega_\nu}+B\boldsymbol{\omega_{\nu\nu}}+C\tilde{\boldsymbol{\omega}}+D\boldsymbol{\omega}=\mathbf{0}, \tag{3.17}$$

where $\boldsymbol{\omega_t}$, $\boldsymbol{\omega_\nu}$, $\boldsymbol{\omega_{\nu\nu}}$ and $\tilde{\boldsymbol{\omega}}$ are $(\overline{q}-\underline{q}+1)\times 1$ vectors given by

$$\boldsymbol{\omega_t}=[\omega_t(t,\nu;q)], \qquad \boldsymbol{\omega_\nu}=[\omega_\nu(t,\nu;q)],$$
$$\boldsymbol{\omega_{\nu\nu}}=[\omega_{\nu\nu}(t,\nu;q)], \qquad \tilde{\boldsymbol{\omega}}=\left[\frac{(\omega_\nu(t,\nu;q))^2}{\omega(t,\nu;q)}\right]$$

with $q=\overline{q},\overline{q}-1,\dots\underline{q}+1,\underline{q}$ and,

$$A=\begin{pmatrix} k(\theta-\nu) & 0 & \cdots & 0\\ 0 & k(\theta-\nu) & \cdots & 0\\ \vdots & \vdots & \ddots & \vdots\\ 0 & 0 & \cdots & k(\theta-\nu)\end{pmatrix},$$

$$B=\begin{pmatrix} \frac{1}{2}\sigma^2\nu & 0 & \cdots & 0\\ 0 & \frac{1}{2}\sigma^2\nu & \cdots & 0\\ \vdots & \vdots & \ddots & \vdots\\ 0 & 0 & \cdots & \frac{1}{2}\sigma^2\nu\end{pmatrix},$$

$$C=\begin{pmatrix} -\frac{1}{2}\sigma^2\nu & 0 & \cdots & 0\\ 0 & -\frac{1}{2}\sigma^2\nu & \cdots & 0\\ \vdots & \vdots & \ddots & \vdots\\ 0 & 0 & \cdots & -\frac{1}{2}\sigma^2\nu\end{pmatrix},$$

$$D = \begin{pmatrix} a & b & 0 & \cdots & 0 & 0 \\ c & a & b & \cdots & 0 & 0 \\ 0 & c & a & \cdots & 0 & 0 \\ \vdots & \vdots & \vdots & \ddots & \vdots & \vdots \\ 0 & 0 & 0 & \cdots & a & b \\ 0 & 0 & 0 & \cdots & c & a \end{pmatrix},$$

with the entries

$$\begin{aligned} a &= \mu q\kappa - \psi\nu q^2\sigma^2\kappa + \lambda^+ q\epsilon^+\kappa - \lambda^- q\epsilon^-\kappa, \\ b &= \lambda^+ e^{-\kappa\left(\frac{1}{\kappa}+\epsilon^+ + \alpha(1-2q)\right)}, \\ c &= \lambda^- e^{-\kappa\left(\frac{1}{\kappa}+\epsilon^- + \alpha(1+2q)\right)}. \end{aligned}$$

Remark 4. An important restriction arises on the negative spreads since the intensities are defined for all real numbers and the trader should keep the admissible strategies where the optimal spreads should be positive and finite. To avoid the negative spreads, we add a constraint for $\delta_t^{\pm *}$ and get the maximum value of them with a very small positive number δ^*:

$$\begin{aligned} \delta_1^{+*}(t,\nu;q) &= \max\left\{\left(\tfrac{1}{\kappa^+} + \epsilon^+ + \alpha(1-2q) - u(t,\nu;q-1) + u(t,\nu;q)\right), \delta^*\right\}, \quad q \neq \underline{q}, \\ \delta_1^{-*}(t,\nu;q) &= \max\left\{\left(\tfrac{1}{\kappa^-} + \epsilon^- + \alpha(1+2q) - u(t,\nu;q+1) + u(t,\nu;q)\right), \delta^*\right\}, \quad q \neq \overline{q}. \end{aligned}$$

3.2.1.2 Case 2: The suggested solution does not include the effect of the stochastic volatility explicitly

In this setup, it is supposed that the suggested solution to (3.6) does not involve the stochastic volatility effect directly.

Proposition 3. Let

$$W(t,x,S,\nu;q) = x + q(S - \alpha q) + u(t;q) \tag{3.18}$$

be a solution to the HJB equation (3.6) which is suggested by the final condition (3.7).

Then, the optimal feedback controls of (3.6) are given by

$$\begin{aligned}
\delta_1^{+*}(t;q) &= \tfrac{1}{\kappa^+} + \epsilon^+ + \alpha(1-2q) - u(t;q-1) + u(t;q), \quad q \neq \underline{q}, \\
\delta_1^{-*}(t;q) &= \tfrac{1}{\kappa^-} + \epsilon^- + \alpha(1+2q) - u(t;q+1) + u(t;q), \quad q \neq \overline{q}.
\end{aligned} \tag{3.19}$$

Proof. Replacing the proposed solution (3.18) into (3.6) and substituting the intensity functions of the filled orders, (3.6) is reduced to

$$\begin{aligned}
\psi\nu q^2\sigma^2 - \mu q = \partial_t u \\
&+ \sup_{\delta_t^+} \lambda^+ \Big\{ q\epsilon^+ \\
&\qquad + e^{-\kappa^+\delta^+}(\delta^+ - \epsilon^+ - \alpha(1-2q) + u(t;q-1) - u(t;q)) \Big\} \\
&+ \sup_{\delta_t^-} \lambda^- \Big\{ - q\epsilon^- \\
&\qquad + e^{-\kappa^-\delta^-}(\delta^- - \epsilon^- - \alpha(1+2q) + u(t;q+1) - u(t;q)) \Big\}
\end{aligned}$$

with final condition $u(T;q) = 0$.

Then, by the first order optimality conditions, the optimal spreads (3.19) can be acquired. □

3.2.2 Verification Argument

Now, we show that a solution $u(t,\nu;q)$ of (3.13) exists and is unique that should be guaranteed by the verification theorem so that this classical solution is the value function of the HJB equation and the spreads, defined by (3.12), are indeed the optimal ones.

Theorem 4. *Let* $u(t,\nu;q)$ *be a solution to* (3.13)*. Then,* $W(t,x,S,\nu;q) = x + q(S - \alpha q) + u(t,\nu;q)$ *is the value function for the control problem* (3.5) *and, moreover, the optimal controls are given by* (3.12)*.*

Proof. Let $t \in [0,T]$, $(\delta_t^{\pm})_{t\le s\le T}$ be admissible controls and $W(t,x,S,\nu;q)$ be the solution to the HJB equation (3.6). Consider the following processes for $s \in [t,T]$:

$$
\begin{aligned}
dS_s^{t,S} &= \mu ds + \sqrt{\nu_s} dB_s^1 + \varepsilon^+ dM_s^+ - \varepsilon^- dM_s^-, \quad S_t^{t,S} = S, \\
d\nu_s^{t,\nu} &= k(\theta - \nu_s)ds + \sigma\sqrt{\nu_s} dB_s^2, \quad \nu_t^{t,\nu} = \nu,
\end{aligned}
$$

as well as

$$
\begin{aligned}
dX_s^{t,x,\delta_s^\pm} &= (S_s + \delta_s^+)dN_s^+ - (S_s - \delta_s^-)dN_s^-, \quad X_t^{t,x,\delta_s^\pm} = x, \\
dq_s^{t,q,\delta_s^\pm} &= dN_s^- - dN_s^+, \quad q_t^{t,q,\delta_s^\pm} = q,
\end{aligned}
$$

such that $dB_s^1 dB_s^2 = \rho ds$, where $M^\pm$ are independent Poisson processes with intensities $\lambda^\pm$ and $N^\pm$ are independent counting processes with filled probabilities $e^{-\kappa^\pm \delta_s^\pm}$. The optimal bid and ask prices are

$$
S_s^- = S_s - \delta_s^- \quad (q \neq \overline{q}) \quad \text{and} \quad S_s^+ = S_s + \delta_s^+ \quad (q \neq \underline{q}),
$$

where the optimal spreads are

$$
\delta_s^{\pm *} = \frac{1}{\kappa^\pm} + \epsilon^\pm + \alpha(1 \pm 2q) - u(s,\nu;q \pm 1) + u(s,\nu;q).
$$

Define

$$
\begin{aligned}
t_n = T \wedge \inf\{s > t : |S_s - S| \geq n \\
&\text{or } |N_s^+ - N_t^+| \geq n \text{ or } |N_s^- - N_t^-| \geq n \\
&\qquad \text{or } |M_s^- - M_t^-| \geq n \text{ or } |M_s^+ - M_t^+| \geq n\}
\end{aligned}
$$

for a given $n \in \mathbb{N}$. Let W be a sufficiently smooth solution to the HJB equation (3.6).

Then, using Itô's formula for W, we have

$$
\begin{aligned}
W(t_n, X_{t_n^-}^{t,x,\delta_s^\pm}, S_{t_n}^{t,S}, \nu_{t_n}^{t,\nu}; q_{t_n^-}^{t,q,\delta_s^\pm}) = W(t,x,S,\nu;q) &+ \int_t^{t_n} \Bigg[\partial_s u(s,\nu_s^{t,\nu}; q_s^{t,q,\delta_s^\pm}) \\
&+ k(\theta-\nu_s)\partial_\nu u(s,\nu_s^{t,\nu}; q_s^{t,q,\delta_s^\pm}) \\
&+ \frac{1}{2}\sigma^2\nu\partial_{\nu\nu}u(s,\nu_s^{t,\nu}; q_s^{t,q,\delta_s^\pm}) + \mu q_s\Bigg] ds \\
&+ \int_t^{t_n} q_s\sqrt{\nu_s}dB_s^1 \\
&+ \int_t^{t_n} \sigma\sqrt{\nu_s}\partial_\nu u(s,\nu_s^{t,\nu}; q_s^{t,q,\delta_s^\pm})dB_s^2 \\
&+ \varepsilon^+\int_t^{t_n} q_{s^-}dM_s^+ - \varepsilon^-\int_t^{t_n} q_{s^-}dM_s^- \\
&+ \int_t^{t_n}\Big[\delta_s^+ + 2\alpha q_{s^-} - \alpha - \varepsilon^+ dM_s^+ \\
&+ u(s,\nu_s; q_{s^-}^{q,\delta_s^+} - 1) - u(s,\nu_s; q_{s^-}^{q,\delta_s^+})\Big] dN_s^+ \\
&+ \int_t^{t_n}\Big[\delta_s^- - 2\alpha q_{s^-} - \alpha - \varepsilon^- dM_s^- \\
&+ u(s,\nu_s; q_{s^-}^{q,\delta_s^-} + 1) - u(s,\nu_s; q_{s^-}^{q,\delta_s^-})\Big] dN_s^-.
\end{aligned}
\tag{3.20}
$$

Note that W is continuous and positive on a compact set on t_n, thus it has a lower bound. We know that $\delta_t^\pm$ are bounded from below and $\delta_s^+ \to +\infty$ ($\delta_s^- \to +\infty$) as $q_s \to \underline{q}$ ($q_s \to \overline{q}$). Hence, all the terms in stochastic integrals in (3.20) are bounded. By Dynkin's formula [19], we get

$$
\begin{aligned}
&\mathbb{E}\left[W(t_n, X_{t_n^-}^{t,x,\delta_s^\pm}, S_{t_n}^{t,S}, \nu_{t_n}^{t,\nu}; q_{t_n^-}^{t,q,\delta_s^\pm})\right] \\
&= W(t,x,S,\nu;q) + \mathbb{E}\Bigg[\int_t^{t_n}\Bigg(\partial_s u(s,\nu_s^{t,\nu}; q_s^{t,q,\delta_s^\pm}) + k(\theta-\nu_s)\partial_\nu u(s,\nu_s^{t,\nu}; q_s^{t,q,\delta_s^\pm}) \\
&\quad + \frac{1}{2}\sigma^2\nu\partial_{\nu\nu}u(s,\nu_s^{t,\nu}; q_s^{t,q,\delta_s^\pm}) + q_{s^-}(\mu+\epsilon^+-\epsilon^-) \\
&\quad + \lambda^+\Big(\delta_s^+ + 2\alpha q_{s^-} - \alpha - \epsilon^+ + u(s,\nu_s; q_{s^-}^{q,\delta_s^+} - 1) - u(s,\nu_s; q_{s^-}^{q,\delta_s^+})\Big) \\
&\quad + \lambda^-\Big(\delta_s^- - 2\alpha q_{s^-} - \alpha - \epsilon^- + u(s,\nu_s; q_{s^-}^{q,\delta_s^-} + 1) - u(s,\nu_s; q_{s^-}^{q,\delta_s^-})\Big)\Bigg)ds\Bigg].
\end{aligned}
$$

Now, by the dominated convergence theorem [38], it can be seen that

$$
\begin{aligned}
\lim_{n\to\infty}\mathbb{E}\left[W(t_n, X^{t,x,\delta_s^\pm}_{t_n^-}, S^{t,S}_{t_n}, \nu^{t,\nu}_{t_n}; q^{t,q,\delta_s^\pm}_{t_n^-})\right] &= \mathbb{E}\left[W(T, X^{t,x,\delta_s^\pm}_{T}, S^{t,S}_{T}, \nu^{t,\nu}_{T}; q^{t,q,\delta_s^\pm}_{T})\right] \\
&= W(t,x,S,\nu;q) \\
&\quad + \mathbb{E}\Bigg[\int_t^T \Bigg(\partial_s u(s,\nu_s^{t,\nu}; q_s^{t,q,\delta_s^\pm}) \\
&\quad + k(\theta-\nu_s)\partial_\nu u(s,\nu_s^{t,\nu}; q_s^{t,q,\delta_s^\pm}) \\
&\quad + \frac{1}{2}\sigma^2\nu\partial_{\nu\nu} u(s,\nu_s^{t,\nu}; q_s^{t,q,\delta_s^\pm}) \\
&\quad + q_{s^-}(\mu+\epsilon^+-\epsilon^-) \\
&\quad + \lambda^+\Big(\delta_s^+ + 2\alpha q_{s^-} - \alpha - \epsilon^+ \\
&\quad + u(s,\nu_s; q_{s^-}^{q,\delta_s^+} - 1) - u(s,\nu_s; q_{s^-}^{q,\delta_s^+})\Big) \\
&\quad + \lambda^-\Big(\delta_s^- - 2\alpha q_{s^-} - \alpha - \epsilon^- \\
&\quad + u(s,\nu_s; q_{s^-}^{q,\delta_s^-} + 1) - u(s,\nu_s; q_{s^-}^{q,\delta_s^-})\Big)\Bigg) ds\Bigg]
\end{aligned}
$$

which holds for all the admissible controls $(\delta_t^\pm)_{t\le s\le T}$.

Using the fact that W solves that the HJB equation (3.6) and similar arguments in Theorem 2.4 in [12], we have

$$
\mathbb{E}\left[W(T, X^{t,x,\delta_s^\pm}_{T}, S^{t,S}_{T}, \nu^{t,\nu}_{T}; q^{t,q,\delta_s^\pm}_{T})\right] \le W(t,x,S,\nu;q) + \psi\sigma^2\mathbb{E}\left[\int_t^T (q_s^{q,\delta_s^\pm})^2 \nu_s^{q,\delta_s^\pm} ds\right].
$$

Therefore, we have

$$
\begin{aligned}
&\sup_{\delta_s^\pm\in\mathcal{A}_s}\mathbb{E}\left[X_T^{t,x,\delta_s^\pm} + q_T^{t,q,\delta_s^\pm}(S_T - \alpha q_T^{t,q,\delta_s^\pm}) - \psi\sigma^2\int_t^T (q_s^{q,\delta_s^\pm})^2\nu_s^{q,\delta_s^\pm} ds\right] \\
&\quad \le W(t,x,S,\nu;q) = \mathbb{E}\left[X_T^{t,x,\delta} + q_T^{t,q,\delta}(S_T - \alpha q_T^{t,q,\delta}) - \psi\sigma^2\int_t^T (q_s^{q,\delta})^2\nu_s^{q,\delta} ds\right].
\end{aligned}
$$

Hence, this proves that $W(t,x,S,\nu;q)$ is the value function of the optimization problem (3.5) and the $\delta_t^{\pm *}$ given by (3.12) are the admissible optimal controls. $\square$

3.3 HJB Equation of the Model for the Value Function Defined with Exponential Utility

The case of the exponential utility function has been investigated earlier by Avellaneda and Stoikov [3], Lehalle *et al.* [31], and Fodra and Labadie [24] for several types of midprice dynamics. In this section, we illustrate the results for the midprice model given by (3.1). Assume that the utility function is defined as exponential having a degree of risk aversion γ for the investor where $\gamma > 0$ with the following related value function:

$$W(t, x, S, \nu; q) = \sup_{(\delta_s^{\pm})_{t \leq s \leq T} \in \mathcal{A}_t} \mathbb{E}\left[-e^{-\gamma(X_T + q_T S_T + \eta(q_T))}\right], \tag{3.21}$$

where $\eta(q_T) = -\alpha q_T^2$ is the penalization function with $\alpha > 0$ as defined in Section 3.2. Now, we display out the corresponding HJB equation for the value function (3.21).

Proposition 4. The value function (3.21) satisfies the following HJB equation,

$$\begin{aligned}
&\partial_t W + \mu \partial_S W + k(\theta - \nu_t)\partial_\nu W + \frac{1}{2}\nu_t \partial_{SS} W + \frac{1}{2}\sigma^2 \nu_t \partial_{\nu\nu} W + \sigma\rho\nu_t \partial_{S\nu} W \\
&\quad + \sup_{\delta_t^+} \Big\{ \Lambda_t^+(\delta_t^+) \mathbb{E}\left[W(t, x + (S_t + \delta_t^+), S_t + \varepsilon^+, \nu_t; q - 1) - W(t, x, S_t, \nu_t; q)\right] \\
&\qquad\quad + (\lambda^+ - \Lambda_t^+(\delta_t^+)) \mathbb{E}\left[W(t, x, S_t + \varepsilon^+, \nu_t; q) - W(t, x, S_t, \nu_t; q)\right] \Big\} \\
&\quad + \sup_{\delta_t^-} \Big\{ \Lambda_t^-(\delta_t^-) \mathbb{E}\left[W(t, x - (S_t - \delta_t^-), S_t - \varepsilon^-, \nu_t; q + 1) - W(t, x, S_t, \nu_t; q)\right] \\
&\qquad + (\lambda^- - \Lambda_t^-(\delta_t^-)) \mathbb{E}\left[W(t, x, S_t - \varepsilon^-, \nu_t; q) - W(t, x, S_t, \nu_t; q)\right] \Big\} = 0,
\end{aligned} \tag{3.22}$$

with the final condition,

$$W(T, x, S, \nu; q) = -e^{-\gamma(x + q(S - \alpha q))}. \tag{3.23}$$

Proof. The proof can be carried out using similar arguments as in Proposition 1. □

For the case of the exponential utility function, now we find the optimal controls obtained by solving the HJB equation (3.22).

Proposition 5. Let

$$W(t, x, S, \nu; q) = -e^{-\gamma(x + q(S - \alpha q) + u(t, \nu; q))} \tag{3.24}$$

be a solution to the HJB equation (3.22) which is suggested by the final condition (3.23). Then, the optimal feedback controls of (3.22) are given by

$$\begin{aligned}
\delta_2^{+*}(t,\nu;q) &= \tfrac{1}{\gamma}\ln\left(1+\tfrac{\gamma}{\kappa^+}\right)+\epsilon^+ +\alpha(1-2q)-u(t,\nu;q-1)+u(t,\nu;q), \;\; q\neq \underline{q},\\
\delta_2^{-*}(t,\nu;q) &= \tfrac{1}{\gamma}\ln\left(1+\tfrac{\gamma}{\kappa^-}\right)+\epsilon^- +\alpha(1+2q)-u(t,\nu;q+1)+u(t,\nu;q), \;\; q\neq \overline{q}.
\end{aligned} \tag{3.25}$$

Proof. First, inserting the suggested solution (3.24) into (3.22) with the functions of filled orders, (3.22) is reduced to

$$\begin{aligned}
&e^{-\gamma(x+q(S-\alpha q)+u(t,\nu;q))}\Big[\gamma\partial_t u+\mu\gamma q-\frac{1}{2}\gamma^2q^2\nu+\left(k(\theta-\nu)\gamma-\sigma\rho\gamma^2q\nu\right)\partial_\nu u\\
&\qquad +\frac{1}{2}\sigma^2\gamma\nu\partial_{\nu\nu}u-\frac{1}{2}\sigma^2\gamma^2\nu(\partial_\nu u)^2\Big]\\
&+\sup_{\delta_t^+}\lambda^+\Big\{e^{-\gamma(x+q(S-\alpha q)+q\epsilon^++u(t,\nu;q))}\left(e^{-\kappa^+\delta^+}-1\right)+e^{-\gamma(x+q(S-\alpha q)+u(t,\nu;q))}\\
&\qquad -e^{-\kappa^+\delta^+}e^{-\gamma(x+q(S-\alpha q)+q\epsilon^++\delta^+-\epsilon^++\alpha(2q-1)+u(t,\nu;q-1))}\Big\}\\
&+\sup_{\delta_t^-}\lambda^-\Big\{e^{-\gamma(x+q(S-\alpha q)-q\epsilon^-+u(t,\nu;q))}\left(e^{-\kappa^-\delta^-}-1\right)+e^{-\gamma(x+q(S-\alpha q)+u(t,\nu;q))}\\
&\qquad -e^{-\kappa^-\delta^-}e^{-\gamma(x+q(S-\alpha q)-q\epsilon^-+\delta^--\epsilon^--\alpha(2q+1)+u(t,\nu;q+1))}\Big\}=0
\end{aligned} \tag{3.26}$$

for $q\in[\underline{q},\overline{q}]$ with final condition $u(T,\nu;q)=0$. Similar to the proof of Proposition 2, the optimal spreads (3.25) can be found by the first order optimality conditions. □

Substituting the optimal spreads into (3.26) yields the verification equation,

$$\begin{aligned}
\frac{1}{2}\gamma q^2\nu-\mu q &= \partial_t u+\left(k(\theta-\nu)-\sigma\rho\gamma q\nu\right)\partial_\nu u+\frac{1}{2}\sigma^2\nu\partial_{\nu\nu}u-\frac{1}{2}\sigma^2\gamma\nu(\partial_\nu u)^2\\
&\quad +\lambda^+\left\{e^{-\gamma q\epsilon^+}e^{-\kappa^+\left(\frac{1}{\gamma}\ln\left(1+\frac{\gamma}{\kappa^+}\right)+\epsilon^++\alpha(1-2q)+u(t,\nu;q)-u(t,\nu;q-1)\right)}\frac{1}{\gamma+\kappa^+}\right.\\
&\qquad \left.+\frac{1}{\gamma}\left(1-e^{-\gamma q\epsilon^+}\right)\right\}\\
&\quad +\lambda^-\left\{e^{\gamma q\epsilon^-}e^{-\kappa^-\left(\frac{1}{\gamma}\ln\left(1+\frac{\gamma}{\kappa^-}\right)+\epsilon^-+\alpha(1+2q)+u(t,\nu;q)-u(t,\nu;q+1)\right)}\frac{1}{\gamma+\kappa^-}\right.\\
&\qquad \left.+\frac{1}{\gamma}\left(1-e^{\gamma q\epsilon^-}\right)\right\}
\end{aligned} \tag{3.27}$$

for $q\in[\underline{q},\overline{q}]$ with final condition $u(T,\nu;q)=0$. Then, the following theorem can be stated.

Theorem 5. *Let $u(t,\nu;q)$ be a solution to* (3.26). *Then,*
$W(t,x,S,\nu;q) = -e^{-\gamma(x+q(S-\alpha q)+u(t,\nu;q))}$ *is the value function for the control problem* (3.21) *and, moreover, the optimal controls are given by* (3.25).

Proof. The proof can be carried out using the similar techniques as done in Theorem 4. □

In the following proposition, we show that how the optimal behaviour of the investor changes when she uses the exponential utility measure in case of the uncertainty in the trades. In fact, this strategy is retrieved as the strategy introduced in Section (3.2.1.1) when $\gamma \to 0^+$.

Proposition 6. If the running inventory penalty parameter ψ and the risk aversion degree parameter γ fulfill the condition

$$\psi = \frac{1}{2\sigma^2}\gamma,$$

then $\delta_2^{\pm *}(t,\nu;q) \to \delta_1^{\pm *}(t,\nu;q)$ holds as $\gamma \to 0^+$.

Proof. We observe that

$$\lim_{\gamma\to 0^+} \frac{1}{\gamma}\ln\left(1+\frac{\gamma}{\kappa^\pm}\right) = \frac{1}{\kappa^\pm}$$

and

$$\lim_{\gamma\to 0^+} \frac{1}{\gamma}\left(1-e^{\mp\gamma q\epsilon^\pm}\right) = \pm q\epsilon^\pm$$

hold, thus it can be easily seen that the verification equation obtained by $\delta_2^{\pm *}$, that is,

$$\begin{aligned}
\frac{1}{2}\gamma q^2\nu - \mu q = {} & \partial_t u + \left(k(\theta-\nu) - \sigma\rho\gamma q\nu\right)\partial_\nu u + \frac{1}{2}\sigma^2\nu\partial_{\nu\nu}u - \frac{1}{2}\sigma^2\gamma\nu(\partial_\nu u)^2 \\
& + \lambda^+\left\{e^{-\gamma q\epsilon^+}e^{-\kappa^+\left(\frac{1}{\gamma}\ln\left(1+\frac{\gamma}{\kappa^+}\right)+\epsilon^+ +\alpha(1-2q)+u(t,\nu;q)-u(t,\nu;q-1)\right)}\frac{1}{\gamma+\kappa^+}\right. \\
& \qquad \left. + \frac{1}{\gamma}\left(1-e^{-\gamma q\epsilon^+}\right)\right\} \\
& + \lambda^-\left\{e^{\gamma q\epsilon^-}e^{-\kappa^-\left(\frac{1}{\gamma}\ln\left(1+\frac{\gamma}{\kappa^-}\right)+\epsilon^- +\alpha(1+2q)+u(t,\nu;q)-u(t,\nu;q+1)\right)}\frac{1}{\gamma+\kappa^-}\right. \\
& \qquad \left. + \frac{1}{\gamma}\left(1-e^{\gamma q\epsilon^-}\right)\right\}
\end{aligned}$$

is identical to the verification equation obtained by $\delta_1^{\pm *}$, that is,

$$\begin{aligned}\psi\nu q^2\sigma^2 - \mu q = \partial_t u + k(\theta-\nu)\partial_\nu u + \frac{1}{2}\sigma^2\nu\partial_{\nu\nu}u \\ + \lambda^+\left[q\epsilon^+ + \frac{1}{\kappa^+}e^{-1-\kappa^+(\epsilon^+ + \alpha(1-2q) - u(t,\nu;q-1)+u(t,\nu;q))}\right] \\ + \lambda^-\left[-q\epsilon^- + \frac{1}{\kappa^-}e^{-1-\kappa^-(\epsilon^- + \alpha(1+2q) - u(t,\nu;q+1)+u(t,\nu;q))}\right]\end{aligned}$$

as $\gamma \to 0^+$ and $\psi = \frac{1}{2\sigma^2}\gamma$. Therefore, the solution $u(t,\nu;q)$ for both strategies are the same. Thus, denoting $\frac{1}{\hat{\kappa}^\pm} = \frac{1}{\gamma}\ln\left(1+\frac{\gamma}{\kappa^\pm}\right)$, we have

$$\delta_2^{\pm *}(t,\nu;q) - \delta_1^{\pm *}(t,\nu;q) = \frac{1}{\hat{\kappa}^\pm} - \frac{1}{\kappa^\pm}.$$

Since $\lim\limits_{\gamma\to 0^+}\frac{1}{\hat{\kappa}^\pm} = \frac{1}{\kappa^\pm}$, we have $\delta_2^{\pm *}(t,\nu;q) \to \delta_1^{\pm *}(t,\nu;q)$ as $\gamma \to 0^+$. The value function of the model with quadratic utility function can be also retrieved by the transformation

$$\begin{aligned}\sup_{(\delta_s^\pm)_{t\le s\le T}\in\mathcal{A}_t} \mathbb{E}\left[X_T + q_T S_T + \eta(q_T) - \psi\sigma^2\int_t^T q_s^2\nu_s ds\right] \\ = -\frac{1}{\gamma}\ln\left(\sup_{(\delta_s^\pm)_{t\le s\le T}\in\mathcal{A}_t}\mathbb{E}\left[-e^{-\gamma(X_T+q_TS_T+\eta(q_T))}\right]\right)\end{aligned}$$

for $\psi = 0$. The result follows from these relationships. □

Figure 3.1 demonstrates the change in $\delta_2^+ - \delta_1^+$ as $\gamma \to 0^+$ for both strategies with quadratic and exponential utility measures with the parameters given in Table 3.1. It is observed that the difference between the optimal spreads for both strategies decreases approaching to zero when γ approaches to zero.

3.4 Effect of the Jumps in Volatility in a LOB model

Now, as another extension of a stock price impact on optimal market making problem, we work on the problem that the stochastic volatility of the asset is influenced by the arrival of market orders and perform this case on the optimal trading prices. The models in literature assume that the stock price is followed by mostly Brownian motion with constant volatility, and in the cases of stochastic volatility, they consider only a diffusive volatility. Picking up the volatility as diffusive is highly permanent

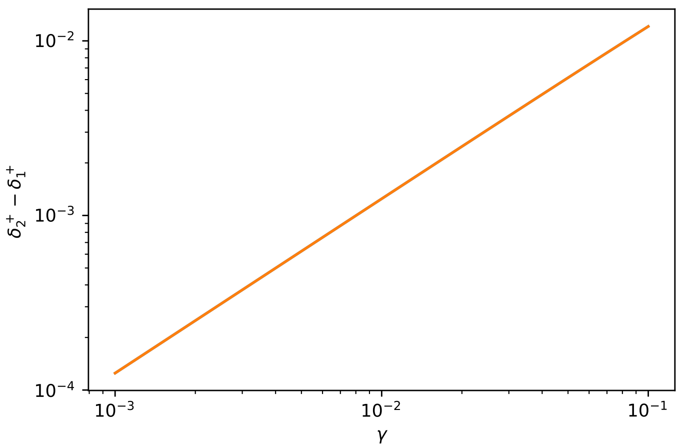

Figure 3.1: Difference between the optimal sell spreads for different γ values

but this dynamics can allow the increments to increase only by a sequence of normally distributions. On the other hand, models with jumps in volatility are more persistent as the jumps fill in the gap between the stock prices and diffusive volatility supplying quick moves to increase the volatility and experiments show that diffusive volatility without jumps causes misdefined effects on prices [20].

Therefore, in this part we consider that the volatility of the asset is stochastic and impacted by the orders including the jump processes as follows:

$$\begin{aligned} dS_t &= \mu dt + \sqrt{\nu_t} dB_t^1, \\ d\nu_t &= k(\theta - \nu_t)dt + \sigma\sqrt{\nu_t} dB_t^2 + \varepsilon^+ dM_t^+ - \varepsilon^- dM_t^-, \\ dB_t^1 dB_t^2 &= \rho dt, \end{aligned} \tag{3.28}$$

with the same assumptions and quadratic utility function as in Case 1 in Section 3.2.1.1. Therefore, the corresponding HJB equation can be obtained by applying the stochastic control approach.

Proposition 7. The value function (3.5) satisfies the HJB equation,

$$\begin{aligned}
&\partial_t W + \mu \partial_S W + k(\theta - \nu_t)\partial_\nu W + \frac{1}{2}\nu_t \partial_{SS} W + \frac{1}{2}\sigma^2 \nu_t \partial_{\nu\nu} W + \sigma\rho\nu_t \partial_{S\nu} W - \psi \nu_t q^2 \sigma^2 \\
&+ \sup_{\delta_t^+} \Big\{ \Lambda_t^+(\delta_t^+) \mathbb{E}\left[W(t, x + (S_t + \delta_t^+), S_t, \nu_t + \varepsilon^+; q-1) - W(t, x, S_t, \nu_t; q) \right] \\
&\qquad + (\lambda^+ - \Lambda_t^+(\delta_t^+)) \mathbb{E}\left[W(t, x, S_t, \nu_t + \varepsilon^+; q) - W(t, x, S_t, \nu_t; q) \right] \Big\} \\
&+ \sup_{\delta_t^-} \Big\{ \Lambda_t^-(\delta_t^-) \mathbb{E}\left[W(t, x - (S_t - \delta_t^-), S_t, \nu_t - \varepsilon^-; q+1) - W(t, x, S_t, \nu_t; q) \right] \\
&\qquad + (\lambda^- - \Lambda_t^-(\delta_t^-)) \mathbb{E}\left[W(t, x, S_t, \nu_t - \varepsilon^-; q) - W(t, x, S_t, \nu_t; q) \right] \Big\} = 0, \quad (3.29)
\end{aligned}$$

with the final condition,

$$W(T, x, S, \nu; q) = x + q(S - \alpha q),$$

where the jump effects in volatility can be properly noticed.

Proof. The proof can be handled similarly as the proof of Proposition 1. □

Proposition 8. The optimal spreads related to the problem (3.29) are given by

$$\begin{aligned}
\delta_3^{+*}(t, \nu; q) &= \tfrac{1}{\kappa^+} + \alpha(1 - 2q) - u(t, \nu + \epsilon^+; q - 1) + u(t, \nu + \epsilon^+; q), \quad q \neq \underline{q}, \\
\delta_3^{-*}(t, \nu; q) &= \tfrac{1}{\kappa^-} + \alpha(1 + 2q) - u(t, \nu - \epsilon^-; q + 1) + u(t, \nu - \epsilon^-; q), \quad q \neq \overline{q}.
\end{aligned} \quad (3.30)$$

Proof. We use the same ansatz in the HJB equation (3.29), that is (3.11). Then, it can be deduced that

$$\begin{aligned}
\psi\nu q^2\sigma^2 - \mu q = \partial_t u &+ k(\theta - \nu)\partial_\nu u + \frac{1}{2}\sigma^2\nu\partial_{\nu\nu} u \\
&+ \sup_{\delta_t^+} \lambda^+ \Big\{ [u(t, \nu + \epsilon^+; q) - u(t, \nu; q)] \\
&+ e^{-\kappa^+\delta^+}(\delta^+ - \alpha(1 - 2q) + u(t, \nu + \epsilon^+; q - 1) - u(t, \nu + \epsilon^+; q)) \Big\} \\
&+ \sup_{\delta_t^-} \lambda^- \Big\{ [u(t, \nu - \epsilon^-; q) - u(t, \nu; q)] \\
&+ e^{-\kappa^-\delta^-}(\delta^- - \alpha(1 + 2q) + u(t, \nu - \epsilon^-; q + 1) - u(t, \nu - \epsilon^-; q)) \Big\}
\end{aligned} \quad (3.31)$$

for $q \in [\underline{q}, \overline{q}]$ with final condition $u(T, \nu; q) = 0$.

Hence, the optimal spreads (3.30) which maximize the supremums in the equation (3.31) can be properly defined to conclude the proof. □

Furthermore, the verification equation that we will calculate the solution $u(t,\nu;q)$ with can be interpreted as

$$\begin{aligned}\psi\nu q^2\sigma^2-\mu q=\partial_t u+k(\theta-\nu)\partial_\nu u+\frac{1}{2}\sigma^2\nu\partial_{\nu\nu}u\\ +\lambda^+\Big\{[u(t,\nu+\epsilon^+;q)-u(t,\nu;q)]\\ +\frac{1}{\kappa^+}e^{-1-\kappa^+(\alpha(1-2q)-u(t,\nu+\epsilon^+;q-1)+u(t,\nu+\epsilon^+;q))}\Big\}\\ +\lambda^-\Big\{[u(t,\nu-\epsilon^-;q)-u(t,\nu;q)]\\ +\frac{1}{\kappa^-}e^{-1-\kappa^-(\alpha(1+2q)-u(t,\nu-\epsilon^-;q+1)+u(t,\nu-\epsilon^-;q)}\Big\}\end{aligned} \tag{3.32}$$

for $q\in[\underline{q},\overline{q}]$ with final condition $u(T,\nu;q)=0$.

3.5 Numerical Results

In this section, we provide the numerical results regarding on the solution of the market making problems given in Sections 3.2, 3.3, and 3.4, and explore the behaviour of the optimal controls δ^{+*} and δ^{-*} for various cases. The parameters that we use in the following analyses are given in Table 3.1.

Table 3.1: The Parameters

T (sec)	Δt	S_0	ν_0	q	$\lambda^\pm$	$\epsilon^\pm$	$\kappa^\pm$	α	ψ	μ	k	θ	σ	ρ
10	0.005	100	0.05	$[-5,5]$	2	0.004	2	0.01	0.1	0.01	1	1	0.1	-0.8

The codes for solving the verification equations of the related HJBs of the models have been written in Spyder Editor of Python Programming Language using the libraries numpy, matplotlib, and scipy [51].

3.5.1 Results with the Quadratic Utility Function

In this part of the numerical applications, we provide the results under two cases where the suggested solution u includes and does not include the effect of the stochastic volatility explicitly, respectively.

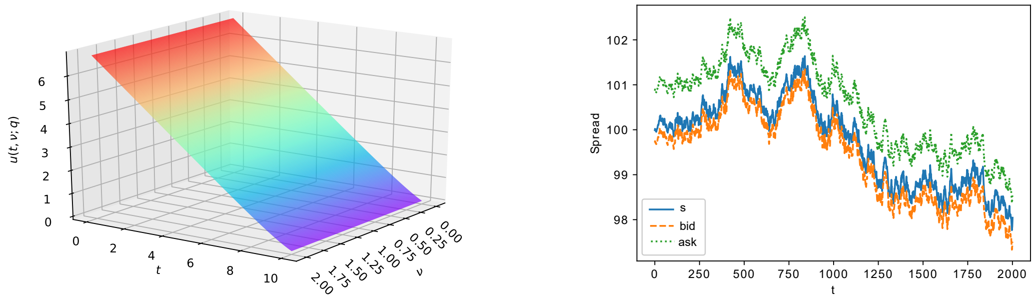

Figure 3.2: Solution of $u(t, \nu; q)$ for $q = 0$ and optimal prices

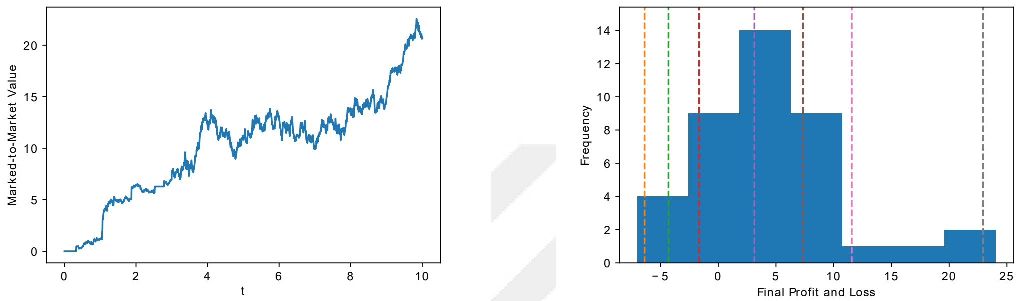

Figure 3.3: A simulated path and histogram of the profit and loss function

3.5.1.1 Results for Case 1

This part intends to show the numerical experiments and the behaviour of the market maker under the results given in Section 3.2.1.1.

Figure 3.2 displays the solution of the value function $u(t, \nu; q)$ for a fixed inventory level q in the left panel. It is shown that the values of u reduces when t approaches to the final time with a fixed value of ν. The figure in the right panel illustrates how the optimal prices which are calculated by the spread formulas in (3.12) change by the strategy. We can see that the strategy is followed as that the trader buys an asset with lower spread and closer price to the midprice while she sells the asset putting higher sell spread and farther price.

Figure 3.3 depicts a simulation of the profit and loss function (PnL) of the market maker at any time t during the trading session in the left panel. The profit and loss performance of the trading are displayed by the histogram in the right panel which is a right skewed distribution. From the Figure 3.3, it is observed that the adverse selection effect in stock prices improves the profitability of the market making strategy.

In Figure 3.4, a simulated path of the inventory process of the trader can be seen for $q \in [-10, 10]$ while the other parameters are fixed as in Table 3.1. It is demonstrated that the trading first occurs when $t \in [0, 1]$ in seconds with buy limit orders and the inventory increases until time $t \in [2, 3]$ in seconds. Another noticeable fact from the figure is that the market buy orders are filled by limit sell orders after the 5th second and then the inventory becomes mean-reverting to zero.

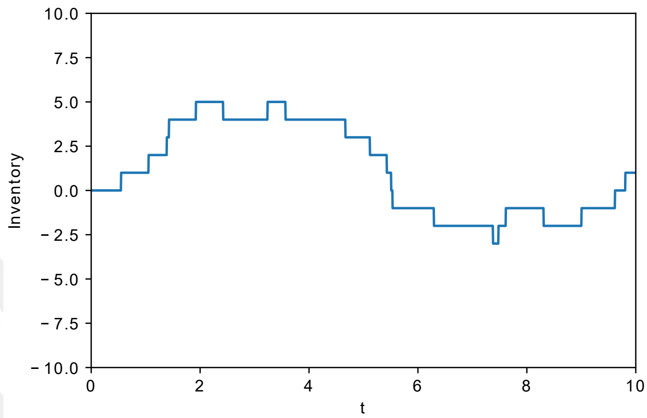

Figure 3.4: A simulated path for inventory process

In Figure 3.5, we can see the optimal spreads δ^+ and δ^- for the trader depending on the each inventory levels monotonically with the liquidation parameter $\alpha = 0.01$ which is a small inventory risk aversion value but enough for the inventory to go back to the average at the end of the trading.

On the negative inventory levels, δ^+ values are larger when $t < T$ since the selling is getting forbidden when approaching to the minimum admitted inventory value so that the trader may sell her assets only if she gets a large premium for selling. As t approaches to T, it is observed that the sell spreads decrease since the trader wants to get rid off her assets rather than paying for the liquidation penalization when the trading ends. On the positive inventory levels, the qualitative behaviour of the trader is just the opposite of the idea for the negative inventory levels. In this case, the trader needs to reduce the number of shares at her hand in order not to have any remaining assets at maturity to sell them with lower price. As the time approaches to T, the trader increases the selling spread since the probability of selling assets at maturity time is higher than that for the time far away from T. Similar interpretation can be adapted for the optimal buy spread δ^- (see Fig. 3.5(b)).

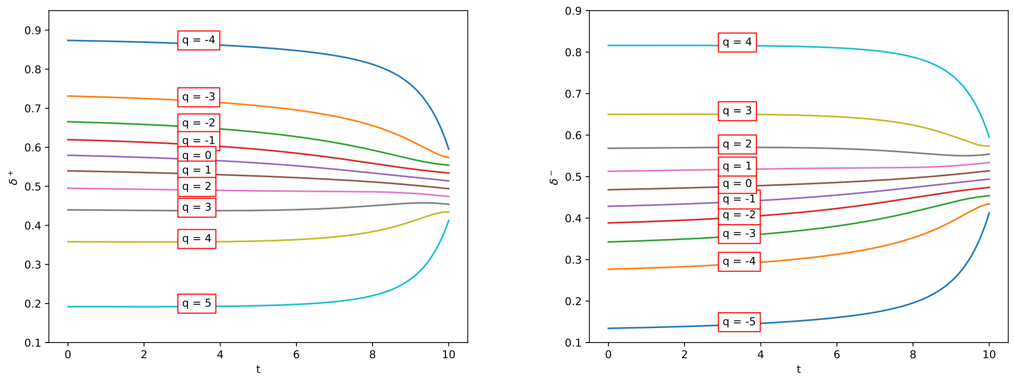

(a) δ^+

(b) δ^-

Figure 3.5: Optimal spreads δ^+ and δ^-

Figure 3.6 is an observation of the optimal prices when the jump amounts are larger, i.e., $\epsilon^{\pm} = 1$ while the other model parameters are kept the same. The impact of the large jump sizes can be obviously noticed by the big jumps in the prices. In this case, it can be also observed that the execution is carried out with very close optimal buy and sell prices to the midprice of the asset.

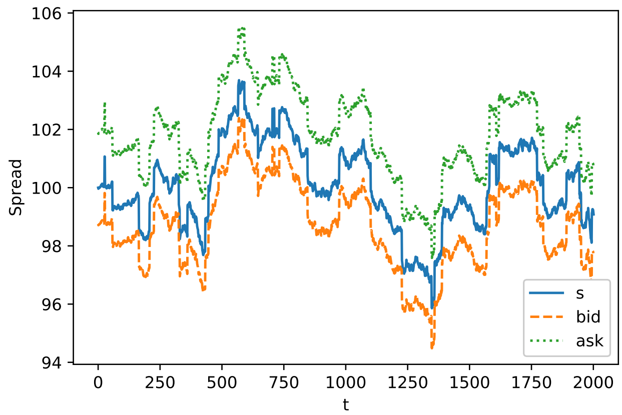

Figure 3.6: Optimal prices for $\epsilon^{\pm} = 1$

Figure 3.7 depicts the trading intensities $\lambda^{\pm} e^{-\kappa^{\pm}\delta_t^{\pm}}$ for each inventory level. It is a fact that the value of a stock price is inversely correlated with the trading intensity. In Figure 3.7, it can be seen that the trading intensity for selling is higher on positive inventory levels while it is the opposite situation on negative inventory levels.

Figure 3.8 presents the δ^+ and δ^- values when the arrival of the market orders is asymmetric. The intensities $\lambda^{\pm}$ of the jump processes in asset price give us the in-

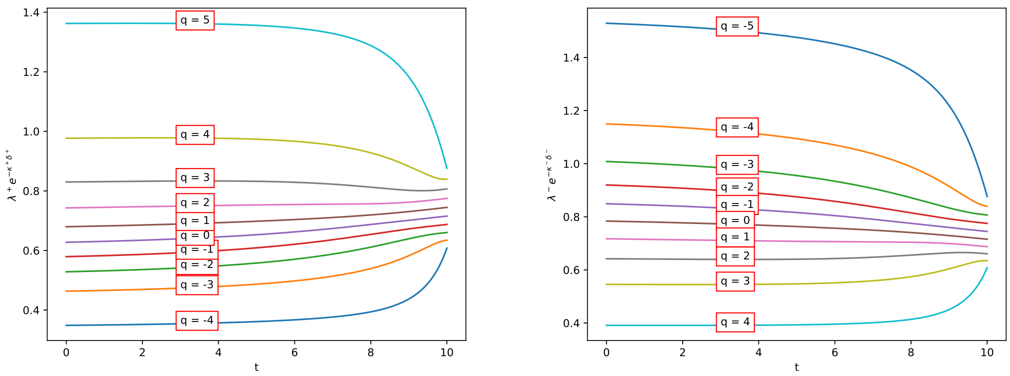

(a) $\lambda^{+}e^{-\kappa^{+}\delta^{+}}$ (b) $\lambda^{-}e^{-\kappa^{-}\delta^{-}}$

Figure 3.7: Trading intensities

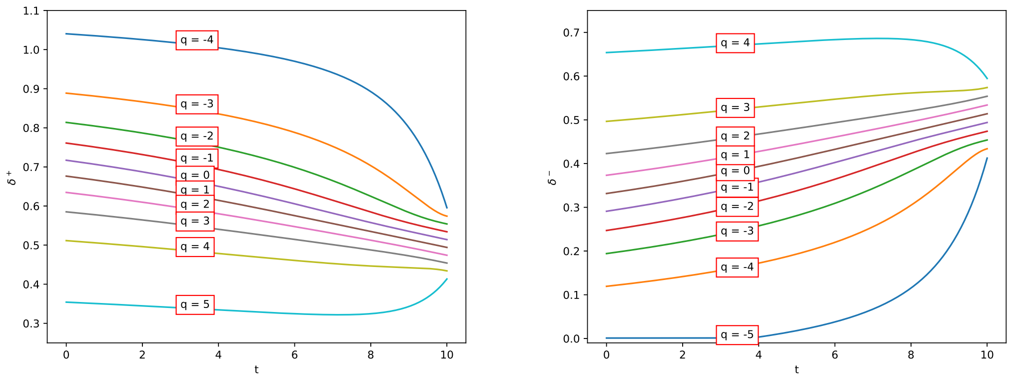

(a) δ^{+} (b) δ^{-}

Figure 3.8: Optimal spreads δ^{+} and δ^{-} for $\lambda^{+} = 2$ and $\lambda^{-} = 1$

formation about the number of market order arrivals. For $\lambda^{+} = 2$ and $\lambda^{-} = 1$ while the other parameters are fixed to those in Table 3.1, we see that there are more buy market orders arriving, thus the optimal filled sell spreads are larger for all inventory levels comparing to the case when the arrival of the market orders is symmetric.

Figure 3.9 displays how δ^{+} and δ^{-} are affected by the amount of the different jump increments ϵ^{+} and ϵ^{-} keeping the rest of the parameters as fixed. A larger ϵ^{+} increment means that more buy market orders arrive and filled by sell orders which causes larger spreads.

In our simulations, we conduct the analyses with proposed risk metrics for HFT which measure the performance of the trader, the final inventory level and their standard

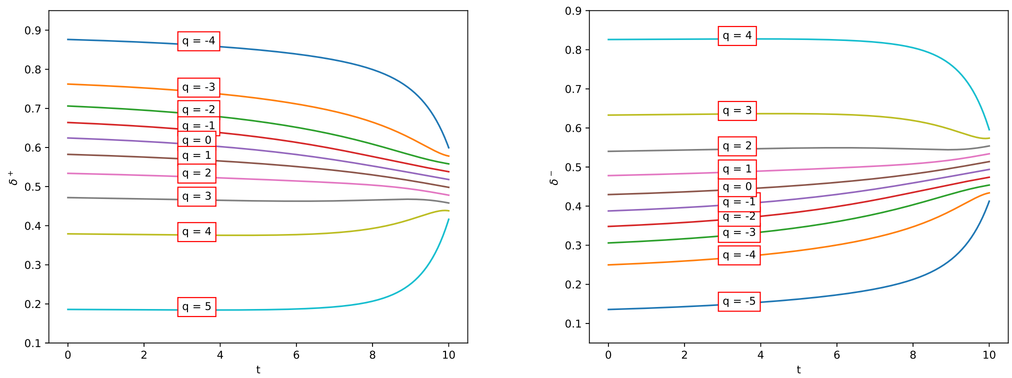

(a) δ^+ (b) δ^-

Figure 3.9: Optimal spreads δ^+ and δ^- for $\epsilon^+ = 0.008$ and $\epsilon^- = 0.004$

deviation which are presented in [12]. For this purpose, we investigate PnL of the trader, its standard deviation, final q, and its standard deviation, as well.

It is observed in Table 3.2 that when we compare our strategy with symmetric strategy that distributes the optimal prices symmetrically around the midprice as done in [3], the profit of the strategy is less than that of the symmetric strategy; on the other hand, it has a lower standard deviation comparing to the symmetric strategy. It can be also seen that the inventory of the trader reverts to zero more quickly than the symmetric strategy and the standard deviation of the inventory is produced less in the strategy.

Table 3.2: Comparison of the strategy with symmetric strategy

	PnL	Std dev of PnL	Final q	Std dev of q
Inventory	3.55	6.24	0.05	2.19
Symmetric	7.95	8.94	-1.51	3.66

We note that when we have $\epsilon^+ = \epsilon^- = 0$ in the model, then it reduces to the Heston stochastic volatility model without jumps. The average spread is found as 1.0402 for the model (3.1) while it is 1.0322 for the model without jumps. We thereby observe that the optimal spread values are higher in the model with jumps (3.1) than those of the model without jumps. In Table 3.3, it is obviously seen that the model with jumps produces larger sell spreads rather than the model without jumps.

Table 3.3: Comparison of two models with jumps and without jumps by the sell spread value $\delta^+(0, \nu_0; q)$

q	Model with jumps	Model without jumps
-4	0.871229	0.867018
-3	0.728921	0.724657
-2	0.663699	0.659419
-1	0.618563	0.614285
0	0.579359	0.575092
1	0.540146	0.535898
2	0.496423	0.492200
3	0.441696	0.437508
4	0.360644	0.356499
5	0.194442	0.190347

Comparative statistics

In this section, we investigate the comparative statistics results of the strategy that we introduce in Section 3.2.1.1.

Table 3.4 presents some significant statistical properties of the strategy in terms of its terminal wealth. The Sharpe ratio which is the return per unit risk, i.e., mean over the standard deviation is found to be 1.0156 for the profit and loss of the trader expressing that we can have an attractive trading performance. We also reveal the skewness and kurtosis values to discover the degree of the normality violation of the distribution. The skewness parameter characterizes the lack of the symmetry that gets the importance because of the fact that the statistical theory generally uses the normal distribution assumption. Meanwhile, the kurtosis parameter refers to the sharpness and height of the central peak of the distribution. By the skewness and kurtosis values given in Table 3.4, we can say that the profit and loss function for this trading session by the strategy have a normal distribution since the values lie in the acceptable range for the normality.

Table 3.4: Statistics of profit-loss (PnL) function

Sharpe ratio	Skewness	Kurtosis
1.0156	-0.5506	0.1716

According to Table 3.5, we may conclude that the inventory approximates to the normal distribution which can be also observed by the histogram of the inventory in Figure 3.10.

Table 3.5: Statistics of inventory

Sharpe ratio	Skewness	Kurtosis
0.3146	-0.4070	0.8640

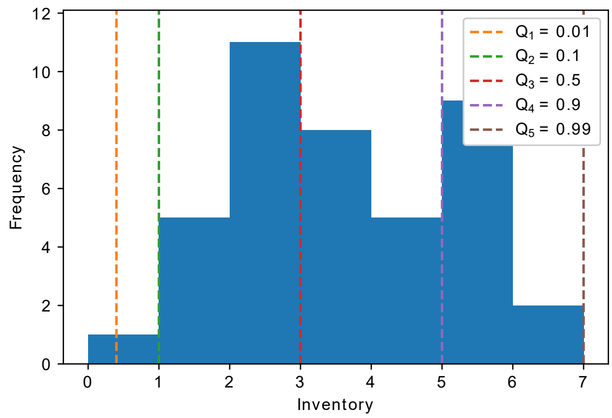

Figure 3.10: Histogram of inventory

By the statistics of the spread $\delta^+ + \delta^-$, as we observe in Table 3.6, it can be deduced that the Sharpe ratio attracts the trader as it is very high since the standard deviation is very low while it has a good expected return. Moreover, the spread can also be considered to be normally distributed due to its skewness and kurtosis values.

Table 3.6: Statistics of spread

Mean	Std dev	Sharpe ratio	Skewness	Kurtosis
1.0402	0.0071	145.8895	-0.4318	-1.3139

Sensitivity to parameters

As we have discussed the behaviours of the optimal spreads and some statistical properties of wealth and inventory processes of the trading in previous part of this section, now we carry out the dependency and sensitivity of the parameters on the optimal spreads and explore the related results in this part.

Effects of μ

By the interpretation of the drift constant and its effect on the optimal spreads and prices, we expect the dependence on μ as

$$\frac{\partial \delta_t^+}{\partial \mu} > 0, \quad \frac{\partial \delta_t^-}{\partial \mu} < 0$$

for all q. We implement our numerical simulations with changing drift constant μ in the set of values $\{-0.01, 0.01, 0.02\}$ as the other parameters in Table 3.1 remain the same.

In Table 3.7, we observe that the optimal sell prices increase when the drift parameter μ increases as the trader expects the price to move up, she sends the orders at higher prices to get profit from the price increase which meets with our expectation.

Table 3.7: Effects of μ on $\delta^+(0, \nu_0; q)$

q	$\mu = -0.01$	$\mu = 0.01$	$\mu = 0.02$
-4	0.813558	0.871229	0.904113
-3	0.647356	0.728921	0.774198
-2	0.566304	0.663699	0.715821
-1	0.511577	0.618563	0.673648
0	0.467854	0.579359	0.634654
1	0.428641	0.540146	0.593511
2	0.389437	0.496423	0.545960
3	0.344301	0.441696	0.485475
4	0.279079	0.360644	0.396444
5	0.136771	0.194442	0.219440

Effects of ψ

Turning to the constant ψ for the penalization of the variations, it can be seen that the optimal sell quotes increase when the risk of penalizing volatilities increases on the negative inventory levels. Eventually, since the trader wants to cover her cost for the variations during the trading, the increase of optimal prices make sense to cover these costs by these amounts. Hence, the following behaviour on optimal spreads is expected:

$$\begin{cases} \frac{\partial \delta_t^+}{\partial \psi} > 0, & \frac{\partial \delta_t^-}{\partial \psi} < 0, \qquad q < 0, \\ \frac{\partial \delta_t^+}{\partial \psi} < 0, & \frac{\partial \delta_t^-}{\partial \psi} > 0, \qquad q = 0, \\ \frac{\partial \delta_t^+}{\partial \psi} < 0, & \frac{\partial \delta_t^-}{\partial \psi} > 0, \qquad q > 0. \end{cases}$$

As we execute our simulations with changing ψ parameter where $\psi \in \{0, 0.01, 0.1\}$ while saving the other parameters the same as given in the Table 3.1, our above expectation matches with the given results in Table 3.8.

Table 3.8: Effects of ψ on $\delta^+(0, \nu_0; q)$

q	$\psi = 0$	$\psi = 0.01$	$\psi = 0.1$
-4	0.862326	0.863225	0.871229
-3	0.718769	0.719799	0.728921
-2	0.655405	0.656251	0.663699
-1	0.614095	0.614550	0.618563
0	0.579601	0.579573	0.579359
1	0.545067	0.544560	0.540146
2	0.505219	0.504319	0.496423
3	0.452891	0.451754	0.441696
4	0.372143	0.370983	0.360644
5	0.203594	0.202676	0.194442

The optimal average spread is therefore affected by the values of ψ where it can be observed in Table 3.9. When the penalty parameter value increases, the average spread increases, as well. This result leads a more traded stock because of the less spread in case of there is no penalty.

Table 3.9: Effects of ψ on average spread

$\psi = 0$	$\psi = 0.01$	$\psi = 0.1$
1.0353	1.0358	1.0402

Effects of k

k represents the mean reversion adjustment rate on the volatility of the model. A large value of k means that the volatility will revert to the average mean faster which increases the optimal spreads for $q > 0$ and reduces them for $q < 0$.

$$\begin{cases} \frac{\partial \delta_t^+}{\partial k} > 0, & \frac{\partial \delta_t^-}{\partial k} < 0, \qquad q < 0, \\ \frac{\partial \delta_t^+}{\partial k} > 0, & \frac{\partial \delta_t^-}{\partial k} > 0, \qquad q = 0, \\ \frac{\partial \delta_t^+}{\partial k} < 0, & \frac{\partial \delta_t^-}{\partial k} > 0, \qquad q > 0. \end{cases} \tag{3.33}$$

In our numerical observations, we take $k \in \{1, 2, 3\}$ while we do not change the rest of the parameters in Table 3.1 and we observe our expectations in the experiments which can be tracked by Table 3.10, in coherence with (3.33).

Table 3.10: Effects of k on $\delta^{+}(0,\nu_0;q)$

q	$k=1$	$k=2$	$k=3$
-4	0.871229	0.873093	0.873933
-3	0.728921	0.73084	0.731654
-2	0.663699	0.665215	0.665841
-1	0.618563	0.619470	0.619846
0	0.579359	0.579581	0.579687
1	0.540146	0.539676	0.539510
2	0.496423	0.495307	0.494880
3	0.441696	0.440047	0.439389
4	0.360644	0.358687	0.357865
5	0.194442	0.192607	0.191778

In the model, since k is just in the multiplication with long-term variance parameter θ, the impact of θ on the optimal quotes will have just the opposite effect of when k is employed.

Effects of σ

Concerning σ, the dependence of optimal spreads is very obvious because a high variance causes an uncertainty and price risk. To reduce this risk and for the higher cost of the variations, the trader increases the prices of the orders. The following result is expected when dependency of σ is considered:

$$\begin{cases} \frac{\partial \delta_t^+}{\partial \sigma} > 0, & \frac{\partial \delta_t^-}{\partial \sigma} < 0, \qquad q < 0, \\ \frac{\partial \delta_t^+}{\partial \sigma} < 0, & \frac{\partial \delta_t^-}{\partial \sigma} > 0, \qquad q > 0. \end{cases}$$

In our numerical simulations, we take $\sigma \in \{0.1, 0.3, 0.5\}$ while keeping the rest of the parameters the same as given in the Table 3.1 and we see that our expectation on changing σ values is met which is shown in Table 3.11.

Effects of α

Now, we work on the dependency of the optimal spreads with respect to the liquidation penalty parameter α. By our numerical results, we observe that the optimal spreads behave in different sense when t approaches to the final trading time with an increasing values of α. Since this parameter refers to the liquidation penalty for the remaining inventories, the trader changes her behaviour at the end of the trade session

Table 3.11: Effects of σ on $\delta^+(0, \nu_0; q)$

q	$\sigma = 0.1$	$\sigma = 0.2$	$\sigma = 0.3$
-4	0.871229	0.896786	0.935502
-3	0.728921	0.757412	0.798962
-2	0.663699	0.686574	0.719139
-1	0.618563	0.630920	0.648724
0	0.579359	0.579104	0.579832
1	0.540146	0.527254	0.510663
2	0.496423	0.472619	0.440225
3	0.441696	0.410499	0.366031
4	0.360644	0.327646	0.278247
5	0.194442	0.167529	0.125368

when α increases. We carry out the simulations with $\alpha \in \{0, 0.001, 0.01\}$ while the other parameters are kept the same as in the Table 3.1.

We investigate the effect of α on the optimal spreads by choosing three specific trade time, that are $t = 0$, $t = 5$, and $t = 10$, respectively, since the behaviour of the trader changes with the trade time in terms of the liquidation cost. In this analysis, we explore the results for all inventory levels and ν_0.

At time $t = 0$, our results show that the change of the optimal spreads does not follow a monotonic way. On the other hand, at time $t = 5$ and $t = 10$, we observe the following behaviour of the optimal spreads:

$$\begin{cases} \frac{\partial \delta_t^+}{\partial \alpha} > 0, & \frac{\partial \delta_t^-}{\partial \alpha} < 0, \qquad q < 0, \\ \frac{\partial \delta_t^+}{\partial \alpha} > 0, & \frac{\partial \delta_t^-}{\partial \alpha} > 0, \qquad q = 0, \\ \frac{\partial \delta_t^+}{\partial \alpha} < 0, & \frac{\partial \delta_t^-}{\partial \alpha} > 0, \qquad q > 0. \end{cases}$$

This result makes sense since the trader should also cover the liquidation cost while selling her assets when $q < 0$, for example. On the other hand, the optimal sell spreads get to decrease when $q > 0$ since it is optimal to post low prices not to have any remaining inventories and pay for the liquidation cost. Therefore, we notice that as the time passes and approaches to the final time, the trader behaves monotonically for an increasing α value on the positive and negative inventory levels, respectively.

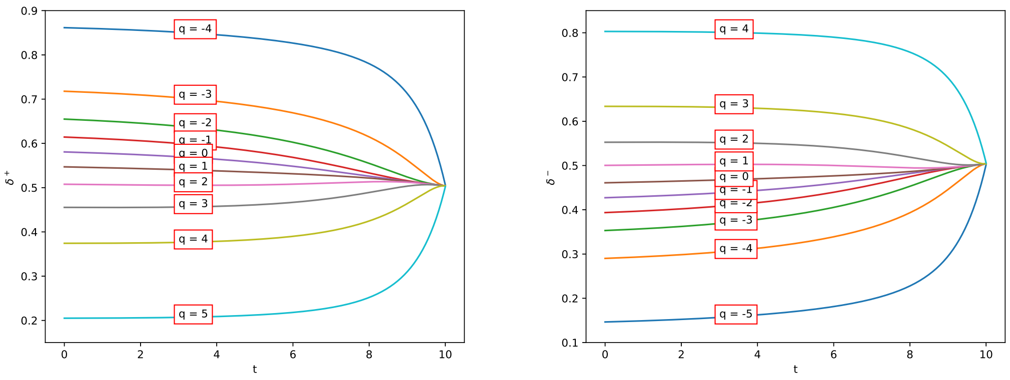

(a) δ^+ (b) δ^-

Figure 3.11: Optimal spreads δ^+ and δ^- for $\alpha = 0, \psi = 0$.

Approaching terminal time strategy

It is worth mentioning that the trader changes her qualitative behaviour depending on the liquidation and penalizing variations of the constants and her positions on inventories as the time approaches to maturity.

For the parameters $\alpha = 0$, $\psi \in \{0, 0.1\}$ when $\epsilon^{\pm} = \epsilon, \kappa^{\pm} = \kappa$ and keeping the rest of the parameters the same, we observe the following behaviour for the optimal spreads:

$$\begin{cases} \lim\limits_{t \to T} \frac{\partial \delta_t^+}{\partial t} > 0, & \lim\limits_{t \to T} \frac{\partial \delta_t^-}{\partial t} < 0, \qquad q > 0, \\ \lim\limits_{t \to T} \frac{\partial \delta_t^+}{\partial t} < 0, & \lim\limits_{t \to T} \frac{\partial \delta_t^-}{\partial t} > 0, \qquad q \leq 0. \end{cases}$$

Figure 3.11 represents the behaviour of the trader for $\alpha = 0, \psi = 0$ when the strategy approaches to the terminal time. In this case, since there are no penalizing parameters, it is easy to understand that the spreads converge to a specific value when $t \to T$.

Remark 5. Note that when $\alpha = 0$, all the optimal spreads converge to the value of $\frac{1}{\kappa^{\pm}} + \epsilon^{\pm}$ as $u(t, \nu; q) - u(t, \nu; q \pm 1)$ tends to zero.

Now, we test the effect of the existing liquidation penalty parameter with the penalty of the variations on the optimal spreads. For being $\alpha = 0.1, \psi \in \{0, 0.1\}$ when $\epsilon^{\pm} = \epsilon, \kappa^{\pm} = \kappa$ having the same values of the other parameters, the following observation

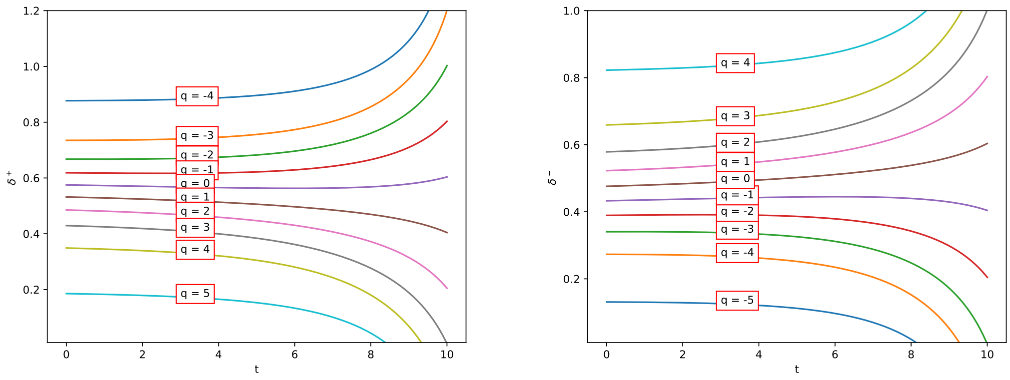

(a) δ^+ (b) δ^-

Figure 3.12: Optimal spreads δ^+ and δ^- for $\alpha = 0.1, \psi = 0.1$.

can be tested:

$$\begin{cases} \lim\limits_{t\to T} \frac{\partial \delta_t^+}{\partial t} < 0, & \lim\limits_{t\to T} \frac{\partial \delta_t^-}{\partial t} > 0, \qquad q > 0, \\ \lim\limits_{t\to T} \frac{\partial \delta_t^+}{\partial t} > 0, & \lim\limits_{t\to T} \frac{\partial \delta_t^-}{\partial t} < 0, \qquad q < 0. \end{cases}$$

Figure 3.12 highlights how the trader behaves when there are liquidation and variations penalty factor such that $\alpha = 0.1$ and $\psi = 0.1$ while the strategy approaches to the terminal time. In this case, the trader should be more cautious since she may have to pay for the liquidating and running variations if she still has the assets at maturity time. Therefore, she increases the optimal sell spreads when $q < 0$ to cover these costs; on the other hand, she reduces the spreads as she is not willing to pay the costs when she has enough assets at hand. It is noticed that the model is efficient as the trader can pay for the liquidation cost until to $\alpha = 0.1$ parameter value without any difficulty.

3.5.1.2 Results for Case 2

Now, the representation for the solution of u and the optimal spreads in the case given in Section 3.2.1.2 are provided in this part using the same parameters in Table 3.1.

In Figure 3.13, the solution of $u(t; q)$ for each inventory level and the optimal prices which are calculated by the formulas (3.19) are shown. Since the effect of the volatility does not seem in the solution of u in this case, the optimal prices distribute almost symmetrically around the midprice which can be observed from the figure.

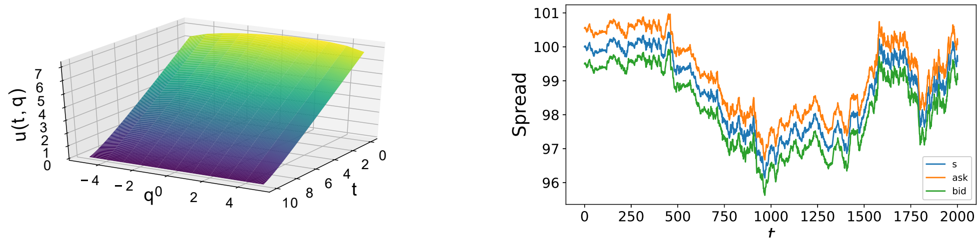

Figure 3.13: Solution of $u(t; q)$ and optimal prices

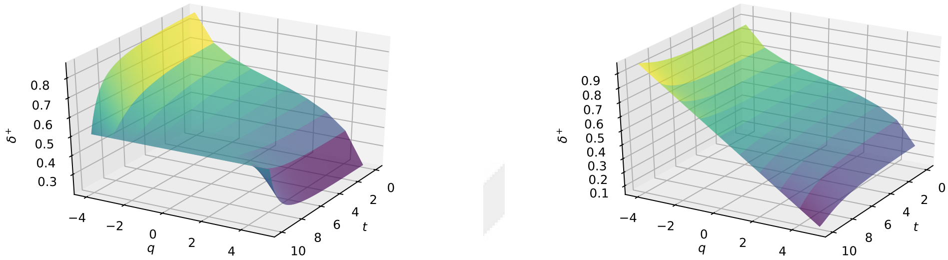

Figure 3.14: Optimal spread δ^+ for different liquidation values $\alpha \in \{0, 0.05\}$

It is easily observable from Figure 3.14 that how the optimal sell spread is changing for an increasing liquidation value. To cover the rising liquidation cost, the market maker shows a behaviour such that expanding the sell spreads and so the sell prices for the negative inventory levels.

On the other hand, changing optimal buy spreads for an increasing liquidation value can be also noticed in Figure 3.15 by the same interpretation as for the optimal sell spread.

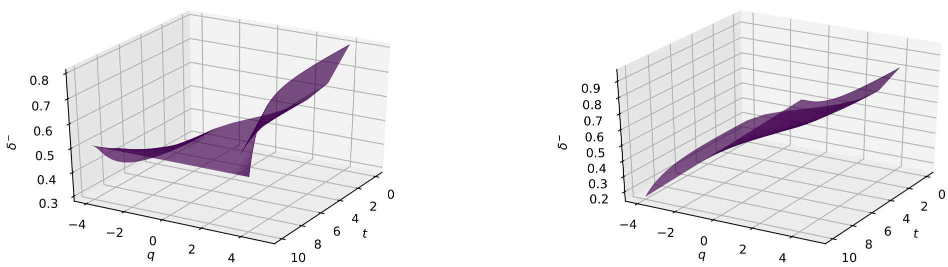

Figure 3.15: Optimal spread δ^- for different liquidation values $\alpha \in \{0, 0.05\}$

3.5.2 Results with the Exponential Utility Function

In this part, the experiment is constructed to discuss the results for $\delta^+(0, \nu_0; q)$ depending of different risk aversion degree γ in the set of values $\{0.0001, 0.001, 0.01\}$ with the same parameters given in Table 3.1. The results for δ^- can be also discussed with the same idea as for δ^+.

The parameter γ shows the risk-averse degree of the investor. When γ increases, the risk-averse degree of the investor increases. Consequently, she will sell the assets with a lower price on the positive inventory levels to reduce both the price risk and liquidation risk. On the other hand, she does not face with the liquidation risk on the negative inventory levels but wants to receive higher amount for selling the assets.

Table 3.12 displays the results for the performance of the strategy with a liquidation parameter $\alpha = 0.01$. Thereby, we observe the following behaviour of the investor:

$$\begin{cases} \frac{\partial \delta_t^+}{\partial \gamma} > 0, & \frac{\partial \delta_t^-}{\partial \gamma} < 0, \qquad q < 0, \\ \frac{\partial \delta_t^+}{\partial \gamma} < 0, & \frac{\partial \delta_t^-}{\partial \gamma} > 0, \qquad q = 0, \\ \frac{\partial \delta_t^+}{\partial \gamma} < 0, & \frac{\partial \delta_t^-}{\partial \gamma} > 0, \qquad q > 0. \end{cases}$$

By the numerical experiments, we can conclude that the above behaviour of the optimal spreads with different values of γ is observed in Table 3.12.

Table 3.12: Effects of γ on $\delta^+(0, \nu_0; q)$

q	$\gamma = 0.0001$	$\gamma = 0.001$	$\gamma = 0.01$
-4	0.862765	0.866689	0.903819
-3	0.719273	0.723774	0.76518
-2	0.655817	0.659483	0.692464
-1	0.614311	0.616237	0.633557
0	0.579575	0.579352	0.577913
1	0.544801	0.542445	0.522182
2	0.504757	0.500643	0.464063
3	0.45231	0.447119	0.399384
4	0.371551	0.366237	0.315636
5	0.203122	0.198878	0.157245

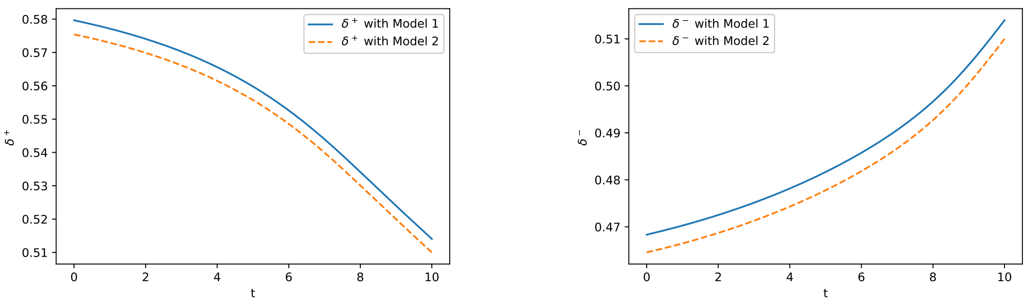

Figure 3.16: Comparison of Model 1 and Model 2

3.5.3 Results of the Model with Jumps in Volatility

Numerical experiments for this case are carried out by linear interpolation and extrapolation techniques in order to calculate the value functions $u(t, \nu + \epsilon^+; q)$ and $u(t, \nu - \epsilon^-; q)$ in the verification equation. To recall the models easier, we call the model in Case 1 in Section 3.2.1.1 with stock price dynamics (3.1) as "Model 1" and the model in Section 3.4 with the dynamics (3.28) as "Model 2".

Figure 3.16 illustrates $\delta^+(t, \nu_0; 0)$ and $\delta^-(t, \nu_0; 0)$ values for both "Model 1" and "Model 2". It is observed that "Model 1" which has the jumps in the price have slightly wider δ^+ and δ^- values. We note that the bid-ask spread for "Model 1" is 1.0402 while it is found as 1.0328 for "Model 2".

Table 3.13 depicts the results of these two strategies. We can see that when the jumps occur in the volatility process, it causes not only larger profits but also larger standard deviation of the profit and loss function.

Table 3.13: Comparison of the strategies Model 1 and Model 2

	PnL	Std dev of PnL	Final q	Std dev of q
Model 1	3.92	4.98	0.07	2.24
Model 2	4.87	5.44	0.73	2.00

3.5.4 Comparison with Some of the Existing Models in the Literature

In this section, we compare the existing optimal market making models based on the stock price impact with the models that we introduce in the previous sections. Numerical experiments are carried out on two different types of utility functions, i.e., quadratic and exponential utility functions.

We first give the results for the value function

$$W(t,x,S,\nu;q) = \sup_{(\delta_s^{\pm})_{t\leq s\leq T}\in\mathcal{A}_t} \mathbb{E}\left(X_T + q_T(S_T - \alpha q_T) - \psi\sigma^2 \int_t^T q_s^2 \nu_s ds\right),$$

for the stock price dynamics which are provided in each model definition.

In this part, we operate the simulations under the quadratic utility function for the comparison purposes for all introduced models in this thesis, although they have been defined with different utility criteria and solved under the different settings in their original papers.

Model a: The model with the stock price dynamics $dS_t = \sigma dB_t$ which is introduced by [3].

The parameters are $T = 10$, $q \in [-5,5]$, $\alpha = 0.01$, $\kappa^{\pm} = 2$, $\psi = 0.1$, and $\sigma = 0.1$.

Model b: The model with the stock price dynamics $dS_t = \sigma dB_t + \varepsilon^+ dM_t^+ - \varepsilon^+ dM_t^-$ that is handled in [12].

The parameters are $T = 10$, $q \in [-5,5]$, $\lambda^{\pm} = 2$, $\epsilon^{\pm} = 0.004$, $\alpha = 0.01$, $\kappa^{\pm} = 2$, $\psi = 0.1$, and $\sigma = 0.1$.

Model c: This is governed by the price dynamics (3.1).

The parameters are $T = 10$, $q \in [-5,5]$, $\lambda^{\pm} = 2$, $\epsilon^{\pm} = 0.004$, $\alpha = 0.01$, $\kappa^{\pm} = 2$, $\psi = 0.1$, $\sigma = 0.01$, $\mu = 0.01$, $k = 1$, $\theta = 1$, and $\rho = -0.8$.

Model d: This is governed by the price dynamics (3.28).

The parameters are $T = 10$, $q \in [-5,5]$, $\lambda^{\pm} = 2$, $\epsilon^{\pm} = 0.004$, $\alpha = 0.01$, $\kappa^{\pm} = 2$, $\psi = 0.1$, $\sigma = 0.01$, $\mu = 0.01$, $k = 1$, $\theta = 1$, and $\rho = -0.8$.

Table 3.14 illustrates that the traders using the "Model c" have relatively higher return but also relatively a higher standard deviation comparing to the other models. The performances of Sharpe ratios of each models indicate that the stock price models with stochastic volatility based on a quadratic utility function produce more attractive portfolios than the other models. It is demonstrated that the "Model d" has a Gaussian normal distribution for both PnL and inventory processes while the other models are positively skewed in terms of their PnL distributions.

Table 3.14: Statistical comparison for PnL and inventory under the quadratic utility function

		Model a	Model b	Model c	Model d
PnL	Mean	0.4751	0.4859	5.5978	5.3605
	Std dev	0.5683	0.5856	3.9561	4.4310
	Sharpe ratio	0.8360	0.8297	1.4150	1.2098
	Skewness	1.2095	1.4313	1.2139	0.2769
	Kurtosis	1.8287	2.6081	2.3427	-0.5726
Inventory	Mean	-0.052	-0.2710	-0.0975	0.0243
	Std dev	0.8736	0.9897	2.2825	2.2029
	Sharpe ratio	0.8360	-0.2738	-0.0427	0.0110
	Skewness	0.1457	-0.3349	0.0831	-0.0309
	Kurtosis	3.3331	1.8898	-0.4861	-0.4321

The next experiment is carried out for the value function

$$W(t,x,S,\nu;q) = \sup_{(\delta_s^{\pm})_{t\leq s\leq T}\in\mathcal{A}_t} \mathbb{E}\left[-e^{-\gamma(X_T+q_T(S_T-\alpha q_T))}\right],$$

using the exponential utility function and the results are provided for the following models.

Model A: The model with the stock price dynamics $dS_t = \sigma dB_t$ that is introduced by [3] and handled by quadratic approximation approach.

The parameters are $T = 10$, $q \in [-5, 5]$, $\alpha = 0.01$, $\kappa^{\pm} = 2$, $\gamma = 0.01$, and $\sigma = 0.1$.

Model B: The model with the stock price dynamics $dS_t = \sigma dB_t + \epsilon^+ dM_t - \epsilon^+ dM_t$ that is introduced with quadratic utility function and solved by providing a closed-form solution.

The parameters are $T = 10$, $q \in [-5, 5]$, $\lambda^{\pm} = 2$, $\epsilon^{\pm} = 0.004$, $\alpha = 0.01$, $\kappa^{\pm} = 2$, $\gamma = 0.01$, and $\sigma = 0.1$.

Model C: The model is governed by the price dynamics (3.1).

The parameters are $T = 10$, $q \in [-5, 5]$, $\lambda^{\pm} = 2$, $\epsilon^{\pm} = 0.004$, $\alpha = 0.01$, $\kappa^{\pm} = 2$, $\gamma = 0.01$, $\sigma = 0.01$, $\mu = 0.01$, $k = 1$, $\theta = 1$, and $\rho = -0.8$.

Table 3.15 demonstrates that the "Model C" which is the stock price modeling with stochastic volatility, has relatively larger expected return, but also a relatively larger standard deviation. Meanwhile, the other stock price modelings in Table 3.15 produce higher Sharpe ratios.

Table 3.15: Statistical comparison for PnL and inventory under the exponential utility function

		Model A	Model B	Model C
PnL	Mean	0.7272	0.7029	3.1546
	Std dev	0.7066	0.6906	3.7787
	Sharpe ratio	1.0291	1.0178	0.8348
	Skewness	1.1525	1.0058	0.4577
	Kurtosis	1.8716	1.2229	-0.4832
Inventory	Mean	0.0860	0.0430	0.2682
	Std dev	1.0471	1.1041	2.3061
	Sharpe ratio	0.0821	0.0389	0.1163
	Skewness	0.1571	-0.0225	-0.1258
	Kurtosis	1.1888	1.2229	-0.4832

3.6 A Further Study: A Model where the Midprice Follows a Mean-reverting Process with Stochastic Volatility

In this part, we present a further study where an asset has stochastic volatility and its underlying stock price employs a mean-reverting process for high-frequency trading in a limit order book. A mean-reverting stock price process with constant volatility has been studied in [1] before. We develop the optimal market making model by adding the jumps in price dynamics and considering the volatility as a stochastic process. Here, we only provide the theoretical development of the model and leave the numerical applications as a further study.

Until now, we consider that the underlying price is implemented by the Heston stochastic volatility model. In reality, the underlying assets of financial instruments mostly reveal both stochastic volatility and mean reversion in price properties [50]. It is apparent that the prices show the behaviour of reverting to their equilibrium mean in financial markets which makes the modeling with mean reversion a significant research area.

Thus, we assume that the midprice S_t of the stock in the market follows the dynamics:

$$
\begin{aligned}
dS_t &= \beta(\mu - S_t)dt + \sqrt{\nu_t}dB_t^1 + \varepsilon^+ dM_t^+ - \varepsilon^- dM_t^-, \\
d\nu_t &= k(\theta - \nu_t)dt + \sigma\sqrt{\nu_t}dB_t^2, \\
dB_t^1 dB_t^2 &= \rho dt,
\end{aligned} \tag{3.34}
$$

which follows a mean-reverting process with an Ornstein-Uhlenbeck (OU) process and stochastic volatility, where β is the mean-reverting rate, μ is the long-term drift, B_t^1 and B_t^2 are Wiener processes, and $\rho \in [-1, 1]$ is the instant correlation coefficient between them. The other parameters in the model have the same meaning as being in the model (3.1).

For a market maker to trade a stock having the dynamics (3.34) in a LOB, we consider again the same value function as presented in Section 3.1 to construct a stochastic control problem as follows:

$$
W(t, x, S, \nu; q) = \sup_{(\delta_s^{\pm})_{t \le s \le T} \in \mathcal{A}_t} \mathbb{E}\left[X_T + q_T(S_T - \alpha q_T) - \psi\sigma^2 \int_t^T q_s^2 \nu_s ds\right]. \tag{3.35}
$$

Proposition 9. The value function (3.35) satisfies the HJB equation,

$$
\begin{aligned}
&\partial_t W + \beta(\mu - S_t)\partial_S W + k(\theta - \nu_t)\partial_\nu W + \frac{1}{2}\nu_t \partial_{SS} W + \frac{1}{2}\sigma^2 \nu_t \partial_{\nu\nu} W + \sigma\rho\nu_t \partial_{S\nu} W - \psi\nu_t q^2 \sigma^2 \\
&+ \sup_{\delta_t^+} \Big\{ \Lambda_t^+(\delta_t^+)\mathbb{E}\left[W(t, x + (S_t + \delta_t^+), S_t + \varepsilon^+, \nu_t; q - 1) - W(t, x, S_t, \nu_t; q)\right] \\
&\qquad + (\lambda^+ - \Lambda_t^+(\delta_t^+))\mathbb{E}\left[W(t, x, S_t + \varepsilon^+, \nu_t; q) - W(t, x, S_t, \nu_t; q)\right] \Big\} \\
&+ \sup_{\delta_t^-} \Big\{ \Lambda_t^-(\delta_t^-)\mathbb{E}\left[W(t, x - (S_t - \delta_t^-), S_t - \varepsilon^-, \nu_t; q + 1) - W(t, x, S_t, \nu_t; q)\right] \\
&\qquad + (\lambda^- - \Lambda_t^-(\delta_t^-))\mathbb{E}\left[W(t, x, S_t - \varepsilon^-, \nu_t; q) - W(t, x, S_t, \nu_t; q)\right] \Big\} = 0,
\end{aligned} \tag{3.36}
$$

with the final condition,

$$
W(T, x, S, \nu; q) = x + q(S - \alpha q). \tag{3.37}
$$

Proof. The proof can be carried out using similar arguments as in Proposition 1. □

Proposition 10. Let

$$
W(t, x, S, \nu; q) = x + q(S - \alpha q) + u(t, \nu, S; q) \tag{3.38}
$$

be a solution to the HJB equation (3.36) which is suggested by the final condition (3.37). Then, the optimal feedback controls of (3.36) are given by

$$\begin{aligned}
\delta^{+*}(t,\nu,S;q) &= \tfrac{1}{\kappa^+} + \epsilon^+ + \alpha(1-2q) - u(t,\nu,S+\epsilon^+;q-1) + u(t,\nu,S+\epsilon^+;q), \quad q \neq \underline{q},\\
\delta^{-*}(t,\nu,S;q) &= \tfrac{1}{\kappa^-} + \epsilon^- + \alpha(1+2q) - u(t,\nu,S-\epsilon^-;q+1) + u(t,\nu,S-\epsilon^-;q), \quad q \neq \overline{q}.
\end{aligned} \tag{3.39}$$

Proof. We plug the proposed solution (3.38) and also substitute the intensity functions for the filled orders into (3.36). Then, the HJB equation is reduced to

$$\begin{aligned}
\psi\nu q^2\sigma^2 = {} & \partial_t u + \beta(\mu - S)(q + \partial_S u) + k(\theta-\nu)\partial_\nu u\\
& + \frac{1}{2}\nu\partial_{SS}u + \frac{1}{2}\sigma^2\nu\partial_{\nu\nu}u + \sigma\rho\nu\partial_{S\nu}u\\
& + \sup_{\delta_t^+}\lambda^+\Big\{q\epsilon^+ + u(t,\nu,S+\epsilon^+;q) - u(t,\nu,S;q) + e^{-\kappa^+\delta^+}\Big(\delta^+ - \epsilon^+\\
& \quad - \alpha(1-2q) + u(t,\nu,S+\epsilon^+;q-1) - u(t,\nu,S+\epsilon^+;q)\Big)\Big\} \qquad (3.40)\\
& + \sup_{\delta_t^-}\lambda^-\Big\{ - q\epsilon^- + u(t,\nu,S-\epsilon^-;q) - u(t,\nu,S;q) + e^{-\kappa^-\delta^-}\Big(\delta^- - \epsilon^-\\
& \quad - \alpha(1+2q) + u(t,\nu,S-\epsilon^-;q+1) - u(t,\nu,S-\epsilon^-;q)\Big)\Big\}
\end{aligned}$$

for $q \in [\underline{q}, \overline{q}]$ with final condition $u(T,\nu,S;q) = 0$.

Then, the optimal spreads (3.39) can be calculated by applying the first order optimality condition in (3.40) which completes the proof. □

Now, inserting the optimal spreads (3.39) in (3.40) yields the verification equation as following:

$$\begin{aligned}
\psi\nu q^2\sigma^2 = {} & \partial_t u + \beta(\mu - S)(q + \partial_S u) + k(\theta-\nu)\partial_\nu u\\
& + \frac{1}{2}\nu\partial_{SS}u + \frac{1}{2}\sigma^2\nu\partial_{\nu\nu}u + \sigma\rho\nu\partial_{S\nu}u\\
& + \lambda^+\Big[q\epsilon^+ + u(t,\nu,S+\epsilon^+;q) - u(t,\nu,S;q)\\
& \qquad + \frac{1}{\kappa^+}e^{-1-\kappa^+\left(\epsilon^+ + \alpha(1-2q) - u(t,\nu,S+\epsilon^+;q-1) + u(t,\nu,S+\epsilon^+;q)\right)}\Big]\\
& + \lambda^-\Big[- q\epsilon^- + u(t,\nu,S-\epsilon^-;q) - u(t,\nu,S;q)\\
& \qquad + \frac{1}{\kappa^-}e^{-1-\kappa^-\left(\epsilon^- + \alpha(1+2q) - u(t,\nu,S-\epsilon^-;q+1) + u(t,\nu,S-\epsilon^-;q)\right)}\Big]
\end{aligned} \tag{3.41}$$

for $q \in [\underline{q}, \overline{q}]$ with the final condition $u(T,\nu,S;q) = 0$.

In order to solve the verification equation (3.41) for $u(t,\nu,S;q)$, the finite difference discretizations for $\partial_t u$, $\partial_S u$, $\partial_\nu u$, $\partial_{SS} u$, $\partial_{\nu\nu} u$ and $\partial_{S\nu} u$ can be applied. The discretizations are provided in Section A.2 in Appendix A. The numerical simulations are not provided here for this modeling case as the computational obstacles arise because of the high dimension of $u(t,\nu,S;q)$ and the mixed derivatives arising in the HJB equation (3.41). We leave it as a future study.

Remark 6. One can also consider to solve the stochastic control problems for limit order book models defined in this chapter with the following value function:

$$W(t,x,S,\nu;q) = x + qS + u_0(t,S) + u_1(t,S)q + u_2(t,\nu)q^2 \tag{3.42}$$

with final conditions $u_0(T,S) = u_1(T,S) = 0$, $u_2(T,\nu) = -\alpha$. Using this proposed solution, we can obtain a PDE system and then an ODE system by reducing the PDE equations. Here, we only provide the PDE system for the model with stock price (3.34).

Inserting (3.42) into HJB equation (3.36), it turns out to

$$\begin{aligned}
\psi\nu q^2\sigma^2 = {} & (\partial_t u_0 + \partial_t u_1 q + \partial_t u_2 q^2) + \beta(\mu - S)(q + \partial_S u_0 + \partial_S u_1 q) \\
& + k(\theta-\nu)(\partial_\nu u_2 q^2) + \frac{1}{2}\nu(\partial_{SS}u_0 + \partial_{SS}u_1 q) + \frac{1}{2}\sigma^2\nu(\partial_{\nu\nu}u_2 q^2) \\
& + \sup_{\delta_t^+}\lambda^+\Big\{q\epsilon^+ + u_0(t,S+\epsilon^+) - u_0(t,S) + u_1(t,S+\epsilon^+) - u_1(t,S) \\
& \qquad + e^{-\kappa^+\delta^+}\left(\delta^+ - \epsilon^+ - u_1(t,S+\epsilon^+) - 2u_2(t,\nu)q + u_2(t,\nu)\right)\Big\} \\
& + \sup_{\delta_t^-}\lambda^-\Big\{-q\epsilon^- + u_0(t,S-\epsilon^-) - u_0(t,S) + u_1(t,S-\epsilon^-) - u_1(t,S) \\
& \qquad + e^{-\kappa^-\delta^-}\left(\delta^- - \epsilon^- + u_1(t,S-\epsilon^-) + 2u_2(t,\nu)q + u_2(t,\nu)\right)\Big\}
\end{aligned} \tag{3.43}$$

with terminal conditions $u_0(T,S) = u_1(T,S) = 0$, $u_2(T,\nu) = -\alpha$.

Then, the optimal spreads are found as

$$\begin{aligned}
\delta^{+*}(t,\nu,S;q) &= \tfrac{1}{\kappa^+} + \epsilon^+ + u_1(t,S+\epsilon^+) + 2qu_2(t,\nu) - u_2(t,\nu), \quad q \neq \underline{q}, \\
\delta^{-*}(t,\nu,S;q) &= \tfrac{1}{\kappa^-} + \epsilon^- - u_1(t,S-\epsilon^-) - 2qu_2(t,\nu) - u_2(t,\nu), \quad q \neq \overline{q}.
\end{aligned} \tag{3.44}$$

Putting the optimal depths (3.44) into (3.43), the verification equation is obtained as

$$\begin{aligned}\psi\nu q^2\sigma^2 &= (\partial_t u_0 + \partial_t u_1 q + \partial_t u_2 q^2) + \beta(\mu - S)(q + \partial_S u_0 + \partial_S u_1 q)\\
&\quad + k(\theta-\nu)(\partial_\nu u_2 q^2) + \frac{1}{2}\nu(\partial_{SS}u_0 + \partial_{SS}u_1 q) + \frac{1}{2}\sigma^2\nu(\partial_{\nu\nu}u_2 q^2)\\
&\quad + \lambda^+\Big[q\epsilon^+ + u_0(t,S+\epsilon^+) - u_0(t,S) + u_1(t,S+\epsilon^+) - u_1(t,S)\\
&\qquad + \frac{1}{\kappa^+}e^{-1-\kappa^+\left(\epsilon^+ + u_1(t,S+\epsilon^+) + 2qu_2(t,\nu) - u_2(t,\nu)\right)}\Big]\\
&\quad + \lambda^-\Big[-q\epsilon^- + u_0(t,S-\epsilon^-) - u_0(t,S) + u_1(t,S-\epsilon^-) - u_1(t,S)\\
&\qquad + \frac{1}{\kappa^-}e^{-1-\kappa^-\left(\epsilon^- + u_1(t,S-\epsilon^-) + 2qu_2(t,\nu) - u_2(t,\nu)\right)}\Big] \qquad (3.45)\end{aligned}$$

with final conditions $u_0(T,S) = u_1(T,S) = 0$, $u_2(T,\nu) = -\alpha$.

Now, assuming that $\epsilon^\pm = 0$ and writing the Taylor series expansion of the exponential functions in (3.45), we get the following PDE system in u_0, u_1 and u_2:

$$\begin{aligned}\partial_t u_0 + \beta(\mu - S)\partial_S u_0 + \frac{1}{2}\nu\partial_{SS}u_0 - (\lambda^+ + \lambda^-)u_1 + (\lambda^+ + \lambda^-)u_2 &= 0,\\
\partial_t u_1 + \beta(\mu - S)(1 + \partial_S u_1) + \frac{1}{2}\nu\partial_{SS}u_1 - 2(\lambda^+ - \lambda^-)u_2 &= 0,\\
\partial_t u_2 + k(\theta - \nu)\partial_\nu u_2 + \frac{1}{2}\sigma^2\nu\partial_{\nu\nu}u_2 - \psi\nu\sigma^2 &= 0,\end{aligned}$$

with final conditions $u_0(T,S) = u_1(T,S) = 0$, $u_2(T,\nu) = -\alpha$. This PDE system can be solved and hence the optimal spreads can be obtained explicitly by rewriting the PDEs in linear equations. This provides with an ODE system to solve. We also leave this problem as a further study related to this topic.

3.7 Summary

In this chapter, we provide optimal market making models for a market maker for high-frequency trading that involve a mean-reverting stochastic volatility model with the influence of arrival market orders in the underlying asset. First, we design a model with variable utilities where the effects of the jumps corresponding to the orders are introduced in returns of the asset and generate the optimal bid and ask prices for trading. Then, we develop another, but novel approach considering an underlying asset model with jumps in stochastic volatility. Such an extension allows one to fit the implied volatility smile better in practice.

In order to analyze the experimental results, we work on the models that we derive in this thesis using the different metrics. It is salient to mention that the market maker modifies her qualitative behaviour in various situations, i.e., changing inventory levels, utility functions. By our numerical results, we deduce that the jump effects and comparative statistics metrics provide us with the information for the traders to gain expected profits. For instance, the model given by (3.1) has a considerable Sharpe ratio and inventory management with a lower standard deviation comparing to the symmetric strategy. Besides, we further quantify the effects of a variety of parameters in the models on the bid and ask spreads and observe that the trader follows different strategies on positive and negative inventory levels, separately. The strategy derived by the model (3.1), for example, illustrates that when the time is approaching to the terminal time, the optimal spreads converge to a fixed, constant value. Furthermore, in case of the jumps in volatility, it is observed that a higher profit can be obtained but with a larger standard deviation.

Consequently, we support our findings by comparing the models proposed within this research with the stock price impact models existing in the literature. Last but not least, we have substantially improved the performance of a market maker in terms of profit and loss distribution of the trade with the proposed models.

CHAPTER 4

APPLICATIONS TO REAL DATA

This section covers a real high-frequency data application for an emerging market, Borsa Istanbul (BIST). For this purpose, we model the asset prices in a limit order book data in an equity market as we define in Chapter 3 and estimate the parameters for each of the model by the quasi-maximum likelihood estimation method. For the estimation of the models issues, we use the yuima package in R programming language [36] which provides precise estimations to predict the market.

We conduct our analyses on two periods, i.e., pre Covid-19 and post Covid-19 pandemic, on the same stocks to see that our optimal market making models still work well and the investors can gain profits even in an exceptional period. Since the pandemic impacts the economies and businesses in all around the world because of the lockdown measures, it has also crushed the stock markets. Due to its negative effects on the stock markets, we investigate whether it affects stock trading and behaviour of the traders who trade with our strategies.

In order to call the models easily in this chapter, let us first summarize them as follows:

Model 1:

Stock price dynamics:

$$\begin{aligned} dS_t &= \mu dt + \sqrt{\nu_t} dB_t^1 + \varepsilon^+ dM_t^+ - \varepsilon^- dM_t^-, \\ d\nu_t &= k(\theta - \nu_t)dt + \sigma\sqrt{\nu_t} dB_t^2, \\ dB_t^1 dB_t^2 &= \rho dt. \end{aligned}$$

Value function: The value function is set up by using quadratic utility function as follows:

$$W(t,x,S,\nu;q) = \sup_{(\delta_s^{\pm})_{t\le s\le T}\in\mathcal{A}_t} \mathbb{E}\left[X_T + q_T S_T + \eta(q_T) - \psi\sigma^2 \int_t^T q_s^2 \nu_s ds\right],$$

where $\eta(q_T) = -\alpha q_T^2$.

Optimal ask and bid spreads:

$$\delta_1^{+*}(t,\nu;q) = \tfrac{1}{\kappa^+} + \epsilon^+ + \alpha(1-2q) - u(t,\nu;q-1) + u(t,\nu;q), \quad q \neq \underline{q},$$
$$\delta_1^{-*}(t,\nu;q) = \tfrac{1}{\kappa^-} + \epsilon^- + \alpha(1+2q) - u(t,\nu;q+1) + u(t,\nu;q), \quad q \neq \overline{q}.$$

Model 2:

Stock price dynamics: Stock price dynamics is the same as given in the Model 1.

Value function: We assume that the utility function is exponential having a degree of the risk aversion for the investor with the following value function:

$$W(t,x,S,\nu;q) = \sup_{(\delta_s^{\pm})_{t\le s\le T}\in\mathcal{A}_t} \mathbb{E}\left[-e^{-\gamma(X_T+q_T S_T+\eta(q_T))}\right].$$

Optimal ask and bid spreads:

$$\delta_2^{+*}(t,\nu;q) = \tfrac{1}{\gamma}\ln\left(1+\tfrac{\gamma}{\kappa^+}\right) + \epsilon^+ + \alpha(1-2q) - u(t,\nu;q-1) + u(t,\nu;q), \quad q \neq \underline{q},$$
$$\delta_2^{-*}(t,\nu;q) = \tfrac{1}{\gamma}\ln\left(1+\tfrac{\gamma}{\kappa^-}\right) + \epsilon^- + \alpha(1+2q) - u(t,\nu;q+1) + u(t,\nu;q), \quad q \neq \overline{q}.$$

Model 3:

Stock price dynamics:

$$\begin{aligned} dS_t &= \mu dt + \sqrt{\nu_t} dB_t^1, \\ d\nu_t &= k(\theta-\nu_t)dt + \sigma\sqrt{\nu_t} dB_t^2 + \varepsilon^+ dM_t^+ - \varepsilon^- dM_t^-, \\ dB_t^1 dB_t^2 &= \rho dt. \end{aligned}$$

Value function: The value function is the same as given in the Model 1.

Optimal ask and bid spreads:

$$\delta_3^{+*}(t,\nu;q) = \tfrac{1}{\kappa^+} + \alpha(1-2q) - u(t,\nu+\epsilon^+;q-1) + u(t,\nu+\epsilon^+;q), \quad q \neq \underline{q},$$
$$\delta_3^{-*}(t,\nu;q) = \tfrac{1}{\kappa^-} + \alpha(1+2q) - u(t,\nu-\epsilon^-;q+1) + u(t,\nu-\epsilon^-;q), \quad q \neq \overline{q}.$$

4.1 Introduction

In this part, we focus on the analysis of the historical price of the stocks with ticker symbols FENER, AGHOL, ARCLK, and EREGL which are traded in Turkish stock market Borsa Istanbul (BIST). We investigate the results on two seperate periods such as before and after the Covid-19 pandemic choosing the specific days of January 10, 2020 and July 8, 2020 in the time between 10.00 am and 18.00 pm leading to a time series of dataset of approximately $68,000$ for each day in total. The data is obtained from Borsa Istanbul Data Store where it is high-frequency and derived in the equity market. The raw data contains the list of the orders which are arrived and filled, and thus shows all the transactions in the limit order book. For each of the orders; we choose the timestamps in milliseconds, order type, trading price, and number of transactions which are obtainable among the other information in the book. The trade session in Borsa Istanbul starts at 09.40 am and ends at 18.05 pm. Nevertheless, there are written orders before the starting time which indicate the opening price of the day and post opening orders which keep going to the time of 18.10 pm. To exclude these events and procure only with the occuring trades, we therefore use the data between 10.00 am and 18.00 pm. The aim of the data representation here is to show that the driven stock price models in Chapter 3 for the limit order books can be employed by practioners in emerging stock markets and would be reasonable and profitable by also providing the liquidity to the market.

Our motivation of defining the BIST data by the Heston stochastic volatility model plus jump components arises from the fact that a high-frequency data mostly has jumps, fluctuating volatility, excess skewness, and kurtosis values [18]. Therefore, indicating these properties of the data with only geometric Brownian motion or stochastic volatility is not sufficient.

For the estimation purposes, we use 2 seconds price data as the time frequency for the determined trading day and calibrate the models provided in Chapter 3. In order to estimate the parameters in the models, we initially need to estimate the volatility ν_t by the realized volatility formula [23].

The list of the companies of the stocks can be found below in Table 4.1. Meanwhile, the stocks are placed in different industry sectors which does not cause an integration between each of them.

Table 4.1: The list of the companies

Company ID	Company name	Sector
FENER	Fenerbahce Futbol AS	Sport
AGHOL	Anadolu Grubu Holding AS	Food
ARCLK	Arcelik AS	Technology
EREGL	Eregli Demir ve Celik Fabrikalari TAS	Iron and steel

4.2 Parameter Estimation

For the sake of the parameter estimation, we take the advantage of the “qmle” function in yuima package which operates the quasi-maximum likelihood method choosing the set of model parameters values that maximize the likelihood function. We additionally use the “optim” function in optimr package which uses a variety of optimization techniques for the calibration of the stochastic differential equations.

We first seek to estimate the unknown parameters $\Theta = \{\mu, k, \theta, \sigma, \rho\}$ of the Heston model assuming that the jump components are zero and then estimate the intensities λ^+ and λ^- of the jumps assuming that there are only jump parts in the same model as this method has been applied before in the literature, see for example [45] and [28]. In order to estimate the jump intensities for buy and sell orders, we seperately use the trading price information of buy and sell orders, respectively.

We consider a multivariate diffusion model

$$\begin{aligned} dX_t &= \mu(X_t, \Theta)dt + \sigma(X_t, \Theta)dW_t, \\ X_0 &= x_0, \end{aligned}$$

where W_t is an m-dimensional Brownian motion, X_t is an m-vector of state variables, $\mu(X_t, \Theta)$ is an m-dimensional function, and $\sigma(X_t, \Theta)$ is and $m \times m$ matrix function. For the given observation $X_1, X_2, \dots, X_n$, the quasi-maximum likelihood estimator of Θ satisfies [36]

$$\hat{\Theta} = \underset{\Theta}{\operatorname{argmax}}\, l_n(X_n, \Theta)$$

with the approximation of the likelihood function for a multivariate diffusion model, i.e.,

$$l_n(X_n, \Theta) = -\frac{1}{2}\sum_{i=1}^{n}\Bigg\{ \ln\big(\det(\Sigma(X_{t_{i-1}}, \Theta))\big) + \frac{1}{\Delta n}\Sigma^{-1}(X_{t_{i-1}}, \Theta)\Big[(\Delta X_i - \Delta n \mu(X_{t_{i-1}}, \Theta))\dot{(}\Delta X_i - \Delta n \mu(X_{t_{i-1}}, \Theta))^T\Big]\Bigg\}$$

with $t_i = i\Delta n$ and $\Delta n \to 0$ as $n \to \infty$, where $\Delta X_i = X_{t_i} - X_{t_{i-1}}$ and $\Sigma = \sigma\sigma^T$.

The estimator is implemented by the "qmle" function in yuima package which can also be implemented to estimate the jump intensities.

4.3 Applications on a Pre Covid-19 Pandemic Period

In this part, we first expose the results on January 10, 2020 which is a time before the global Covid-19 pandemic.

Tables 4.2, 4.3, 4.4, and 4.5 reveal the descriptive properties of the chosen and listed stocks in Table 4.1 on January 10, 2020 exhibiting the excess skewness and kurtosis values of both prices and volatilities for each stock.

Table 4.2: Descriptive statistics on the price and volatility for the stock FENER

	Mean	Std dev	Skewness	Kurtosis
Price	14.85757	0.06753039	0.4560056	3.482695
Volatility	0.4114614	0.1474814	1.121215	4.506218

Table 4.3: Descriptive statistics on the price and volatility for the stock AGHOL

	Mean	Std dev	Skewness	Kurtosis
Price	18.16659	0.07211792	-0.7015099	2.352282
Volatility	0.3045807	0.123605	0.3470168	2.428909

Table 4.4: Descriptive statistics on the price and volatility for the stock ARCLK

	Mean	Std dev	Skewness	Kurtosis
Price	21.68509	0.1057809	-1.05381	3.013819
Volatility	0.462925	0.1571043	0.2878955	2.693471

Table 4.5: Descriptive statistics on the price and volatility for the stock EREGL

	Mean	Std dev	Skewness	Kurtosis
Price	9.287843	0.0272914	0.4073723	2.71716
Volatility	0.5779547	0.1844738	0.1864868	2.3377

Figure 4.1 shows the price while Figure 4.2 represents the volatility of the stocks FENER, AGHOL, ARCLK, and EREGL on the day of January 10, 2020 and the time between 10.00 am and 18.00 pm. The figures of the stock prices also demonstrate the non-integration between each stock.

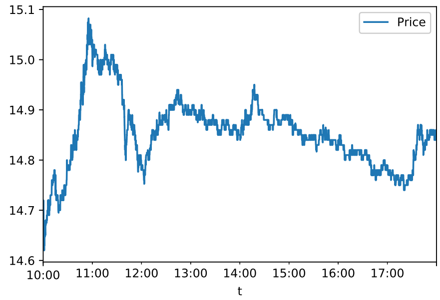

(a) FENER

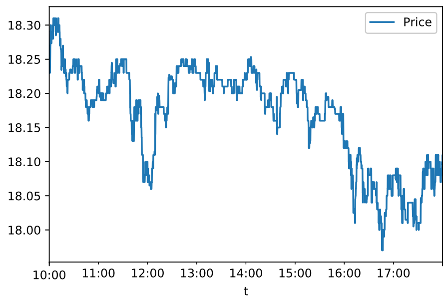

(b) AGHOL

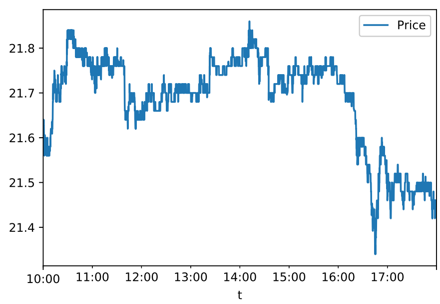

(c) ARCLK

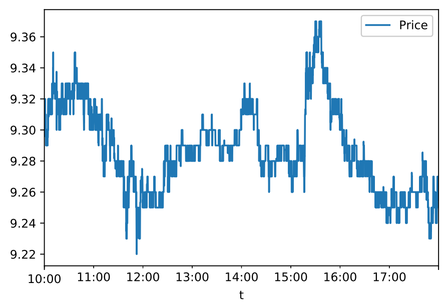

(d) EREGL

Figure 4.1: Illustration of the stock prices

4.3.1 Parameter Estimation and Applications for Model 1

Table 4.6 presents the estimated values of the parameters of "Model 1" for each stock and their standard errors which are quite small values. Moreover, it is seen that the stock FENER has considerably larger jump intensities comparing to the other stocks.

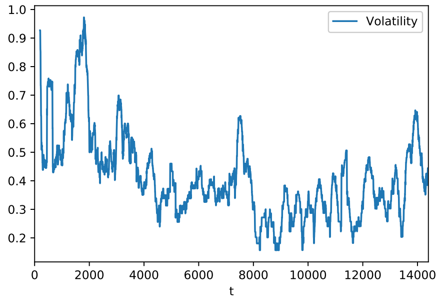

(a) FENER

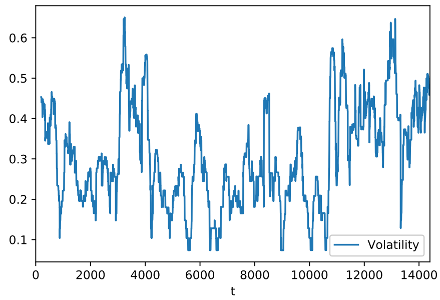

(b) AGHOL

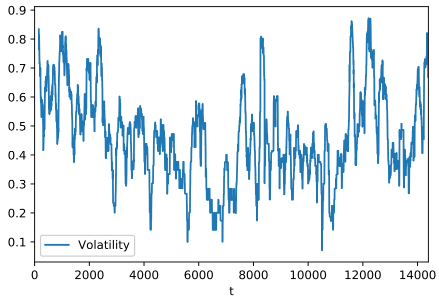

(c) ARCLK

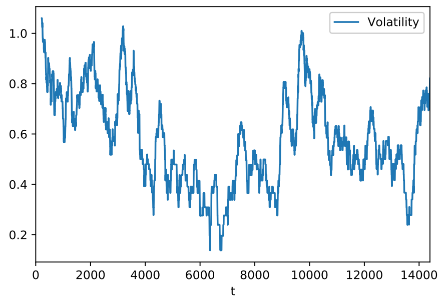

(d) EREGL

Figure 4.2: Illustration of the volatilities

Besides, there is a positive but low correlation between the price and volatility of the stock AGHOL.

Table 4.6: Estimation results for the stocks for Model 1 and Model 2

		Estimate	Std error
FENER	$\hat{\rho}$	-0.367579371	0.141935501
	$\hat{\sigma}$	0.165582174	0.009993511
	$\hat{\mu}$	-0.002577744	0.080611373
	$\hat{k}$	0.358303422	0.096038288
	$\hat{\theta}$	0.389447560	0.037853592
	$\hat{\lambda^+}$	0.4147828	0.009834001
	$\hat{\lambda^-}$	0.411985	0.009800777
AGHOL	$\hat{\rho}$	0.178438055	0.064817902
	$\hat{\sigma}$	0.233059741	0.003078144
	$\hat{\mu}$	-0.005674979	0.066279721
	$\hat{k}$	0.511847115	0.128105181
	$\hat{\theta}$	0.306111173	0.033599105
	$\hat{\lambda^+}$	0.04632192	0.001792756
	$\hat{\lambda^-}$	0.04632872	0.001792756
ARCLK	$\hat{\rho}$	-0.2892213482	0.047795044
	$\hat{\sigma}$	0.2701155459	0.004321504
	$\hat{\mu}$	-0.0009525923	0.084354563
	$\hat{k}$	0.7785487472	0.139258674
	$\hat{\theta}$	0.4582132795	0.030874946
	$\hat{\lambda^+}$	0.09016745	0.002502413
	$\hat{\lambda^-}$	0.09009799	0.002501449
EREGL	$\hat{\rho}$	-0.193997520	0.092728178
	$\hat{\sigma}$	0.166512780	0.003255053
	$\hat{\mu}$	-0.002462423	0.095412680
	$\hat{k}$	0.292166191	0.085181457
	$\hat{\theta}$	0.565964490	0.056797135
	$\hat{\lambda^+}$	0.08447185	0.002422057
	$\hat{\lambda^-}$	0.08447177	0.002422055

In order to agree that the estimated parameters of only the Heston stochastic volatility model fit "Model 1" for the real data of each stock with zero jump components assumption, we operate the hypotheses testing problem for the two hypotheses

$$H_0 : \hat{\Theta} = \Theta_0,$$

$$H_A : \hat{\Theta} \neq \Theta_0$$

using the yuima package where Θ_0 is the set of the estimated parameters.

The following first result for the stock FENER shows that the hypotheses test accepts the null hypotheses with a p-value of 0.9133889 and the quasi-maximum likelihood estimator produces quite well results.

$$\text{Test statistics} = 1.497, \quad df = 5, \quad p - \text{value} = 0.9133889,$$

where df is the degree of freedom.

The upcoming hypotheses testing results also indicate that the null hypotheses are not rejected with their p-values for the other stocks AGHOL, ARCLK, and EREGL.

$$\text{Test statistics} = 1.886, \quad df = 5, \quad p - \text{value} = 0.8646639,$$

$$\text{Test statistics} = 1.670, \quad df = 5, \quad p - \text{value} = 0.8926096,$$

$$\text{Test statistics} = 1.883, \quad df = 5, \quad p - \text{value} = 0.8650839.$$

In the next parts, the numerical results and experiments are carried out for the estimated values given in the Table 4.6 and the fixed parameters as in the Table 4.7.

Table 4.7: The Parameters

T (sec)	Δt	q	$\epsilon^{\pm}$	κ	α	ψ
10	0.005	$[-5, 5]$	0.004	2	0.01	0.1

Now, we provide the results on “Model 1” which uses quadratic utility function for the stocks FENER, AGHOL, ARCLK, and EREGL for the estimated parameters given in Table 4.6.

Results for the stock FENER

Figure 4.3 shows the solution of the value function $u(t, \nu; q)$ of the associated HJB equation for a fixed inventory level q in the left panel. A path of the profit and loss function (PnL) for this stock obtained by “Model 1” is demonstrated in the right panel where the improved profitability can be obviously seen.

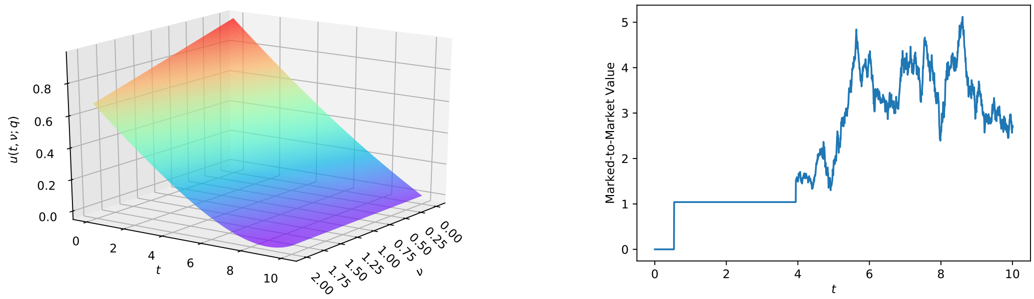

Figure 4.3: Solution of $u(t, \nu; q)$ for $q = 0$ and one path of the simulated PnL for the stock FENER

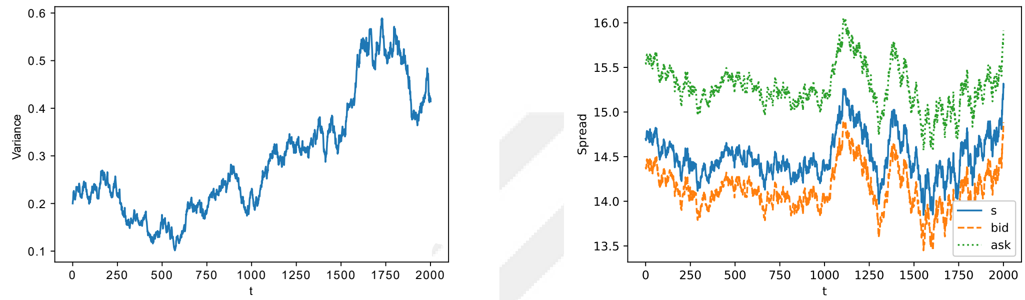

Figure 4.4: Simulated volatility and the optimal prices for the stock FENER

Figure 4.4 is an illustration for the simulated volatility and optimal prices for trading. In the right figure, it is displayed out that the market maker buys the stock with an optimal bid price which is close to the market price, but sells it with a quite far optimal ask price that leads to a large profit which is shown in Figure 4.3.

Figure 4.5 presents the optimal spreads δ^+ and δ^- of the trader for each inventory level. We can see the classical behaviour that the trader puts smaller price to get rid of the assets when the inventory is on the positive levels, but the higher values when the inventory is already negative at any trading time t since she may only want to sell the assets for a large ask price.

Results for the stock AGHOL

Now, we provide the results of the numerical experiments for the stock AGHOL which is traded in BIST market.

Figure 4.6 is a demonstration for the solution of the value function $u(t, \nu; q)$ of the as-

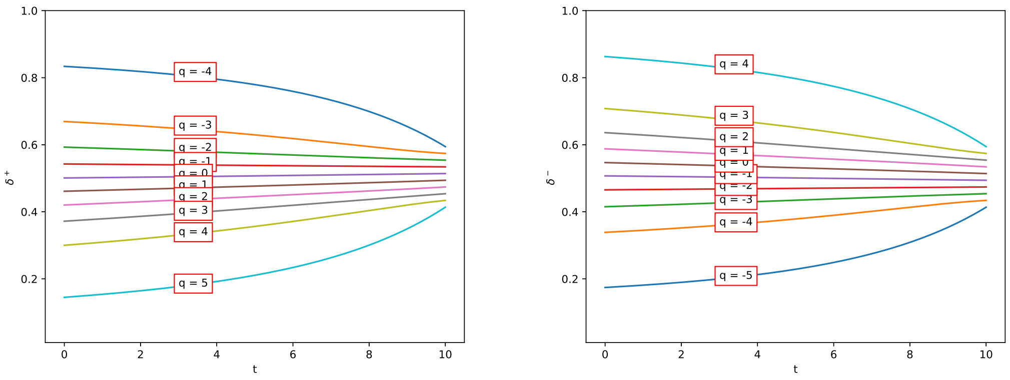

(a) δ^+ (b) δ^-

Figure 4.5: Optimal spreads δ^+ and δ^- for the stock FENER

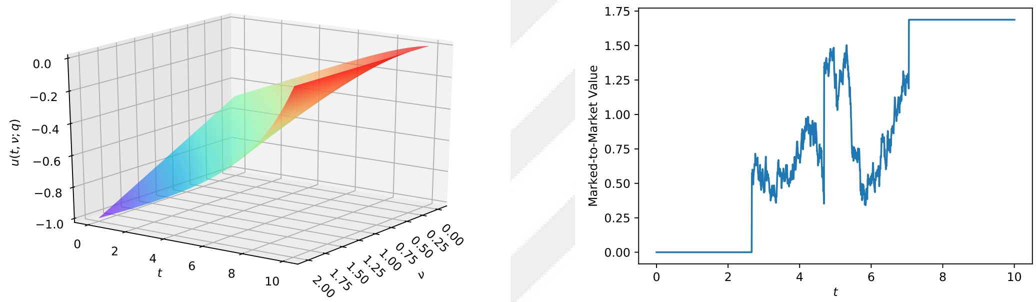

Figure 4.6: Solution of $u(t, \nu; q)$ for $q = 0$ and one path of the simulated PnL for the stock AGHOL

sociated HJB equation for a fixed inventory level q and for a path of the PnL achieved with the estimated parameters of the stock. From the left picture, we observe that the values of the function u are negative and it is an increasing function of time t for any fixed value of ν for this stock.

In Figure 4.7, we can see the estimated volatility and the optimal buy and sell prices.

Figure 4.8 shows that how the optimal spreads δ^+ and δ^- are changing for all inventory levels. The same qualitative behaviour of the trader for the stock FENER can be also observed for this stock in terms of the interpretation of the optimal spreads. In the calibrated values, we point to the stock AGHOL with the lowest estimated intensities resulting in the lowest spreads comparing to the spread graphs of the other stocks.

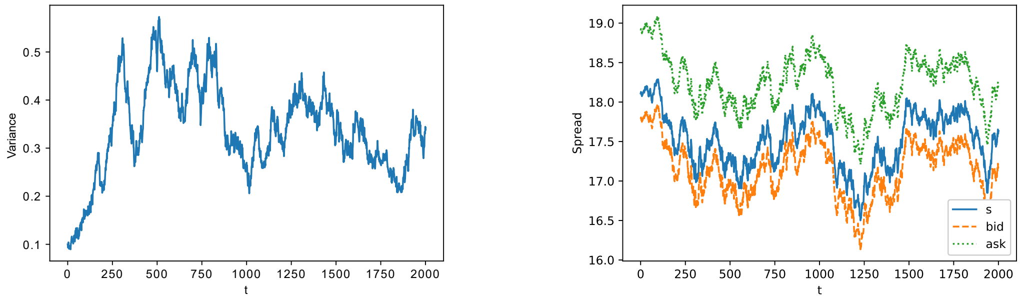

Figure 4.7: Simulated volatility and the optimal prices for the stock AGHOL

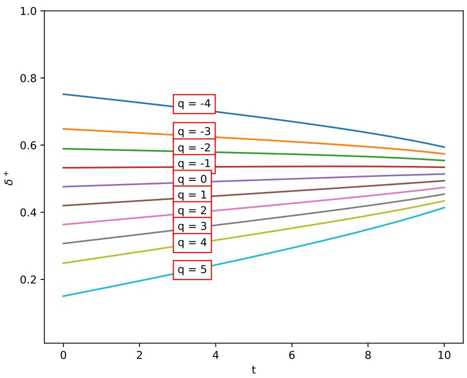

(a) δ^+

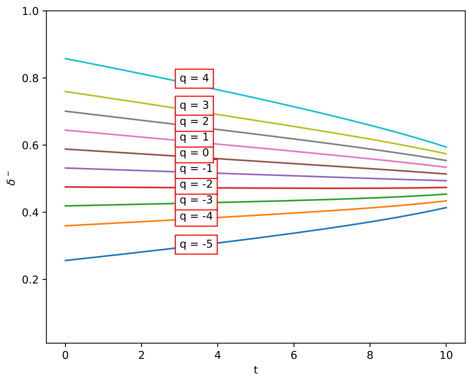

(b) δ^-

Figure 4.8: Optimal spreads δ^+ and δ^- for the stock AGHOL

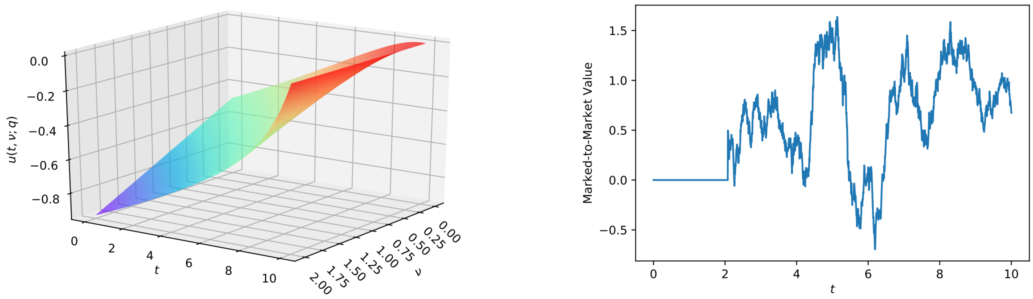

Figure 4.9: Solution of $u(t, \nu; q)$ for $q = 0$ and one path of the simulated PnL for the stock ARCLK

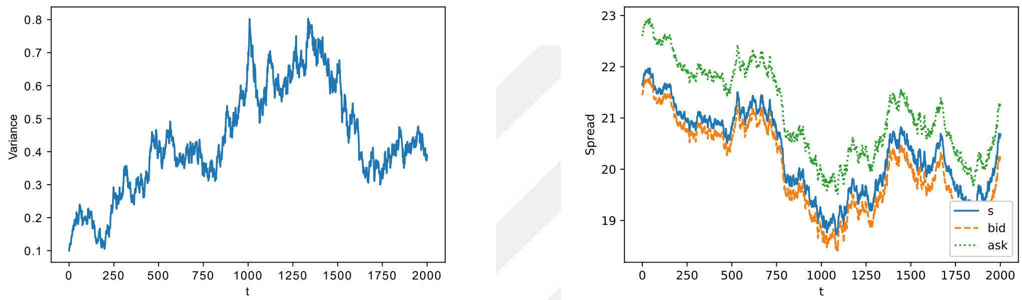

Figure 4.10: Simulated volatility and the optimal prices for the stock ARCLK

Results for the stock ARCLK

As a next numerical experiment, we provide the results for the stock ARCLK.

In Figure 4.9, the solution of the value function $u(t, \nu; q)$ of the related HJB equation and a path of the PnL calculated by the estimated parameters for the stock are provided. The values of the function u are also obtained as negative for this stock, as well.

Figure 4.10 is a demonstration for the estimated volatility and the optimal prices.

Figure 4.11 is a plot to see how the optimal spreads δ^+ and δ^- change for all inventory levels. In these figures, it can be observed that the spread values are greater than the spreads of the other stocks which can be caused because of the higher estimated standard deviation σ and the mean reversion adjustment rate value k.

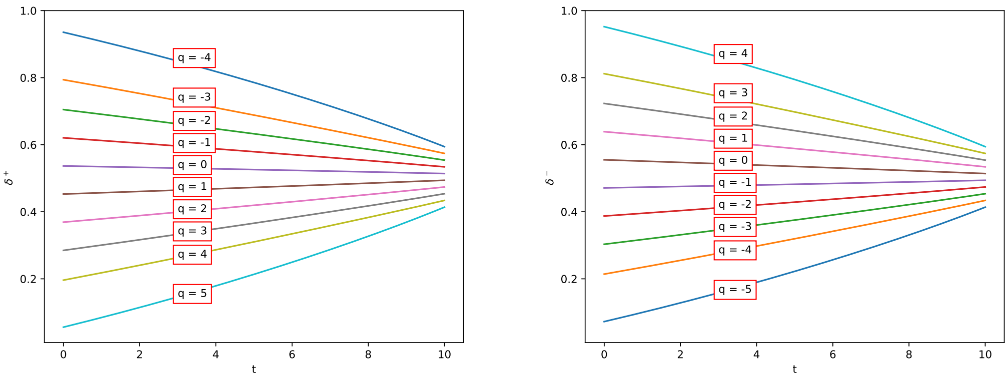

(a) δ^+ (b) δ^-

Figure 4.11: Optimal spreads δ^+ and δ^- for the stock ARCLK

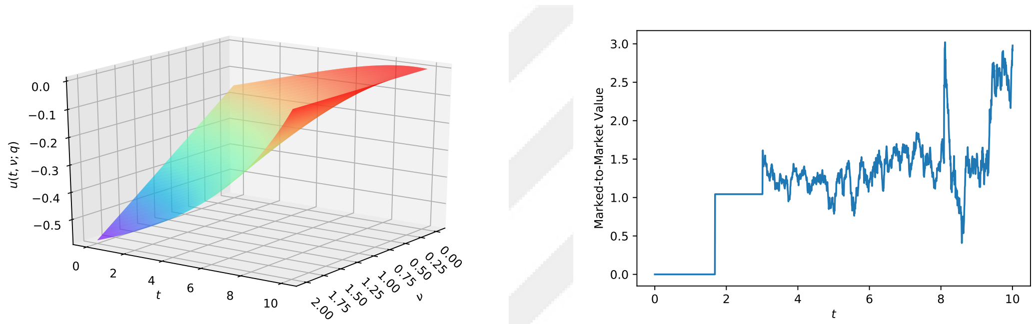

Figure 4.12: Solution of $u(t, \nu; q)$ for $q = 0$ and one path of the simulated PnL for the stock EREGL

Results for the stock EREGL

Figure 4.12 interprets the performance of the solution of the value function $u(t, \nu; q)$ and one path of the PnL for the stock EREGL. The negative u values are also achieved for this stock, hence we can make a conclusion that the very small jump intensities in the price lead negative u values.

Next, Figure 4.13 displays the estimated volatility and the optimal prices for the stock EREGL.

Figure 4.14 demonstrates the behaviour of the optimal spreads δ^+ and δ^- which are obtained by the formulas (3.12) for each inventory level. For example, a decreasing behaviour of the optimal sell spreads when $t \to T$ is seen in the figure of the optimal prices given by Figure 4.13.

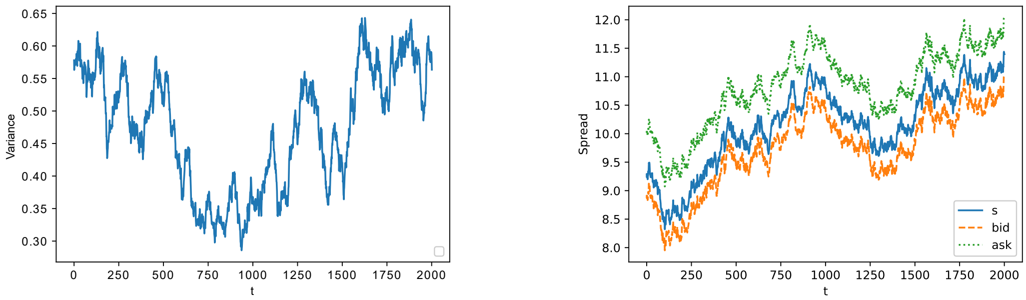

Figure 4.13: Simulated volatility and the optimal prices for the stock EREGL

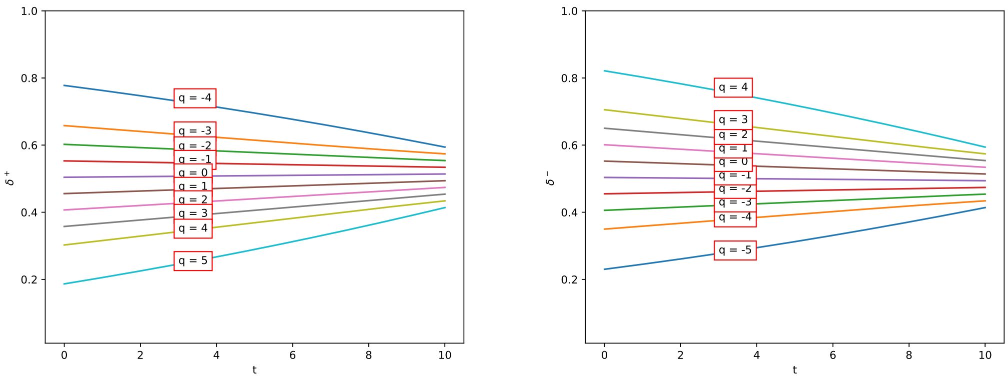

(a) δ^+ (b) δ^-

Figure 4.14: Optimal spreads δ^+ and δ^- for the stock EREGL

As a next illustration, we provide values of the optimal spreads of the model, that is "Model 1", by also giving the results of the model when there are no jumps in the stock price in the same model. Therefore, Tables 4.8 and 4.9 exhibit the optimal spreads of each stock where $q \in [-3, 3]$. The results indicate that larger spreads occur when there are jump effects in the stock price dynamics.

Table 4.8: $\delta^{+}(0, \nu_0; q)$ for the model with jump and without jumps

	q	Model with jumps	Model without jumps
	-2	0.77788	0.774227
	-1	0.60005	0.596332
FENER	0	0.515289	0.511367
	1	0.451834	0.44768
	2	0.371151	0.366811
	3	0.202215	0.19784
	-2	0.622228	0.618619
	-1	0.520973	0.517026
AGHOL	0	0.471142	0.467149
	1	0.42482	0.420826
	2	0.375757	0.371727
	3	0.280466	0.276138
	-2	0.764837	0.761233
	-1	0.616139	0.612212
ARCLK	0	0.532997	0.528999
	1	0.456727	0.452726
	2	0.373905	0.369837
	3	0.226769	0.222387
	-2	0.673899	0.670432
	-1	0.550525	0.54665
EREGL	0	0.500784	0.496801
	1	0.459128	0.455122
	2	0.410269	0.406165
	3	0.291059	0.286571

Table 4.9: $\delta^{-}(0, \nu_0; q)$ for the model with jump and without jumps

	q	Model with jumps	Model without jumps
FENER	-3	0.23012	0.225773
	-2	0.40795	0.403668
	-1	0.492711	0.488633
	0	0.556166	0.55232
	1	0.636849	0.633189
	2	0.805785	0.802159
AGHOL	-3	0.385772	0.381381
	-2	0.487027	0.482974
	-1	0.536858	0.532851
	0	0.58318	0.579174
	1	0.632243	0.628273
	2	0.727534	0.723862
ARCLK	-3	0.243163	0.238767
	-2	0.391861	0.387788
	-1	0.475003	0.471001
	0	0.551273	0.547274
	1	0.634095	0.630163
	2	0.781231	0.777613
EREGL	-3	0.334101	0.329568
	-2	0.457475	0.45335
	-1	0.507216	0.503199
	0	0.548872	0.544878
	1	0.597731	0.593835
	2	0.716941	0.713429

Table 4.10 provides the optimal average spreads for each of the stock. From the results, we can conclude that the stock with lower average spread, that is FENER, produces a higher PnL and standard deviation of both PnL and inventory.

Table 4.11 reveals some statistics of "Model 1" for each stock comparing the results with the symmetric strategy. It is undoubtedly observable that the optimal strategy results in very slightly lower PnL but lower standard deviation at the same time. Through these stocks, the higher value of the estimated intensities for the stock FENER draw the attention. Such a sign indicates a salient relatively high PnL and standard deviation for this stock as shown in Table 4.11. By this evidence, we can also associate the higher and positive values of the function $u(t, \nu; q)$ for the stock

Table 4.10: Average spreads

	FENER	AGHOL	ARCLK	EREGL
Average spread	1.0434	1.0560	1.0689	1.0486

FENER comparing to the results of $u(t, \nu; q)$ for other stocks.

Altogether, when the model with quadratic utility function is applied on the stocks which are traded in an emerging market, i.e., Turkish stock market Borsa Istanbul, it satisfies a profitable strategy in terms of the terminal PnL and the standard deviation, and a mean-reverting inventory process which reverts to zero.

Table 4.11: Comparison of the strategy with symmetric strategy for each stock

		PnL	Std dev of PnL	Final q	Std dev of q
FENER	Inventory	2.02	2.11	-0.17	1.65
	Symmetric	1.94	2.43	-0.46	1.64
AGHOL	Inventory	0.25	0.75	0.0	0.54
	Symmetric	0.28	0.87	-0.07	0.60
ARCLK	Inventory	0.56	0.87	0.02	0.81
	Symmetric	0.61	0.92	0.07	0.75
EREGL	Inventory	0.53	1.05	0.07	0.77
	Symmetric	0.54	1.26	-0.2	0.74

Effects of the intensities $\lambda^{\pm}$

In the parameter estimation results, it is observable that the jump intensities $\lambda^{\pm}$ for the stock FENER are higher compared to that of the other stocks. With this observation, we notice that the optimal spreads for the stocks with lower intensities are changing more rapidly in their graphs. This shows that the larger jump intensities are the meaning of more trades resulting in narrow spreads. This fact is illustrated in the Table 4.12 which is performed only with the estimated parameters for the stock FENER for different symmetric intensities.

Table 4.12: Effects of $\lambda^{\pm}$

	$\lambda^{\pm} = 0.2$	$\lambda^{\pm} = 0.4$	$\lambda^{\pm} = 0.6$
Average spread	1.0442	1.0435	1.0432

4.3.2 Parameter Estimation and Applications for Model 2

In this part, we provide the numerical results for the case of the exponential utility function, that is "Model 2", with the estimated parameters given by the Table 4.6 and the fixed parameters given by the Table 4.7.

Table 4.13 involves the consequences for different risk aversion degrees γ only on the optimal sell spreads $\delta^{+}(0, \nu_0; q)$ for each stock. We hereby notice that the optimal sell spreads increase when the risk aversion degree of the investor increases on the negative levels of inventories. However, the spreads decrease on the positive inventory levels with an increasing risk aversion degree of the investor which is a consistent result in terms of the price and liquidation risks.

Table 4.14 presents the change of the average spreads corresponding to the different risk aversion degree of the investor. It is shown that when the degree of the risk aversion increases, the average spread increases for all stocks. This result is meaningful since the liquidity of the stock decreases when the investor is more risk averse which causes larger spreads.

Table 4.14: Average spreads for different risk aversion degrees

	$\gamma = 0.0001$	$\gamma = 0.001$	$\gamma = 0.01$
FENER	1.0277	1.0302	1.0537
AGHOL	1.0281	1.0302	1.0513
ARCLK	1.0280	1.0303	1.0536
EREGL	1.0281	1.0313	1.0626

Table 4.13: Effects of γ on $\delta^{+}(0,\nu_0;q)$

	q	$\gamma=0.0001$	$\gamma=0.001$	$\gamma=0.01$
FENER	-2	0.764506	0.766626	0.787587
	-1	0.58855	0.590363	0.608131
	0	0.510569	0.511248	0.517811
	1	0.455759	0.454982	0.447329
	2	0.382185	0.380216	0.360789
	3	0.215463	0.213129	0.189919
AGHOL	-2	0.564006	0.568749	0.616326
	-1	0.482408	0.485534	0.51669
	0	0.457833	0.45884	0.468846
	1	0.437416	0.436243	0.424588
	2	0.413757	0.410452	0.377605
	3	0.338819	0.333833	0.284114
ARCLK	-2	0.651285	0.658229	0.72736
	-1	0.537719	0.54255	0.590199
	0	0.50575	0.507366	0.523225
	1	0.483506	0.481694	0.463811
	2	0.451986	0.446946	0.397018
	3	0.340301	0.333122	0.261251
EREGL	-2	0.633135	0.639744	0.705621
	-1	0.521886	0.526527	0.572302
	0	0.490695	0.492261	0.507615
	1	0.468775	0.467054	0.450083
	2	0.438602	0.43378	0.386059
	3	0.331853	0.325001	0.25647

Table 4.15: Comparison of the strategy with symmetric strategy for each stock with the risk aversion degree $\gamma = 0.01$

		PnL	Std dev of PnL	Final q	Std dev of q
FENER	Inventory	1.33	1.59	0.51	1.51
	Symmetric	1.46	1.59	-0.07	1.22
AGHOL	Inventory	0.13	0.30	0.07	0.34
	Symmetric	0.15	0.38	0.05	0.58
ARCLK	Inventory	0.42	0.77	0.09	0.76
	Symmetric	0.43	1.12	0.02	0.75
EREGL	Inventory	0.43	0.57	0.05	0.66
	Symmetric	0.40	0.51	0.12	0.63

As a next illustration, Table 4.15 shows that the statistical results for both PnL and standard deviation evaluated by the estimated parameters for each stock. We again observe that the stock FENER has relatively higher PnL and standard deviation compared to the other ones because of the higher jump intensities. The table also indicates that the strategy generates appropriate PnL and standard deviation compared to the symmetric strategy for all analyzed stocks.

4.3.3 Parameter Estimation and Applications for Model 3

In this part, while we provide the results for "Model 3", we also compare the consequences with "Model 1". The experiments are carried out with the calibrated parameters for the model given by Table 4.16 and the fixed parameters given by the Table 4.7. The aim is to see the behavior of the trader for the optimal spreads generated by both models on the stocks in an emerging market.

In Table 4.17, it can be observed that the average spreads which are obtained by "Model 1" are slightly larger than that of "Model 3". Hence, the stocks will be more traded ones with "Model 3" as they have smaller spreads.

Table 4.17: Average spreads for the given stocks

		Average spread
FENER	Model 1	1.0434
	Model 3	1.0404
AGHOL	Model 1	1.0560
	Model 3	1.0480
ARCLK	Model 1	1.0689
	Model 3	1.0609
EREGL	Model 1	1.0486
	Model 3	1.0405

Table 4.18 exhibits that both models produce quite well results. Nevertheless, "Model 3" usually provides smaller but less riskier profit and loss at the end of the trade for the analyzed stocks according to the results.

Table 4.16: Estimation results for the stocks for Model 3

		Estimate	Std error
FENER	$\hat{\rho}$	-0.367579371	0.141935501
	$\hat{\sigma}$	0.165582174	0.009993511
	$\hat{\mu}$	-0.002577744	0.080611373
	$\hat{k}$	0.358303422	0.096038288
	$\hat{\theta}$	0.389447560	0.037853592
	$\hat{\lambda^+}$	0.6448054	0.01231161
	$\hat{\lambda^-}$	0.6429248	0.01229364
AGHOL	$\hat{\rho}$	0.178438055	0.064817902
	$\hat{\sigma}$	0.233059741	0.003078144
	$\hat{\mu}$	-0.005674979	0.066279721
	$\hat{k}$	0.511847115	0.128105181
	$\hat{\theta}$	0.306111173	0.033599105
	$\hat{\lambda^+}$	0.1063646	0.002734256
	$\hat{\lambda^-}$	0.1063652	0.002734272
ARCLK	$\hat{\rho}$	-0.2892213482	0.047795044
	$\hat{\sigma}$	0.2701155459	0.004321504
	$\hat{\mu}$	-0.0009525923	0.084354563
	$\hat{k}$	0.7785487472	0.139258674
	$\hat{\theta}$	0.4582132795	0.030874946
	$\hat{\lambda^+}$	0.1695126	0.003449993
	$\hat{\lambda^-}$	0.1694423	0.003449278
EREGL	$\hat{\rho}$	-0.193997520	0.092728178
	$\hat{\sigma}$	0.166512780	0.003255053
	$\hat{\mu}$	-0.002462423	0.095412680
	$\hat{k}$	0.292166191	0.085181457
	$\hat{\theta}$	0.565964490	0.056797135
	$\hat{\lambda^+}$	0.1561535	0.003319274
	$\hat{\lambda^-}$	0.1561551	0.003319309

Table 4.18: Comparison of Model 1 and Model 3 for the given stocks

		PnL	Std dev of PnL	Final q	Std dev of q
FENER	Model 1	2.02	2.11	-0.17	1.65
	Model 3	2.21	1.91	0.58	1.18
AGHOL	Model 1	0.25	0.75	0.0	0.54
	Model 3	0.17	0.63	0.02	0.71
ARCLK	Model 1	0.56	0.87	0.02	0.81
	Model 3	0.43	0.66	0.09	0.65
EREGL	Model 1	0.53	1.05	0.07	0.77
	Model 3	0.38	0.85	0.07	0.71

4.3.4 Comparison with Existing Models

This section covers the comparison of the models that we work on Chapter 3 with the existing models defined in Section 3.5.4 for the fixed parameters given by Table 4.7 and, the estimated parameters given by Table 4.6 and Table 4.16.

First, let us provide the estimated σ variables in Table 4.19 for each stock to use in "Model a" and "Model b".

Table 4.19: Estimation results for the stocks for Model a and Model b

		Estimate	Std error
FENER	$\hat{\sigma}$	0.05393771	0.0003139071
AGHOL	$\hat{\sigma}$	0.04959306	0.0002873309
ARCLK	$\hat{\sigma}$	0.08808467	0.0005178277
EREGL	$\hat{\sigma}$	0.04675763	0.0002704871

Table 4.20 and Table 4.21 are the representations for the comparison of the models in Section 3.5.4 by the means of the estimated parameters.

First of all, we observe that the higher jump intensities of the stock FENER leads to higher PnL and Sharpe ratios comparing to the results of other stocks. In addition, "Model c" and "Model d" produce relatively larger standard deviations, but also the larger means of PnL with well Sharpe ratios. The skewness and kurtosis values reveal that both PnL and inventory processes approximate to the normal distribution. Coherently, “Model c” and “Model d” perform with well results on the high-frequency data of Turkish stock market and also cover the stochastic volatility reality with jump effects in the stock price dynamics.

Table 4.20: Statistical comparison for PnL and inventory under the quadratic utility function

			Model a	Model b	Model c	Model d
FENER	PnL	Mean	1.4403	1.4004	2.2447	2.4837
		Std dev	0.9371	0.9384	1.4633	2.1846
		Sharpe ratio	1.5368	1.4923	1.5340	1.1369
		Skewness	0.5972	0.8134	-0.2454	1.5317
		Kurtosis	0.1262	1.1052	-0.0597	2.8881
	Inventory	Mean	-0.056	0.216	0.0731	-0.6829
		Std dev	1.4010	1.4083	1.1973	1.8797
		Sharpe ratio	-0.0399	0.1533	0.0611	-0.3632
		Skewness	0.0101	0.0711	0.3705	0.4622
		Kurtosis	0.4269	0.2318	0.1502	0.9331
AGHOL	PnL	Mean	0.2254	0.2175	0.4231	0.7829
		Std dev	0.3831	0.3908	0.7362	0.9628
		Sharpe ratio	0.5884	0.5566	0.5747	0.8131
		Skewness	1.7080	2.0525	1.5800	0.8939
		Kurtosis	2.2707	4.3748	1.2790	-0.5954
	Inventory	Mean	0.033	0.035	0.024	0.2195
		Std dev	0.5530	0.5251	0.6043	0.8698
		Sharpe ratio	0.0596	0.0666	0.0403	0.2523
		Skewness	0.0158	0.1657	-0.6735	0.6720
		Kurtosis	5.6410	3.8849	2.0349	-0.1029

Table 4.22 and Table 4.23 report the results for the comparison of the models in Section 3.5.4 under the exponential utility function with a risk aversion degree $\gamma = 0.01$. We can observe that “Model C” creates higher profit with also higher standard deviation for the stock FENER with the property of larger jump intensities. Besides, the model approaches to the normal distribution for the same stock. For the other analyzed stocks, we can easily notice that adding jumps to a stock price model reduces the Sharpe ratio. Meanwhile, “Model C” expresses the reality well as it has the jumps in prices and stochastic volatility dynamics also producing good results in terms of profits and standard deviation.

Table 4.21: Statistical comparison for PnL and inventory under the quadratic utility function

			Model a	Model b	Model c	Model d
ARCLK	PnL	Mean	0.2193	0.3923	0.4929	0.8524
		Std dev	0.3854	0.5223	0.9444	1.2947
		Sharpe ratio	0.5691	0.7510	0.5219	0.6584
		Skewness	1.9711	1.6813	1.8840	0.1069
		Kurtosis	4.1604	3.7659	3.6548	0.3853
	Inventory	Mean	0.078	0.169	-0.0731	0.4878
		Std dev	0.5309	0.7592	0.7119	0.9658
		Sharpe ratio	0.1469	0.2225	-0.1027	0.5050
		Skewness	0.5582	0.4202	-0.2989	-0.6152
		Kurtosis	2.5815	2.2638	2.2254	0.3476
EREGL	PnL	Mean	0.4223	0.3507	0.4400	0.6375
		Std dev	0.5385	0.4840	0.8289	1.0776
		Sharpe ratio	0.7841	0.7245	0.5307	0.5916
		Skewness	1.4988	1.6306	1.7397	0.1094
		Kurtosis	2.3887	3.2560	3.5336	0.5898
	Inventory	Mean	0.112	0.097	0.0731	0.3170
		Std dev	0.7664	0.6925	0.6768	1.0462
		Sharpe ratio	0.1461	0.1400	0.1081	0.3030
		Skewness	0.1670	0.1581	0.3824	0.3621
		Kurtosis	1.8852	2.9887	0.3678	-0.0696

4.3.5 Comparison of Model 1 and Model 2

Now, we compare the model under the quadratic utility function, that is “Model 1”, with the model defined under the exponential utility function, that is “Model 2”, with a risk aversion degree of $\gamma = 0.01$ and for $\psi = 0$ in Tables 4.24 and 4.25. In the light of the below results, it is clear that the stocks are more liquid when a quadratic utility function is used in the value function. This evidence is relevant to higher profits and standard deviation of profits for this type of the utility function comparing to the exponential utility function. Moreover, when the risk averse degree is increased, it should be expected to have less slightly profits for each stock.

Table 4.22: Statistical comparison for PnL and inventory under the exponential utility function

			Model A	Model B	Model C
FENER	PnL	Mean	0.8535	0.9914	1.9275
		Std dev	0.7131	0.8026	1.8953
		Sharpe ratio	1.1969	1.2352	1.0169
		Skewness	0.7715	0.8952	0.1631
		Kurtosis	0.2837	0.7166	0.6030
	Inventory	Mean	0.057	0.193	-0.4634
		Std dev	1.0889	1.1856	1.6978
		Sharpe ratio	0.0523	0.1627	-0.2729
		Skewness	-0.029	-0.0276	0.3258
		Kurtosis	1.0103	0.9466	-0.1178
AGHOL	PnL	Mean	0.7840	0.5170	0.2499
		Std dev	0.7265	0.5817	0.5410
		Sharpe ratio	1.0791	0.8887	0.4619
		Skewness	1.0804	1.2232	1.7037
		Kurtosis	1.1932	1.5215	3.1995
	Inventory	Mean	0.007	0.121	0.17073
		Std dev	0.5530	0.5251	0.5365
		Sharpe ratio	0.0068	0.1509	0.3181
		Skewness	-0.0195	0.1282	1.0655
		Kurtosis	1.4093	1.5183	2.3814

Table 4.24: Average spreads for the models with quadratic and exponential utility functions

	Quadratic	Exponential
FENER	1.0274	1.0537
AGHOL	1.0278	1.0513
ARCLK	1.0277	1.0536
EREGL	1.0278	1.0626

Table 4.23: Statistical comparison for PnL and inventory under the exponential utility function

			Model A	Model B	Model C
ARCLK	PnL	Mean	0.8293	0.4249	0.6896
		Std dev	0.7508	0.5553	1.2856
		Sharpe ratio	1.1045	0.7651	0.5364
		Skewness	1.2387	1.4914	2.5974
		Kurtosis	2.4698	2.4501	6.1763
	Inventory	Mean	0.12	0.105	0.3170
		Std dev	1.1788	0.7210	0.7789
		Sharpe ratio	0.1018	0.1456	0.4070
		Skewness	-0.0060	0.4802	0.6206
		Kurtosis	1.5699	2.1072	0.0686
EREGL	PnL	Mean	0.6607	0.3675	0.5517
		Std dev	0.6199	0.5188	1.2303
		Sharpe ratio	1.0658	0.7084	0.4485
		Skewness	0.9464	1.8526	-0.6051
		Kurtosis	0.9633	5.2871	3.8539
	Inventory	Mean	0.074	0.019	0.1707
		Std dev	0.9718	0.7104	0.7933
		Sharpe ratio	0.0761	0.0267	0.2152
		Skewness	-0.0371	-0.0439	0.2725
		Kurtosis	2.0632	3.0830	1.1032

Table 4.25: Comparison of the models with quadratic and exponential utility functions

		PnL	Std dev of PnL	Final q	Std dev of q
FENER	Quadratic	1.80	2.18	-0.17	1.74
	Exponential	1.62	2.10	0.60	1.55
AGHOL	Quadratic	0.30	0.63	0.04	0.54
	Exponential	0.22	0.60	0.21	0.41
ARCLK	Quadratic	0.55	1.39	0.21	0.97
	Exponential	0.27	0.78	0.07	0.67
EREGL	Quadratic	0.39	1.15	0.02	0.81
	Exponential	0.30	0.67	0.41	0.66

4.4 Applications on a Post Covid-19 Pandemic Period

This part includes the results for the analyses of the models defined in Chapter 3 in a period of Covid-19 pandemic which leads to deep economic consequences globally because of the lockdowns.

Tables 4.26 – 4.29 present the descriptive properties of the listed stocks in Table 4.1 on July 8, 2020 where we can simply see the excess skewness and kurtosis values of both prices and volatilities for each stock.

Table 4.26: Descriptive statistics on the price and volatility for the stock FENER

	Mean	Std dev	Skewness	Kurtosis
Price	12.95407	0.05364403	1.345411	8.158702
Volatility	0.5483445	0.2853055	2.552679	13.79426

Table 4.27: Descriptive statistics on the price and volatility for the stock AGHOL

	Mean	Std dev	Skewness	Kurtosis
Price	21.53372	0.1736499	-1.522491	8.725423
Volatility	0.6149144	0.3626831	1.73732	6.514356

Table 4.28: Descriptive statistics on the price and volatility for the stock ARCLK

	Mean	Std dev	Skewness	Kurtosis
Price	19.71222	0.04462048	-1.146808	12.98358
Volatility	0.3710144	0.1453511	1.48314	5.577385

Table 4.29: Descriptive statistics on the price and volatility for the stock EREGL

	Mean	Std dev	Skewness	Kurtosis
Price	8.655773	0.04351151	-1.081301	4.202644
Volatility	0.9031066	0.1963276	0.1077365	2.505967

4.4.1 Parameter Estimation and Applications for Model 1

Estimated parameters of “Model 1” with their standard errors are given by Table 4.30 for each stock.

Table 4.30: Estimation results for the stocks for Model 1 and Model 2

		Estimate	Std error
FENER	$\hat{\rho}$	-0.421229046	0.037574188
	$\hat{\sigma}$	0.256615364	0.005114366
	$\hat{\mu}$	-0.006947857	0.089204015
	$\hat{k}$	0.596926810	0.098729747
	$\hat{\theta}$	0.488550133	0.038860900
	$\hat{\lambda}^{+}$	0.1289176	0.002992245
	$\hat{\lambda}^{-}$	0.1289183	0.002992262
AGHOL	$\hat{\rho}$	-0.05226043	0.069559012
	$\hat{\sigma}$	0.23675135	0.001658542
	$\hat{\mu}$	0.01823702	0.090685443
	$\hat{k}$	0.26549365	0.080919894
	$\hat{\theta}$	0.53854776	0.084129167
	$\hat{\lambda}^{+}$	0.09771853	0.00260486
	$\hat{\lambda}^{-}$	0.09764908	0.002603934
ARCLK	$\hat{\rho}$	-0.394852202	0.03481117
	$\hat{\sigma}$	0.234183508	0.00400153
	$\hat{\mu}$	0.001687635	0.07577822
	$\hat{k}$	0.646702107	0.13420949
	$\hat{\theta}$	0.364845396	0.02863185
	$\hat{\lambda}^{+}$	0.1376509	0.003091749
	$\hat{\lambda}^{-}$	0.1376504	0.003091738
EREGL	$\hat{\rho}$	-0.097725808	0.195622907
	$\hat{\sigma}$	0.216993272	0.004369507
	$\hat{\mu}$	0.000406516	0.123018873
	$\hat{k}$	0.564929853	0.134304291
	$\hat{\theta}$	0.905965023	0.048638867
	$\hat{\lambda}^{+}$	0.1736946	0.003473082
	$\hat{\lambda}^{-}$	0.1736942	0.003473074

Results for the stock FENER

Figure 4.15 demonstrates a path of the profit and loss function and the optimal prices for the stock FENER in a post Covid-19 time period. In the right figure, it is observed that the price of the stock and the optimal spreads have been decreased comparing to

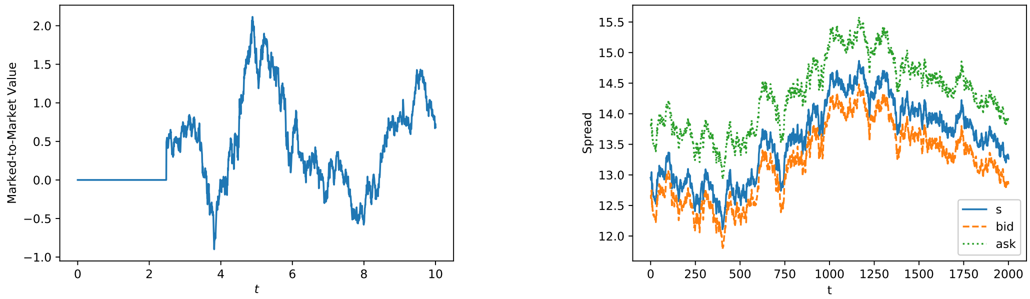

Figure 4.15: A path of the simulated PnL and the optimal prices for the stock FENER

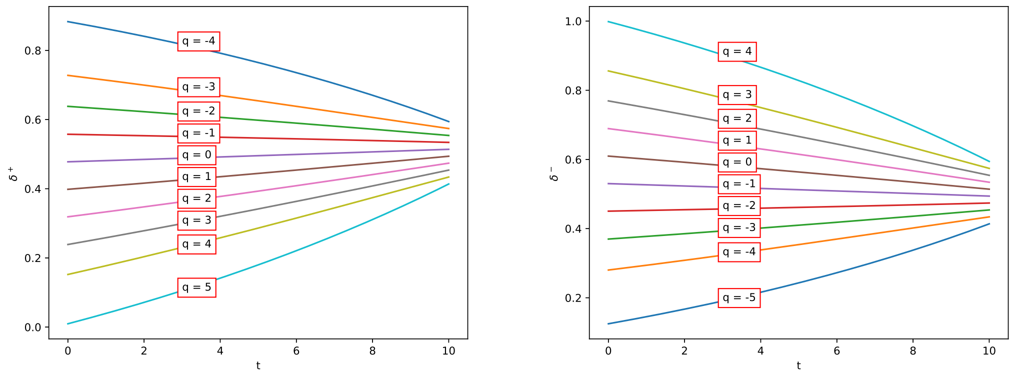

(a) δ^+ (b) δ^-

Figure 4.16: Optimal spreads δ^+ and δ^- for the stock FENER

the figure which is obtained in time before Covid-19. This result can be related with the sector of the stock as it is a much affected sector due to the pandemic. As a further result, the intensities $\lambda^\pm$ of the jumps in the stock price dynamics are less than the intensities achieved in the before Covid-19 time which may cause a less traded stock. Table 4.31 shows that the resulting profit and the standard deviation of the profit obtained by the strategy of "Model 1" are also less than comparing to the previous term, but the strategy still produces higher profit standard deviation comparing to the symmetric strategy, as well.

Figure 4.16 is a representation of the optimal spreads for the stock FENER on the given time.

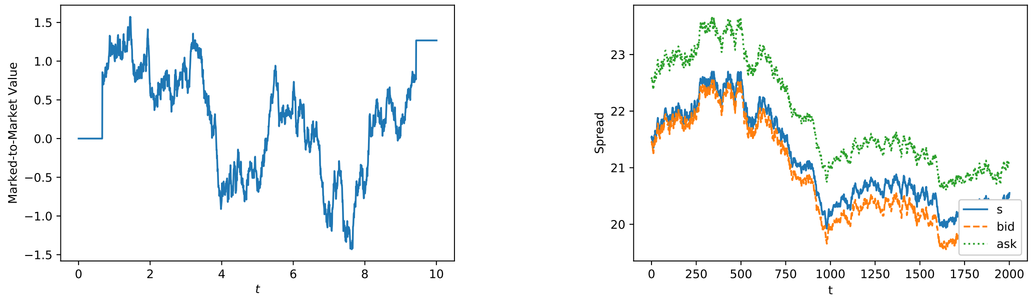

Figure 4.17: A path of the simulated PnL and the optimal prices for the stock AGHOL

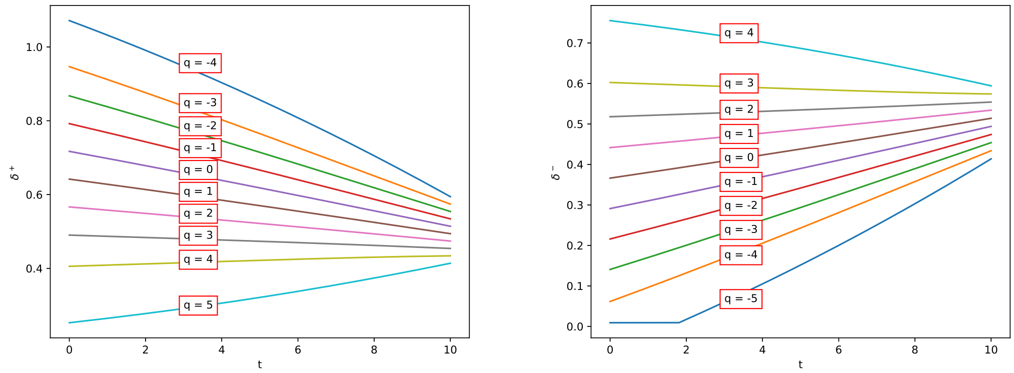

(a) δ^+ (b) δ^-

Figure 4.18: Optimal spreads δ^+ and δ^- for the stock AGHOL

Results for the stock AGHOL

In the right panel of the Figure 4.17, we can see that the stock AGHOL is bought very close to the midprice especially at the beginnings of the trading session. Comparing with the previous experiments, it can be deduced that the stock is more traded in the post Covid-19 period as the jump intensities are higher and provide larger profit according to the symmetric strategy, as well.

Results for the stock ARCLK

The stock ARCLK is traded with optimal buy prices which are very close to the midprice which can be seen in the Figure 4.19. On the other hand, it is observed that the depth of the optimal buy spreads are larger in contrast to the depth of the optimal sell spreads comparing to the pre Covid-19 period. Table 4.31 illustrates that the stock

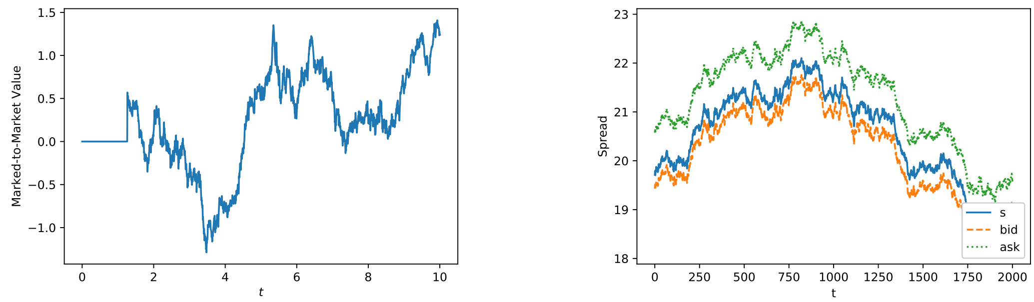

Figure 4.19: A path of the simulated PnL and the optimal prices for the stock ARCLK

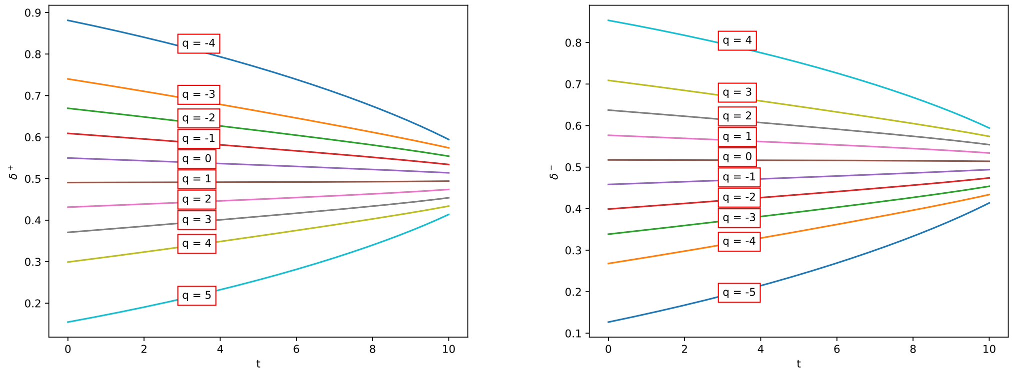

(a) δ^{+} (b) δ^{-}

Figure 4.20: Optimal spreads δ^{+} and δ^{-} for the stock ARCLK

creates larger profit comparing to both the time before Covid-19 and the symmetric strategy but with also larger standard deviation.

Results for the stock EREGL

For the stock EREGL, we observe that it leads higher jump intensities in the post Covid-19 term which may cause a more traded stock. Figure 4.21 shows an increasing path of the profit and loss function with the optimal prices.

Table 4.31 demonstrates that the strategy of “Model 1” results in a less profit compared to the symmetric strategy. Moreover, the risk of the strategy is less than the risk of the symmetric strategy for this stock. Additionally, an investor can obtain more profit with higher risk by trading the stock AGHOL at the chosen day in post Covid-19 term rather than the pre Covid-19 term.

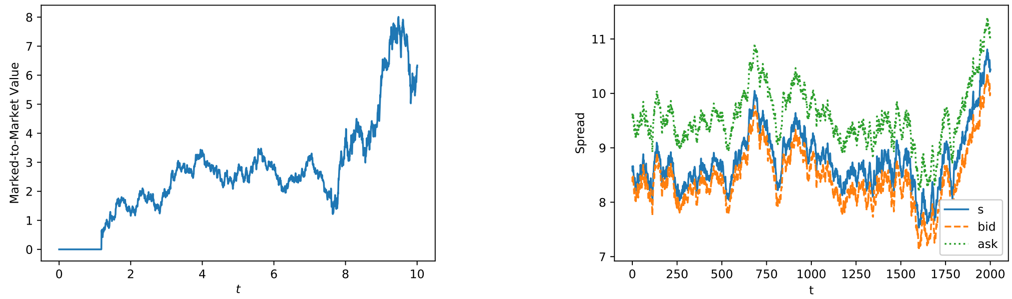

Figure 4.21: A path of the simulated PnL and the optimal prices for the stock EREGL

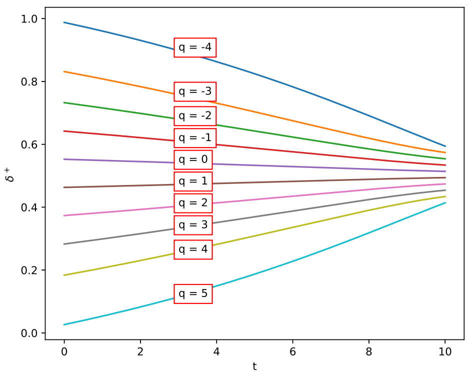

(a) δ^+

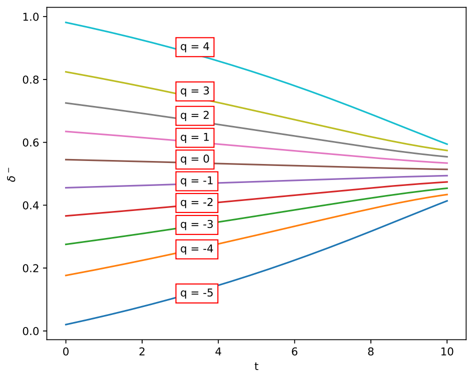

(b) δ^-

Figure 4.22: Optimal spreads δ^+ and δ^- for the stock EREGL

Table 4.31: Comparison of the strategy "Model 1" with symmetric strategy for each stock

		PnL	Std dev of PnL	Final q	Std dev of q
FENER	Inventory	1.16	1.38	-0.05	0.96
	Symmetric	0.73	1.22	0.02	1.04
AGHOL	Inventory	0.57	1.42	0.09	0.69
	Symmetric	0.34	1.38	-0.14	0.92
ARCLK	Inventory	0.83	1.39	0.02	0.97
	Symmetric	0.33	1.09	0.17	0.96
EREGL	Inventory	1.05	1.35	-0.09	0.75
	Symmetric	1.22	1.49	0.12	1.13

4.4.2 Parameter Estimation and Applications for Model 2

Now, we repeat the numerical experiments for the case of the exponential utility function expressed by "Model 2" with the estimated parameters and the fixed parameters given in Table 4.30 and Table 4.7, respectively.

We first examine the effect of the different risk averse parameter, γ, on the average spread given in Table 4.32. As in the pre Covid-19 pandemic time, it is observed that the average spread increases when γ increases since an investor who is highly risk averse is not willing to trade more which causes larger spreads.

Table 4.32: Average spreads for different risk aversion degrees

	$\gamma = 0.0001$	$\gamma = 0.001$	$\gamma = 0.01$
FENER	1.0279	1.0305	1.0557
AGHOL	1.0280	1.0312	1.0623
ARCLK	1.0278	1.0299	1.0509
EREGL	1.0279	1.0318	1.0689

In comparison with the previous results under the exponential utility function, we realize that the profit and standard deviation of the stock FENER have been declined on July, 2020 which can be noticed from Table 4.33 while the other stocks have been increased. Beside, a decrease in both profit and risk can be observed for the stocks

FENER and AGHOL in contrast to the results under the quadratic utility function at the same time.

Table 4.33: Comparison of the strategy of “Model 2” with symmetric strategy for each stock with the risk aversion degree $\gamma = 0.01$

		PnL	Std dev of PnL	Final q	Std dev of q
FENER	Inventory	0.89	1.31	0.02	0.89
	Symmetric	0.26	1.06	0.02	0.87
AGHOL	Inventory	0.44	1.37	0.53	0.88
	Symmetric	0.14	0.93	-0.26	0.58
ARCLK	Inventory	1.08	1.55	0.48	1.11
	Symmetric	0.92	1.19	-0.19	1.02
EREGL	Inventory	1.45	2.57	0.85	1.28
	Symmetric	0.78	1.82	-0.19	0.94

4.4.3 Parameter Estimation and Applications for Model 3

This part examines the results for “Model 3” which includes jump components in the volatility dynamics. The estimation of the parameters for the model are given by Table 4.34 for each stock. From the table, we see that the stock EREGL has higher jump intensities compared to the others.

The average spreads for each stock are provided in Table 4.35. As in the pre Covid-19 time, the optimal spreads obtained by “Model 1” are larger than that of the “Model 3”.

Table 4.35: Average spreads for the given stocks

		Average spread
FENER	Model 1	1.0677
	Model 3	1.0583
AGHOL	Model 1	1.0692
	Model 3	1.0599
ARCLK	Model 1	1.0558
	Model 3	1.0469
EREGL	Model 1	1.0689
	Model 3	1.0587

The related comparison of “Model 1” and “Model 3” in terms of profit and loss function for each stock with their risks are provided in Table 4.36. It can be observed that the stock AGHOL which has the less intensity produces less PnL as a result of the largest bid-ask spread among the others. Moreover, it can be said that “Model 3” is riskier for an investor to trade on these stocks on this time period because of the higher standard deviations and generally less PnL which can be seen from the Table 4.36.

Table 4.36: Comparison of Model 1 and Model 3 for the given stocks

		PnL	Std dev of PnL	Final q	Std dev of q
FENER	Model 1	1.16	1.38	-0.05	0.96
	Model 3	0.69	1.06	0.53	1.06
AGHOL	Model 1	0.57	1.42	0.09	0.69
	Model 3	0.51	2.22	0.58	1.58
ARCLK	Model 1	0.83	1.39	0.02	0.97
	Model 3	0.61	1.34	-0.07	1.29
EREGL	Model 1	1.05	1.35	-0.09	0.75
	Model 3	1.28	2.72	0.60	1.24

4.4.4 Comparison with Existing Models

In this part, we compare the models studied in Chapter 3 with the existing models which are mentioned in Section 3.5.4 using the estimated parameters in Table 4.30 and Table 4.34 for the post Covid-19 time.

For “Model a” and “Model b” defined in Chapter 3, the estimations of σ for each stock are given in Table 4.37.

Table 4.37: Estimation results for the stocks for Model a and Model b

		Estimate	Std error
FENER	$\hat{\sigma}$	0.06433965	0.0003756643
AGHOL	$\hat{\sigma}$	0.1255504	0.0007423953
ARCLK	$\hat{\sigma}$	0.06514671	0.0003800451
EREGL	$\hat{\sigma}$	0.06634283	0.0003873817

Table 4.38 and Table 4.39 represent the comparison of the models with existing models under the quadratic utility function for the given time in this part. It is observable that “Model c” and “Model d” are still profitable in the specified time after Covid-19, but they are considerably riskier than the other models. Hence, these models are suitable for a trader who can take more risk.

Table 4.38: Statistical comparison for PnL and inventory under the quadratic utility function

			Model a	Model b	Model c	Model d
FENER	PnL	Mean	0.4286	0.4480	1.0798	0.9584
		Std dev	0.6475	0.7267	1.3453	1.2959
		Sharpe ratio	0.6619	0.6164	0.8026	0.7395
		Skewness	0.8414	1.0112	0.7448	1.4637
		Kurtosis	1.8987	3.2216	0.1178	1.4477
	Inventory	Mean	0.2890	0.3500	0.1219	1.2927
		Std dev	0.9578	0.9096	0.8022	0.9433
		Sharpe ratio	0.3017	0.3847	0.1520	0.3102
		Skewness	0.5195	0.5290	-0.5067	-0.2633
		Kurtosis	1.3172	1.6399	0.8777	0.1892
AGHOL	PnL	Mean	0.2732	0.3896	0.5226	0.8662
		Std dev	0.5700	0.6108	0.9440	1.6827
		Sharpe ratio	0.4793	0.6378	0.5536	0.5147
		Skewness	0.7455	0.9358	0.1225	1.4640
		Kurtosis	4.4343	2.3058	-0.2360	2.1528
	Inventory	Mean	0.2720	0.4640	0.3170	0.4634
		Std dev	0.7694	0.8524	0.7469	0.9395
		Sharpe ratio	0.3535	0.5443	0.4244	0.4932
		Skewness	0.8359	0.8047	0.4640	1.6054
		Kurtosis	2.4993	1.2788	0.0335	3.8619

Table 4.39: Statistical comparison for PnL and inventory under the quadratic utility function

			Model a	Model b	Model c	Model d
ARCLK	PnL	Mean	0.4695	0.4826	0.8034	0.8686
		Std dev	0.3854	0.5223	0.9444	1.2947
		Sharpe ratio	0.6834	0.6822	1.0113	1.1734
		Skewness	0.7410	0.8200	-0.6316	0.1819
		Kurtosis	2.8085	1.2683	1.2159	1.4879
	Inventory	Mean	0.3150	0.3770	0.1951	0.1390
		Std dev	0.9432	0.9544	0.8328	1.0370
		Sharpe ratio	0.3339	0.3950	0.2342	0.1340
		Skewness	0.3513	0.3948	-0.1246	0.0973
		Kurtosis	0.9785	1.2407	0.1302	-0.1396
EREGL	PnL	Mean	0.5388	0.6364	1.2583	0.9249
		Std dev	0.6766	0.7600	1.7123	1.8954
		Sharpe ratio	0.7963	0.8373	0.7348	0.4879
		Skewness	1.0164	0.8682	1.9322	0.5342
		Kurtosis	1.6376	2.0285	4.7341	2.0480
	Inventory	Mean	0.1550	0.4400	0.1219	0.5053
		Std dev	0.9720	1.0480	1.1086	1.1888
		Sharpe ratio	0.1594	0.4198	0.1100	0.4923
		Skewness	0.1957	0.3204	0.2951	0.6677
		Kurtosis	1.3547	1.1785	0.1397	0.6175

For an investor having a risk averse degree, the introduced models are also considerable as it can be seen from Table 4.40 and Table 4.41. While the models are more profitable for each stock, they have higher standard deviation which decreases the Sharpe ratio in comparison with the existing models.

Table 4.40: Statistical comparison for PnL and inventory under the exponential utility function

			Model A	Model B	Model C
FENER	PnL	Mean	0.5854	0.5570	0.5636
		Std dev	0.7860	0.7281	0.9729
		Sharpe ratio	0.7448	0.7650	0.5793
		Skewness	1.7734	1.1557	1.9891
		Kurtosis	6.3523	1.4730	3.3780
	Inventory	Mean	0.0840	0.2010	-0.0731
		Std dev	0.8549	0.8744	0.6768
		Sharpe ratio	0.0982	0.2298	-0.1081
		Skewness	0.1363	0.4245	-1.7985
		Kurtosis	1.6162	1.1563	6.7301
AGHOL	PnL	Mean	0.4537	0.4566	1.2729
		Std dev	0.6330	0.6522	2.1667
		Sharpe ratio	0.7168	0.7000	0.5875
		Skewness	1.4843	1.3983	1.9170
		Kurtosis	2.3227	2.0942	4.3051
	Inventory	Mean	0.007	0.121	0.17073
		Std dev	0.5530	0.5251	0.5365
		Sharpe ratio	0.0068	0.1509	0.3181
		Skewness	-0.0195	0.1282	1.0655
		Kurtosis	1.4093	1.5183	2.3814

Table 4.41: Statistical comparison for PnL and inventory under the exponential utility function

			Model A	Model B	Model C
ARCLK	PnL	Mean	0.5821	0.5735	0.7805
		Std dev	0.7301	0.7074	1.0935
		Sharpe ratio	0.7974	0.8107	0.7138
		Skewness	1.4333	1.1611	1.3775
		Kurtosis	2.9090	1.7875	1.0586
	Inventory	Mean	0.0240	0.0900	0.3414
		Std dev	0.9525	0.9251	0.8441
		Sharpe ratio	0.0251	0.0972	0.4044
		Skewness	0.2715	0.1846	0.2608
		Kurtosis	2.1812	1.5234	-0.4927
EREGL	PnL	Mean	0.7451	0.7423	0.8616
		Std dev	0.8199	0.8075	1.5887
		Sharpe ratio	0.9088	0.9191	0.5423
		Skewness	1.4559	1.1524	0.6068
		Kurtosis	4.3007	1.6515	1.8717
	Inventory	Mean	0.0930	0.1030	0.1602
		Std dev	1.0140	1.0170	0.9344
		Sharpe ratio	0.0917	0.1012	0.1714
		Skewness	0.1412	-0.0130	-0.1656
		Kurtosis	1.4073	1.2400	0.0218

4.5 Analysis on Global Stocks

In this part, we perform the numerical experiments on "Model 1" for the stocks JUVE (Juventus Football Club SpA) traded in Borsa Italiana and MT (Arcelor Mittal) traded in the New York Stock Exchange (NYSE) comparing with the stocks FENER and EREGL in BIST since they take place in the same industries, respectively.

Figures 4.23 and 4.24 are the presentations of the prices and realized volatilities of the stocks JUVE and MT on the day of June 30, 2020 through the whole trading session.

The following tables 4.42 and 4.43 report the descriptive statistics properties of these stocks.

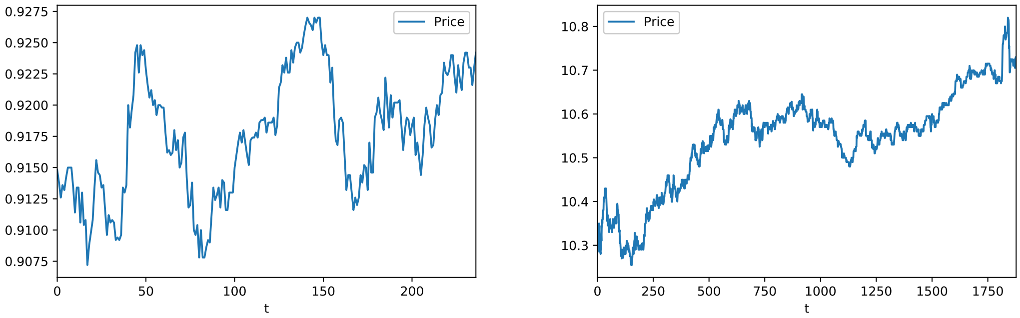

(a) JUVE (b) MT

Figure 4.23: Illustration of the stock prices of JUVE and MT

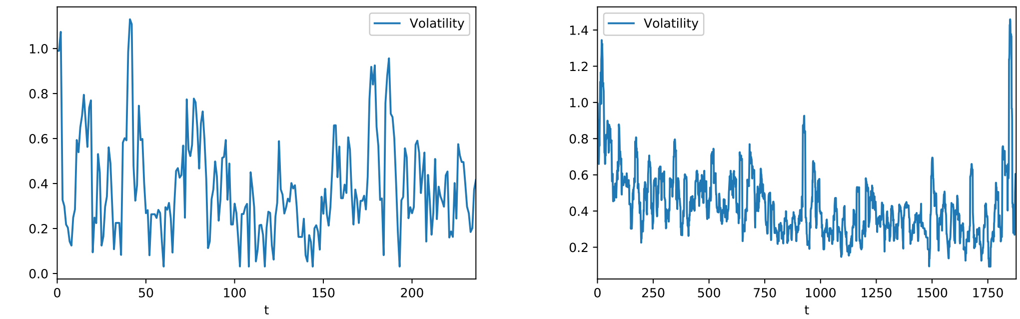

(a) JUVE (b) MT

Figure 4.24: Illustration of the volatilities of JUVE and MT

Table 4.42: Descriptive statistics on the price and volatility for the stock JUVE

	Mean	Std dev	Skewness	Kurtosis
Price	0.9175401	0.004831986	-0.01553123	2.155233
Volatility	0.3853216	0.2226497	0.9337616	3.770949

Table 4.43: Descriptive statistics on the price and volatility for the stock MT

	Mean	Std dev	Skewness	Kurtosis
Price	10.54354	0.1125986	-0.6144726	3.045242
Volatility	0.4366808	0.1891995	1.596987	7.660528

Now, we apply the optimal spreads formulas which are derived by the “Model 1” on the stocks JUVE and MT, and compare their results with the analyses on the stocks

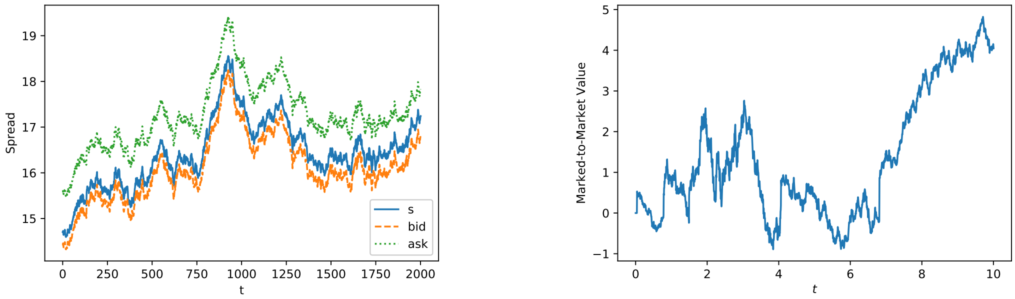

Figure 4.25: Optimal prices and a path of PnL for the stock JUVE

FENER and EREGL under the quadratic utility function.

Table 4.44 provides the estimated parameters of the model for the chosen assets.

Table 4.44: Estimation results for the stocks JUVE and MT for Model 1

		Estimate	Std error
JUVE	$\hat{\rho}$	-0.4270035386	0.05386165
	$\hat{\sigma}$	0.1803846288	0.00515994
	$\hat{\mu}$	0.0003199191	0.09541278
	$\hat{k}$	0.2934722245	0.08488954
	$\hat{\theta}$	0.5641174121	0.6064603
	$\hat{\lambda}^{+}$	0.7331465	0.04538055
	$\hat{\lambda}^{-}$	0.7554352	0.04530791
MT	$\hat{\rho}$	-0.4554403637	0.060222999
	$\hat{\sigma}$	0.1835452848	0.006424682
	$\hat{\mu}$	0.0004785057	0.095412422
	$\hat{k}$	0.2917415027	0.084957901
	$\hat{\theta}$	0.5637339403	0.061928032
	$\hat{\lambda}^{+}$	0.28973	0.008377659
	$\hat{\lambda}^{-}$	0.2842219	0.008312755

Using the estimated parameters, we first proceed with the graphs of the optimal prices, PnL, and optimal spreads for the stocks. As shown in the optimal prices graphs, which are, Figure 4.25 and Figure 4.27, the strategy allows to buy with a lower and closer price to the market value and to sell with a quite larger price as similar in the case of the stocks traded in BIST.

We first test the performance of the strategy on "Model 1" using the estimated pa-

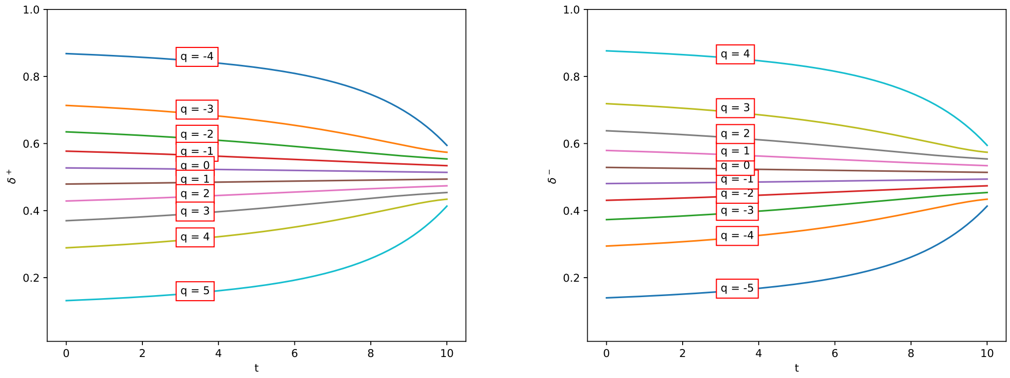

(a) δ^+ (b) δ^-

Figure 4.26: Optimal spreads δ^+ and δ^- for the stock JUVE

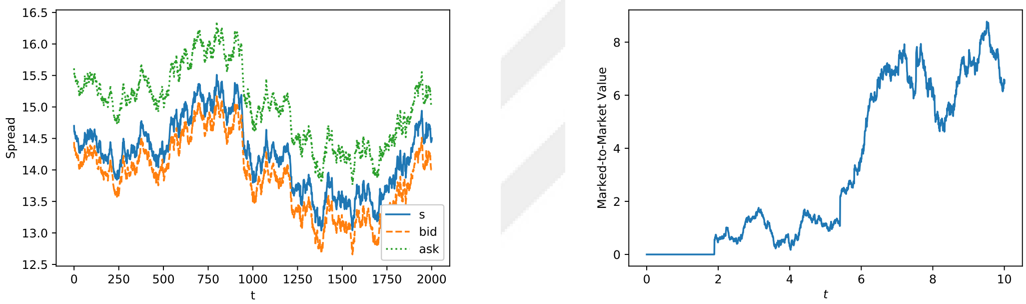

Figure 4.27: Optimal prices and a path of PnL for the stock MT

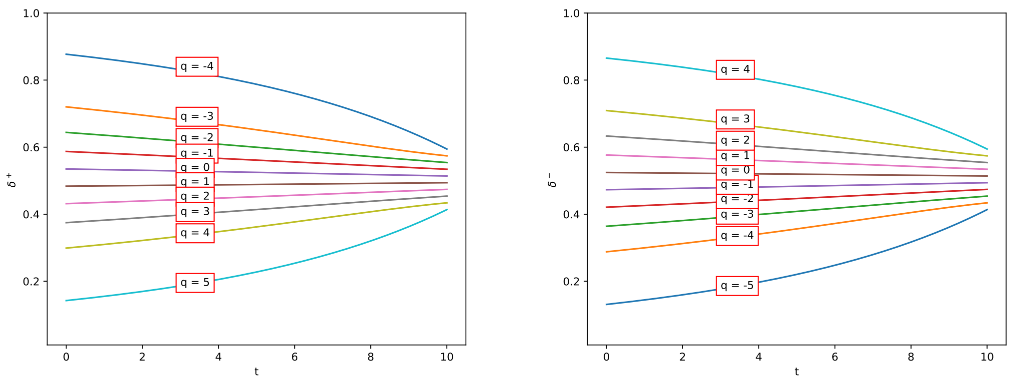

(a) δ^+ (b) δ^-

Figure 4.28: Optimal spreads δ^+ and δ^- for the stock MT

rameters of the stocks in terms of their optimal average spreads as represented in Table 4.45. It is noteworthy to mention that the results indicate higher spreads on the stocks JUVE and MT and thus, it can be concluded that the model causes more liquidation on the stocks in BIST.

Table 4.45: Average spreads for each stock

	Average spread
FENER	1.0434
JUVE	1.0488
EREGL	1.0486
MT	1.0513

Table 4.46 provides the details concerning the profit and standard deviation results on each stock comparing with the baseline symmetric strategy. For instance, while the stock FENER performs with a relatively higher profit and lower standard deviation, the stock JUVE which is in the same industry with FENER but traded in a different market performs absolutely fine, as well. In addition, it can be seen that the model produces well results both on PnL and inventory processes for the stock MT. In the light of these results, “Model 1” achieves profitable trades by taking behind the advantage of Heston model and market impact of the orders.

Table 4.46: Comparison of the strategy with symmetric strategy for each stock

		PnL	Std dev of PnL	Final q	Std dev of q
FENER	Inventory	2.02	2.11	-0.17	1.65
	Symmetric	1.94	2.43	-0.46	1.64
JUVE	Inventory	3.69	2.11	-0.14	1.47
	Symmetric	3.73	2.91	-0.19	2.03
EREGL	Inventory	0.53	1.05	0.07	0.77
	Symmetric	0.54	1.26	-0.2	0.74
MT	Inventory	1.53	1.50	0.21	1.13
	Symmetric	1.48	1.61	-0.17	1.18

4.6 Summary

In this section, we develop the applications of the models derived in Chapter 3 for optimal trading in a limit order book in different perspectives using a high-frequency real data which is obtained in a limit order book on emerging Turkish stock market, BIST. We first perform each derived model on the chosen stocks and then execute the performances on comparison of the models with existing models and on the global stocks. For this aim, we analyze our results in two different time slot as before and after Covid-19 pandemic in order to see that the models still succeed well in an exceptional time by looking at the statistical values of the models. To the best of our knowledge, the models derived in this thesis are the novel approaches based on the stock price dynamics for optimal market making problem in a limit order book enclosing both stochastic volatility and market impacts of the number of the orders. The numerical experiments present that when an investor trades with the usage of our models, she can obtain a well profit and meaningful standard deviation of both profits and inventories which make the models useful for practioners on both emerging and global markets.

Table 4.34: Estimation results for the stocks for Model 3

		Estimate	Std error
FENER	$\hat{\rho}$	-0.421229046	0.037574188
	$\hat{\sigma}$	0.256615364	0.005114366
	$\hat{\mu}$	-0.006947857	0.089204015
	$\hat{k}$	0.596926810	0.098729747
	$\hat{\theta}$	0.488550133	0.038860900
	$\hat{\lambda^+}$	0.2248137	0.003972862
	$\hat{\lambda^-}$	0.2248134	0.003972857
AGHOL	$\hat{\rho}$	-0.05226043	0.069559012
	$\hat{\sigma}$	0.23675135	0.001658542
	$\hat{\mu}$	0.01823702	0.090685443
	$\hat{k}$	0.26549365	0.080919894
	$\hat{\theta}$	0.53854776	0.084129167
	$\hat{\lambda^+}$	0.183341	0.003589987
	$\hat{\lambda^-}$	0.1832707	0.003589987
ARCLK	$\hat{\rho}$	-0.394852202	0.03481117
	$\hat{\sigma}$	0.234183508	0.00400153
	$\hat{\mu}$	0.001687635	0.07577822
	$\hat{k}$	0.646702107	0.13420949
	$\hat{\theta}$	0.364845396	0.02863185
	$\hat{\lambda^+}$	0.2472877	0.00416029
	$\hat{\lambda^-}$	0.2472891	0.004160313
EREGL	$\hat{\rho}$	-0.097725808	0.195622907
	$\hat{\sigma}$	0.216993272	0.004369507
	$\hat{\mu}$	0.000406516	0.123018873
	$\hat{k}$	0.564929853	0.134304291
	$\hat{\theta}$	0.905965023	0.048638867
	$\hat{\lambda^+}$	0.3087764	0.004639143
	$\hat{\lambda^-}$	0.3087754	0.004639127

CHAPTER 5

OPTIMAL MARKET MAKING MODELS WITH STOCHASTIC LATENCY

We dedicate this chapter for deriving the optimal bid and ask spreads in the presence of latency between the submission and execution of an order. More specifically, the latency can be described as a time delay between submitting an order, operating the information by the trader, admitting the order from the trader, and executing the order. The latency occurs commonly in real situations and it is stochastic which impacts the decisions and behaviour of the market maker within the trading period.

The topic has been a warm research area in optimal market making models since the latency affects the qualitative behaviour of the market maker. When there exists a latency during the trading, it may cause a fluctuation on the midprice and optimal quotes of the asset on this time interval. This results in higher risk and negative performance of the trader [25]. In [28], the latency is modeled as an Ornstein-Uhlenbeck (OU) process with zero mean and it exists in the underlying asset for the optimal liquidation process. In the literature, there exists time delay financial models which are applied on option pricing and portfolio optimization. For instance, Lee *et al.* introduce an extended delayed stochastic volatility model to develop a theory for option pricing in [42]. Carmona *et al.* [11] present a stochastic game model with delay and they introduce the HJB equation of the problem by using stochastic control theory. Larssen [41] studies the dynamic programming in stochastic control problems with delay.

Here, we consider the time delay as a stochastic latency which appears in the price as a novelty approach. We model the latency as a mean-reverting process and work with the difference between the price and latency. By this approach, we propose and discuss optimal market making models when the latency impact is taken into account in the line of the models studied in Chapter 3 and explore the behaviour of the market maker in the strategies.

5.1 A Limit Order Book Modeling with the Impact of Stochastic Latency

We build an optimal market making model with stock price having the stochastic latency where it is derived by Ornstein-Uhlenbeck (OU) process and also the jump components. In the model, the latency is included in the price and we assume that it is followed with a Wiener process since it causes fluctuations in the asset price.

We suppose that the midprice S_t of the stock is influenced by the latency where it is a mean-reverting stochastic process:

$$\begin{aligned} dS_t &= \sigma(S_t + \tau_t)dB_t^1 + \varepsilon^+ dM_t^+ - \varepsilon^- dM_t^-, \\ d\tau_t &= k(\theta - \tau_t)dt + \beta dB_t^2, \\ dB_t^1 dB_t^2 &= \rho dt. \end{aligned} \tag{5.1}$$

Here, we assume that there is no correlation between two Wiener processes dB_t^1 and dB_t^2, i.e., $\rho = 0$. σ denotes the constant volatility and β is the volatility of the latency.

In this chapter, we use the same assumptions given in Chapter 3, Section 3.1.1 for the wealth and inventory processes of the trader.

In order to see the effect of the stochastic latency on the behaviour of the optimal strategy, we consider the following value function to form a stochastic control problem:

$$W(t, x, S, \tau; q) = \sup_{(\delta_s^\pm)_{t \le s \le T} \in \mathcal{A}_t} \mathbb{E}\left[X_T + q_T(S_T - \alpha q_T) - \psi\sigma^2 \int_t^T q_s^2 \tau_s ds\right], \tag{5.2}$$

where the last term $\psi\sigma^2 \int_t^T q_s^2 \tau_s ds$ penalizes the inventory for $\psi > 0$.

Proposition 11. The dynamic programming suggests that the value function (5.2) is the unique solution of the HJB equation:

$$\partial_t W+k(\theta-\tau_t)\partial_\tau W+\frac{1}{2}\sigma^2(S_t+\tau_t)^2\partial_{SS}W+\frac{1}{2}\beta^2\partial_{\tau\tau}W+\sigma\rho\beta(S_t+\tau_t)\partial_{S\tau}W-\psi\tau_t q^2\sigma^2$$
$$+\sup_{\delta_t^+}\Big\{\Lambda_t^+(\delta_t^+)\mathbb{E}\left[W(t,x+(S_t+\delta_t^+),S_t+\varepsilon^+,\tau_t;q-1)-W(t,x,S_t,\tau_t;q)\right]$$
$$+(\lambda^+-\Lambda_t^+(\delta_t^+))\mathbb{E}\left[W(t,x,S_t+\varepsilon^+,\tau_t;q)-W(t,x,S_t,\tau_t;q)\right]\Big\}$$
$$+\sup_{\delta_t^-}\Big\{\Lambda_t^-(\delta_t^-)\mathbb{E}\left[W(t,x-(S_t-\delta_t^-),S_t-\varepsilon^-,\tau_t;q+1)-W(t,x,S_t,\tau_t;q)\right]$$
$$+(\lambda^--\Lambda_t^-(\delta_t^-))\mathbb{E}\left[W(t,x,S_t-\varepsilon^-,\tau_t;q)-W(t,x,S_t,\tau_t;q)\right]\Big\}=0, \quad (5.3)$$

with the final condition,

$$W(T,x,S,\tau;q)=x+q(S-\alpha q). \quad (5.4)$$

Proof. By the similar arguments in Proposition 1 in Chapter 3, the proof can be completed. □

Proposition 12. Let

$$W(t,x,S,\tau;q)=x+q(S-\alpha q)+u(t,\tau;q) \quad (5.5)$$

be a solution to the HJB equation (5.3) recommended by the final condition (5.4). Then, the optimal controls of (5.3) are found as

$$\begin{aligned}\delta^{+*}(t,\tau;q)&=\tfrac{1}{\kappa^+}+\epsilon^++\alpha(1-2q)-u(t,\tau;q-1)+u(t,\tau;q), \quad q\neq \underline{q},\\ \delta^{-*}(t,\tau;q)&=\tfrac{1}{\kappa^-}+\epsilon^-+\alpha(1+2q)-u(t,\tau;q+1)+u(t,\tau;q), \quad q\neq \overline{q}.\end{aligned} \quad (5.6)$$

Proof. Upon inserting the suggested solution and the intensity functions for the filled orders into (5.3), it turns out to

$$\psi\tau q^2\sigma^2=\partial_t u+k(\theta-\tau)\partial_\tau u+\frac{1}{2}\beta^2\partial_{\tau\tau}u$$
$$+\sup_{\delta_t^+}\lambda^+\Big\{q\epsilon^+$$
$$+e^{-\kappa^+\delta^+}\left(\delta^+-\epsilon^+-\alpha(1-2q)+u(t,\tau;q-1)-u(t,\tau;q)\right)\Big\}$$
$$+\sup_{\delta_t^-}\lambda^-\Big\{-q\epsilon^-$$
$$+e^{-\kappa^-\delta^-}\left(\delta^--\epsilon^--\alpha(1+2q)+u(t,\tau;q+1)-u(t,\tau;q)\right)\Big\}$$
$$(5.7)$$

for $q \in [\underline{q}, \overline{q}]$ with terminal condition $u(T, \tau; q) = 0$.

After that, the optimal spreads (5.6) can be achieved applying the first order optimality measures in (5.7) which completes the proof. □

The optimal spreads given by (5.6) yields the following equation:

$$\begin{aligned}
\psi\tau q^2\sigma^2 &= \partial_t u + k(\theta - \tau)\partial_\tau u + \frac{1}{2}\beta^2\partial_{\tau\tau} u \\
&+ \lambda^+\Big[q\epsilon^+ + \frac{1}{\kappa^+}e^{-1-\kappa^+\left(\epsilon^+ + \alpha(1-2q) - u(t,\tau;q-1) + u(t,\tau;q)\right)}\Big] \\
&+ \lambda^-\Big[-q\epsilon^- + \frac{1}{\kappa^-}e^{-1-\kappa^-\left(\epsilon^- + \alpha(1+2q) - u(t,\tau;q+1) + u(t,\tau;q)\right)}\Big]
\end{aligned} \tag{5.8}$$

for $q \in [\underline{q}, \overline{q}]$ with the final condition $u(T, \tau; q) = 0$.

For the purpose of discovering the performance of the model with the latency impact, we need to solve (5.8) numerically. The numerical scheme of the equation is very similar to the one given in Section A.1 in Appendix A.

Remark 7. We remark that the stock price dynamics with the impact of the latency can be also modeled assuming that there is a correlation between the price and latency, i.e., $\rho \neq 0$, as in the Heston model.

Remark 8. Notice that we consider the volatility in this section as a constant, but one can take into this model account with a stochastic volatility. In this case, the model should include one more stochastic process to produce the volatility σ_t resulting a variance-covariance matrix for S_t, τ_t, and σ_t and mixed derivatives in the finite difference scheme in the verification equation. We leave this problem as a further study.

5.1.1 Numerical Results

Using the solutions for the optimal spreads having the latency effect in the model, we demonstrate the performance of the strategy with the given parameter values in Table 5.1.

Table 5.1: The Parameters

T (sec)	Δt	S_0	τ_0	q	$\lambda^\pm$	$\epsilon^\pm$	$\kappa^\pm$	α	ψ	σ	k	θ	β
10	0.005	100	0.05	$[-5, 5]$	2	0.004	2	0.01	0.001	0.02	0.005	0.1	0.01

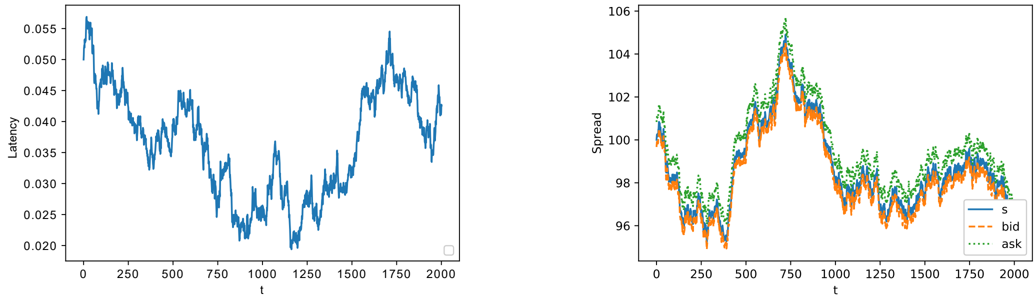

Figure 5.1: The paths of the latency and optimal prices

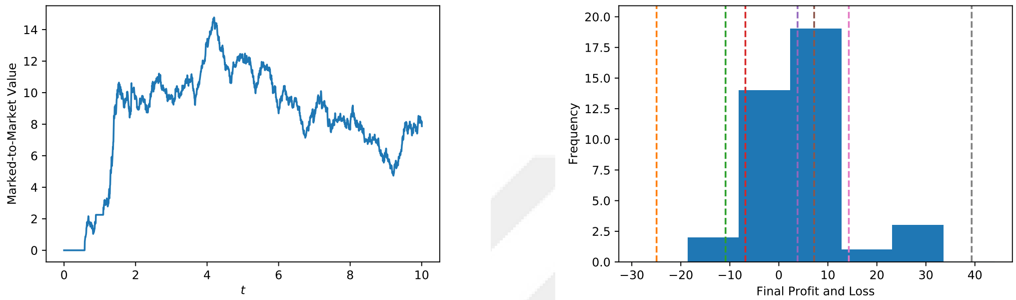

Figure 5.2: A simulated path and histogram of the profit and loss function

By Figure 5.1, we can see the latency dynamics and the optimal prices which are evaluated by the spread formulas in (5.6). Here, a mean-reverting behaviour can be observed in the latency process. The strategy allows to buy with a price closer to and sell far away from the midprice. The jump effects can be also noticed in the prices.

Figure 5.2 exhibits a path of the PnL process and histogram PnL for the strategy which shows that when the investor starts with a zero wealth, she can get approximately 9 units profit at the end of the trading day. The histogram reveals that the strategy approximates to the normal distribution.

One path of the simulated inventory process q_t is shown in Figure 5.3 for $q \in [-10, 10]$ with other parameters given in Table 5.1. The trade starts at a time between $[0, 1]$ seconds and the inventory remains stable until a time $[2, 3]$. When t approaches to the final time T, the investor is willing to sell her assets which causes a decrease and a mean-reverting to zero behaviour in the inventory.

Figure 5.4 demonstrates the optimal spreads δ^+ and δ^- for the strategy with latency on the each inventory levels with a very small inventory penalty parameter $\psi = 0.001$. Comparing the strategy with that in Chapter 3 having the stock price modeling (3.1),

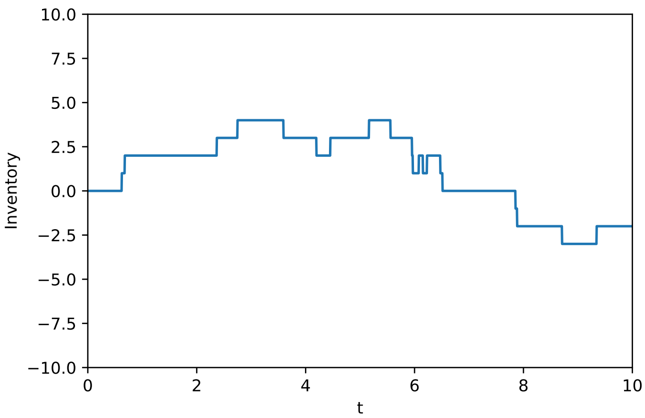

Figure 5.3: A simulated path for inventory process

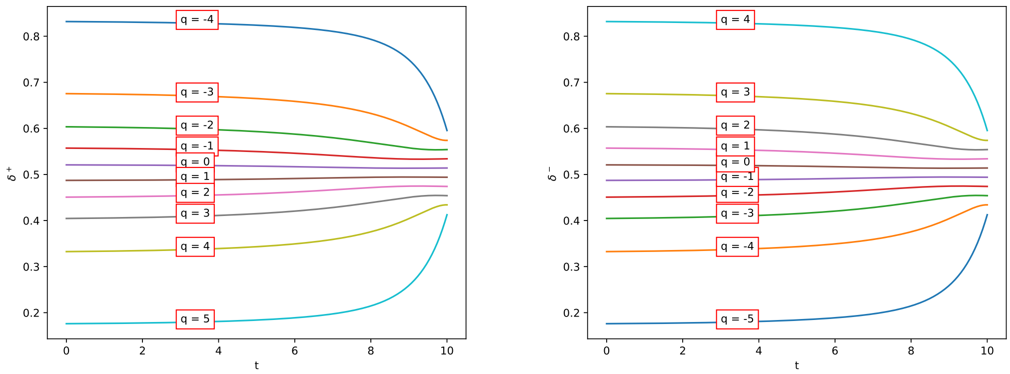

(a) δ^+ (b) δ^-

Figure 5.4: Optimal spreads δ^+ and δ^-

less sell spreads and higher buy spreads occur in this strategy. This result may be a consequence of the latency. The trader decreases the sell prices and increases the buy prices because of the stochastic latency as it causes an uncertainty on the execution of the assets.

Table 5.2 compares the results of the strategy with the results of the symmetric strategy for the same model. It indicates that the strategy again creates a smaller value of PnL with a smaller risk compared to the symmetric strategy. Further, it is also seen that the latency impact causes a higher standard deviation since it may increase the asset fluctuating.

Remark 9. In order to see the behaviour of the optimal market making strategy when the latency occurs between the submission and execution time of the order, we make

Table 5.2: Comparison of the strategy

	PnL	Std dev of PnL	Final q	Std dev of q
Inventory	5.66	10.11	0.02	2.21
Symmetric	10.58	13.53	-0.34	3.94

a comparison between this strategy and the one with stock price dynamics which does not include the latency impact. When there is no latency impact on trading, the stock price reduces to

$$dS_t = \sigma S_t dB_t^1 + \varepsilon^+ dM_t^+ - \varepsilon^- dM_t^- . \tag{5.9}$$

The HJB and verification equations can be similarly generated for the price model (5.9).

In Table 5.3, we provide the results for the comparison of the strategy in the case of no latency. First, it is observed that the model provides more PnL with extremely higher standard deviation if a stochastic latency appears. By the strategy (5.6), the trader can obtain a bit more attractive investment with the related Sharpe ratio if she is a risk lover investor. By this comparison, it is shown that the latency causes additional risk since the stock price fluctuates more with its existence.

Table 5.3: Comparison of the model with the model without latency

		Latency	Without Latency
PnL	Mean	2.6233	0.6938
	Std dev	10.0143	5.4990
	Sharpe ratio	0.2619	0.1261
	Skewness	-0.8941	0.3162
	Kurtosis	2.2119	5.1860
Inventory	Mean	-0.1707	0.1800
	Std dev	1.7655	1.1373
	Sharpe ratio	-0.0967	0.1582
	Skewness	0.0472	-0.0260
	Kurtosis	1.3823	1.0068

Figure 5.5 shows that the difference between the spreads of two strategies such that without latency and with latency, respectively, for fixed $q = -4$ and τ_0. From the figure, we see that the latency effect decreases when the time approaches to maturity.

Moreover, the investor sells the assets with higher price (buys with lower price) when there is no latency effect. This strategy results in a larger optimal spread in the case of without the latency.

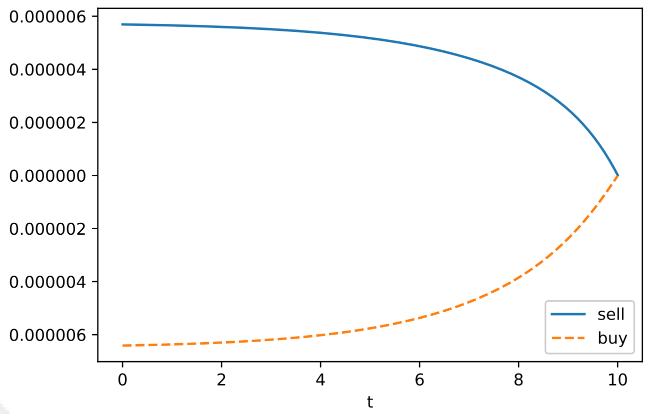

Figure 5.5: Difference between the spreads

5.2 Effect of the Jumps in Latency in a LOB model

In this part, we model the price dynamics containing the mean-reverting process and jump components in the latency process. With this assumption, the underlying price process follows the dynamics as follows:

$$\begin{aligned} dS_t &= \sigma(S_t + \tau_t)dB_t^1, \\ d\tau_t &= k(\theta - \tau_t)dt + \beta dB_t^2 + \varepsilon^+ dM_t^+ - \varepsilon^- dM_t^-, \\ dB_t^1 dB_t^2 &= \rho dt, \end{aligned} \tag{5.10}$$

where we take the correlation coefficient $\rho = 0$.

Considering the same value function given by (5.2), the HJB equation of the control problem can be obtained as

$$
\begin{aligned}
&\partial_t W+k(\theta-\tau_t)\partial_\tau W+\frac{1}{2}\sigma^2(S_t+\tau_t)^2\partial_{SS}W+\frac{1}{2}\beta^2\partial_{\tau\tau}W+\sigma\rho\beta(S_t+\tau_t)\partial_{S\tau}W-\psi\tau_t q^2\sigma^2\\
&+\sup_{\delta_t^+}\Big\{\Lambda_t^+(\delta_t^+)\mathbb{E}\left[W(t,x+(S_t+\delta_t^+),S_t,\tau_t+\varepsilon^+;q-1)-W(t,x,S_t,\tau_t;q)\right]\\
&\qquad+(\lambda^+-\Lambda_t^+(\delta_t^+))\mathbb{E}\left[W(t,x,S_t,\tau_t+\varepsilon^+;q)-W(t,x,S_t,\tau_t;q)\right]\Big\}\\
&+\sup_{\delta_t^-}\Big\{\Lambda_t^-(\delta_t^-)\mathbb{E}\left[W(t,x-(S_t-\delta_t^-),S_t,\tau_t-\varepsilon^-;q+1)-W(t,x,S_t,\tau_t;q)\right]\\
&\quad+(\lambda^--\Lambda_t^-(\delta_t^-))\mathbb{E}\left[W(t,x,S_t,\tau_t-\varepsilon^-;q)-W(t,x,S_t,\tau_t;q)\right]\Big\}=0, \quad (5.11)
\end{aligned}
$$

with the final condition,

$$W(T,x,S,\tau;q)=x+q(S-\alpha q).$$

Then, using the ansatz (5.5) in the HJB equation (5.11), it reduces to the following equation:

$$
\begin{aligned}
\psi\tau q^2\sigma^2 = {}&\partial_t u+k(\theta-\tau)\partial_\tau u+\frac{1}{2}\beta^2\partial_{\tau\tau}u\\
&+\sup_{\delta_t^+}\lambda^+\Big\{[u(t,\tau+\epsilon^+;q)-u(t,\tau;q)]\\
&+e^{-\kappa^+\delta^+}(\delta^+-\alpha(1-2q)+u(t,\tau+\epsilon^+;q-1)-u(t,\tau+\epsilon^+;q))\Big\}\\
&+\sup_{\delta_t^-}\lambda^-\Big\{[u(t,\tau-\epsilon^-;q)-u(t,\tau;q)]\\
&+e^{-\kappa^-\delta^-}(\delta^--\alpha(1+2q)+u(t,\tau-\epsilon^-;q+1)-u(t,\tau-\epsilon^-;q))\Big\}
\end{aligned}
\quad (5.12)
$$

with the final condition $u(T,\tau;q)=0$.

By the first order optimality conditions in (5.12), the optimal spreads can be found as

$$
\begin{aligned}
\delta^{+*}(t,\tau;q)&=\tfrac{1}{\kappa^+}+\alpha(1-2q)-u(t,\tau+\epsilon^+;q-1)+u(t,\tau+\epsilon^+;q), \quad q\neq \underline{q},\\
\delta^{-*}(t,\tau;q)&=\tfrac{1}{\kappa^-}+\alpha(1+2q)-u(t,\tau-\epsilon^-;q+1)+u(t,\tau-\epsilon^-;q), \quad q\neq \overline{q},
\end{aligned}
$$

with the verification equation

$$
\begin{aligned}
\psi\tau q^2\sigma^2 = \partial_t u &+ k(\theta-\tau)\partial_\tau u + \frac{1}{2}\beta^2\partial_{\tau\tau}u \\
&+ \lambda^+\Big\{[u(t,\tau+\epsilon^+;q) - u(t,\tau;q)] \\
&\qquad + \frac{1}{\kappa^+}e^{-1-\kappa^+(\alpha(1-2q)-u(t,\tau+\epsilon^+;q-1)+u(t,\tau+\epsilon^+;q))}\Big\} \\
&+ \lambda^-\Big\{[u(t,\tau-\epsilon^-;q) - u(t,\tau;q)] \\
&\qquad + \frac{1}{\kappa^-}e^{-1-\kappa^-(\alpha(1+2q)-u(t,\tau-\epsilon^-;q+1)+u(t,\tau-\epsilon^-;q)}\Big\}
\end{aligned} \tag{5.13}
$$

for $q \in [\underline{q}, \overline{q}]$ with final condition $u(T,\tau;q) = 0$.

Besides the finite difference method in backwards starting from the final time, the verification equation (5.13) is solved by applying the linear interpolation and extrapolation methods to calculate the functions $u(t,\tau+\epsilon^+;q)$ and $u(t,\tau+\epsilon^+;q)$. Finally, we obtain the solution of $u(t,\tau;q)$.

5.2.1 Numerical Results

For the purpose of the numerical demonstration, we call the latency model with the dynamics (5.1) as “Jumps in price model” and the model with the dynamics (5.10) as “Jumps in latency model” in this part.

Figure 5.6 is an illustration to showcase $\delta^+(t,\tau_0;-1)$ and $\delta^-(t,\tau_0;-1)$ values for “Jumps in price model” and “Jumps in latency model”. We note that the average spread is 1.0350 for “Jumps in price model”, while it is evaluated as 1.0271 for “Jumps in latency model”. It is noticed that both sell and buy spreads are greater in the case when the jumps are in the price dynamics.

By the comparison of two strategies provided in Table 5.4, it can be realized that the strategy including jumps in the price process yields a wider PnL with a wider standard deviation which is the opposite result of the one given by Table 3.13 since there is no correlation between the latency and price.

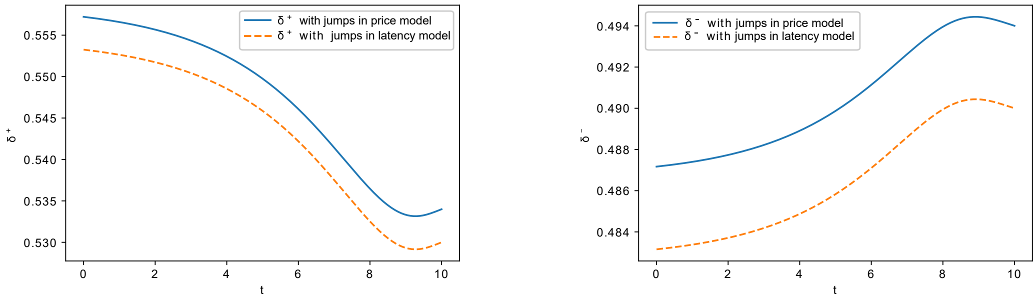

Figure 5.6: Spreads of “Jumps in price model” and “Jumps in latency model”

Table 5.4: Comparison of the strategies by “Jumps in price model” and “Jumps in latency model”

	PnL	Std dev of PnL	Final q	Std dev of q
Jumps in price model	7.29	6.97	-0.04	2.25
Jumps in latency model	3.05	1.80	-0.12	2.11

5.3 Summary

In this chapter, we approach to the optimal market making models in high-frequency trading in the case of existence of stochastic latency in the midprice of the asset and provide an insight on the qualitative behaviour of the trader. Here, we define the time delay between the submission and execution of the orders as stochastic latency since it always takes time for the orders to get into the high-frequency trading system. Therefore, we consider the delayed model in the continuous part of the price process as an additional source of randomness. Another possible contribution for optimal market making models with delay will be to consider a stochastic price process with delay in time and to establish the associate optimal stochastic control problem where the case of a portfolio optimization model with delay has been studied in [47].

By the numerical experiments, we observe that the latency rises fluctuating of the asset which leads to an additional risk source for the trader. Furthermore, we analyze this case when the jump components are either in price or latency process. Obviously, we find that the trader takes different actions in the manner of optimal quotes and the jumps in the price cause larger standard deviation with also larger PnL. Lastly, the real data application can be executed for the latency models as done in Chapter 4, but we leave it as a further study.

CHAPTER 6

CONCLUSION

The main subject of this thesis is optimal market making models for high-frequency trading when the midprice process of an asset is followed by stochastic volatility. Herewith, we present optimal trading strategies to execute the limit buy and sell orders where the strategies stand on the price impact models. For this reason, we build optimal stochastic control problems which aims to gain maximum profit for the market maker while updating the orders and inventories continuously. In order to achieve the optimal quotes, we penalize the gathered inventories both during and at the end of the trading. Then, we provide numerical illustrations which show the optimal behaviour of the trader and some statistical analysis of both PnL and inventory process. Further, we discuss these analyses on the high-frequency data which is obtained from BIST. Also, we propose optimal market making models in the presence of the stochastic latency.

Chapter 2 first addresses some important characteristics of LOBs to understand the concept. Then, we briefly give some definitions and results on stochastic processes and stochastic optimal control. This chapter is concluded with an introduction on optimal market making problem with some of the classical models that exist in the literature.

In Chapter 3, we introduce optimal market making models with the goal of finding the best prices in a limit order book for an asset by finding the optimal spreads where the price is procedured by Heston stochastic volatility model. In the literature, there exists the strategies which are described by the price models with constant volatility. In our models, we define the price processes with stochastic volatility and add jump components corresponding to the number of arrived orders. As the volatility of a stock is a significant component in option pricing, it also takes a crucial role in high-frequency trading. Since the volatility of an asset fluctuates and is not constant, deriving optimal strategies with stochastic volatility in the price dynamics reflects the reality better in markets. Moreover, the number of the arrived orders also causes a price change. Hence, we indicate this fact as adding jump processes in price dynamics. First, we can see that when the value function is not a function of the volatility, the optimal prices distribute around the midprice of the asset almost symmetrically. The inventory level and model parameters play an important role on the behaviour of the market maker. For instance, when the inventory level is on positive side and there is a liquidation cost, she wishes to get rid of her assets not to pay for the remaining assets at expiry time and thus, she sells with lower price. Approaching to the end of the trading, the trader behaves differently and a bit increases the sell spreads to cover the liquidation cost, otherwise she may get less profit.

Our analyses reveal that the strategy obtained with quadratic utility function generates less profit and less standard deviation in comparison with the symmetric strategy. The Sharpe ratio of the strategy with a value greater than 1 indicates a noticeable performance. Besides, we observe that there is a considerable effect of the model parameters on the optimal spreads. By the strategy with the exponential utility function, one can sell the assets with the larger spreads on positive inventory levels being a less risk averse investor. Hence, we can say that the behaviour of the trader changes according to the different utility functions. Additionally, we illustrate that the strategy is resulted in a large PnL and standard deviation of PnL when the impact of the arrival orders are considered in the stochastic volatility. Comparing the models to the existing works in the literature, it can be realized that our models provide significantly higher PnL and higher risks at the same time. This shows us that a market maker who loves to take risk can trade with our models which also express the fluctuating volatility in real markets. We further propose a strategy theoretically at the end of this chapter where the asset price follows a mean-reverting process with stochastic volatility.

Chapter 4 pays attention to the high-frequency data applications of the models derived in Chapter 3 for the pre and post Covid-19 pandemic times. After parameter estimation for each stock used in this work, we get the results to describe the trading strategies. In the pre pandemic term, the stock with ticker name FENER has the higher jump intensities in comparison with others. Then, by our analysis, we conclude that the higher intensities procure the lowest optimal average spread, the highest PnL and risk of both PnL and inventory. By the comparison of the models with the ones in the literature, it can be seen that our models derive higher PnL and risks, but explain the characteristics of the data more reasonable and realistic. Further, we provide the applications of the models on some stocks traded in global markets and we get the result of that the strategies are profitable and meaningful even traded on global stocks. Then, we conduct our analysis on the same stocks in BIST for the post pandemic time and we obtain that the stock with ticker name EREGL has the higher jump intensities in price dynamics and so that the highest PnL and standard deviations.

In Chapter 5, we focus on optimal market making models with stochastic latency in the price dynamics. To the best of our knowledge, the models developed in this chapter are the first models which can be applied to HFT. With the same assumptions for the derived models in Chapter 3, we derive the first model with price dynamics including the jump components and solve for the optimal controls. By this application, we aim to measure the qualitative behaviour of the trader when there is a stochastic latency between the submission and execution of the limit orders. We first come to the conclusion that the latency impact leads an increase on the risk of the strategy because of the additional randomness. The effect also increases the PnL, as well. Then, when we compare the latency model with the one which has no latency, it can be deduced that the profit and standard deviation of the PnL are higher in the latency model. Further, we consider the strategy when the stochastic latency is affected by the number of the arrived orders. In results, it is shown that this model is less risky providing less PnL compared to the first model.

The models and results presented in this thesis will serve as extended models for HFT on optimal market making problem. One can describe a high-frequency data properties using the price models of our strategies and apply the optimal controls even for an emerging market to obtain profitable tradings. As a further study, numerical results can be achieved for the model where the midprice is processed with a mean-reverting system with stochastic volatility by solving the PDE system which is obtained by the quadratic approximation of the inventory. As another solution technique, the related verification equation of the problem can be solved by applying the mixed derivatives by finite differences. Another future research direction is to apply the strategies of the latency models on a high-frequency data since the latency is a fact of the markets and there is a waiting time for the execution of the orders which is random. Moreover, using Double Heston stochastic volatility model on optimal market making problems will be an important future study since it provides more flexibility on capturing the stochastic volatility [27]. Such applications and results can be used in financial markets.

REFERENCES

[1] S. Ahuja, G. Papanicolaou, W. Ren, and T. Yang, Limit order trading with a mean reverting reference price, Risk and Decision Analysis, 6(2), pp. 121–136, 2016.

[2] R. Almgren, Optimal execution of portfolio transactions, Journal of Risk, 3, pp. 5–40, 2001.

[3] M. Avellaneda and S. Stoikov, High-frequency trading in a limit order book, Quantitative Finance, 8(3), pp. 217–224, 2008.

[4] A. Bachouch, C. Huré, N. Langrené, and H. Pham, Deep neural networks algorithms for stochastic control problems on finite horizon: numerical applications, arXiv:1812.05916, 2020.

[5] B. Baldacci, P. Bergault, and O. Guéant, Algorithmic market making for options, Quantitative Finance, 21(1), pp. 85–97, 2021.

[6] B. Baldacci, I. Manziuk, T. Mastrolia, and M. Rosenbaum, Market making and incentives design in the presence of a dark pool: a deep reinforcement learning approach, arXiv:1912.01129, 2019.

[7] F. Baudoin, *Diffusion Processes and Stochastic Calculus*, EMS Textbooks in Mathematics, European Mathematical Society, 2014.

[8] E. Bayraktar and M. Ludkovski, Liquidation in limit order books with controlled intensity, Mathematical Finance, 24(4), pp. 627–650, 2014.

[9] R. Bellman, Dynamic programming and stochastic control processes, Information and Control, 1, pp. 228–239, 1958.

[10] T. Björk, *Equilibrium Theory in Continuous Time, Lecture Notes*, Stockholm School of Economics, 2012.

[11] R. Carmona, J. P. Fouque, S. M. Mousavi, and L. H. Sun, Systemic risk and stochastic games with delay, Journal of Optimization Theory and Applications, 179, pp. 366–399, 2018.

[12] A. Cartea and S. Jaimungal, Risk metrics and fine tuning of high frequency trading strategies, Mathematical Finance, 25(3), pp. 576–611, 2013.

[13] A. Cartea, S. Jaimungal, and J. Penalva, *Algorithmic and High Frequency Trading*, Cambridge University Press, 2015.

[14] A. Cartea, S. Jaimungal, and J. Ricci, Buy low sell high: A high frequency trading perspective, SIAM Journal of Financial Mathematics, 5, pp. 415–444, 2014.

[15] W. Ching, J. Gu, T. Siu, and Q. Yang, Trading strategy with stochastic volatility in a limit order book market, arXiv:1602.00358, 2016.

[16] R. Cont, Statistical modeling of high-frequency financial data, IEEE Signal Processing Magazine, 28(5), pp. 16–25, 2011.

[17] R. Courant, K. Friedrichs, and H. Lewy, Über die partiellen differenzengleichungen der mathematischen physik, Mathematische Annalen, 100(1), pp. 32–74, 1928.

[18] R. Craine, L. A. Lochstoer, and K. Syrtveit, Estimation of a stochastic volatility jump diffusion model, Economic Analysis Review, 15(1), pp. 61–87, 2000.

[19] E. B. Dynkin, *Markov processes, Volume I*, New York: Academic Press, 1965.

[20] B. Eraker, M. Johannes, and N. G. Polson, The impact of jumps in volatility and returns, The Journal of Finance, 58(3), pp. 1269–1300, 2003.

[21] O. Ersan and E. Cumhur, Algorithmic and high-frequency trading in borsa istanbul, Borsa Istanbul Review, 16(4), pp. 233–248, 2016.

[22] W. Feller, Two singular diffusion problems, Annals of Mathematics Second Series, 54(1), pp. 173–182, 1951.

[23] S. Figlewski, Forecasting volatility, Financial Markets, Institutions and Instruments, 6(1), pp. 1–88, 1997.

[24] P. Fodra and M. Labadie, High-frequency market-making with inventory constraints and directional bets, arXiv:1206.4810, 2012.

[25] X. Gao and Y. Wang, Optimal market making in the presence of latency, Quantitative Finance, 20(9), pp. 1495–1512, 2020.

[26] M. Garman, Market microstructure, Journal of Fiancial Economics, 3(3), pp. 257–275, 1976.

[27] P. Gauthier and D. Possamaï, Efficient simulation of the double heston model, IUP Journal of Computational Mathematics, 4(3), pp. 23–75, 2011.

[28] H. Gong, *Automatic trading using stochastic methods*, Ph.D. thesis, University College London, 2018.

[29] S. J. Grossman and M. Miller, Liquidity and market structure, The Journal of Finance, 43(3), pp. 617–633, 1988.

[30] O. Guéant, *The Financial Mathematics of Market Liquidity: From Optimal Execution to Market Making*, New York: Chapman and Hall/CRC, 2016.

[31] O. Guéant, C. A. Lehalle, and J. Fernandez-Tapia, Dealing with the inventory risk: a solution to the market making problem, Mathematics and Financial Economics, 7(4), pp. 477–507, 2013.

[32] F. Guilbaud and H. Pham, Optimal high-frequency trading with limit and market orders, Quantitative Finance, 13(1), pp. 79–94, 2013.

[33] J. Hasbrouck, *Empirical Market Microstructure*, Oxford University Press, 2007.

[34] S. Heston, A closed-form solution for options with stochastic volatility with applications to bond and currency options, The Review of Financial Studies, 6(2), pp. 327–343, 1993.

[35] T. Ho and H. Stoll, Optimal dealer pricing under transactions and return uncertainty, Journal of Financial Economics, 9(1), pp. 47–73, 1981.

[36] S. M. Iacus and N. Yoshida, *Simulation and Inference for Stochastic Processes with YUIMA: A Comprehensive R Framework for SDEs and other Stochastic Processes*, Springer, 2018.

[37] S. M. Kakade, M. Kearns, Y. Mansour, and L. E. Ortiz, Competitive algorithms for vwap and limit order trading, Social and Behavioral Sciences Economics, pp. 189–198, 2004.

[38] F. C. Klebaner, *Introduction to Stochastic Calculus with Applications*, World Scientific Publishing Co Inc, 2005.

[39] B. Øksendal, *Stochastic Differential Equations: An Introduction with Applications*, Springer Berlin, 2003.

[40] D. Lamberton and B. Lapeyre, *Introduction to Stochastic Calculus Applied to Finance*, Chapman and Hall/CRC, 2007.

[41] B. Larssen, Dynamic programming in stochastic control of systems with delay, Stochastics and Stochastic Reports, 74(3-4), pp. 651–673, 2002.

[42] M. K. Lee, J. H. Kim, and J. Kim, A delay financial model with stochastic volatility; martingale method, Physica A, 390, pp. 2909–2919, 2011.

[43] R. J. Leveque, *Finite-Volume Methods for Hyperbolic Problems*, Cambridge University Press, 2002.

[44] R. C. Merton, Optimum consumption and portfolio rules in a continuous-time model, Journal of Economic Theory, 3(4), pp. 373–413, 1971.

[45] C. P. Ogbogbo, Jump diffusion model for crude oil spot price process: parameter estimation for predicting the market, Ghana Journal of Science, 58, pp. 59–69, 2018.

[46] M. O'Hara, *Market Microstructure Theory*, Blackwell Publishing, 1997.

[47] T. Pang and A. Hussain, An infinite time horizon portfolio optimization model with delays, Mathematical Control and Related Fields, 6(4), pp. 629–659, 2016.

[48] H. Pham, *Continuous-time Stochastic Control and Optimization with Financial Applications*, Stochastic Modelling and Applied Probability, Springer Berlin Heidelberg, 2009.

[49] S. E. Shreve, *Stochastic Calculus for Finance II: Continuous-time Models*, Springer, 2004.

[50] H. Y. Wong and Y. W. Lo, Option pricing with mean reversion and stochastic volatility, European Journal of Operational Research, 197(1), pp. 179–187, 2009.

[51] Y. Yan, *Python for Finance: Build real-life Python applications for quantitative finance and financial engineering*, Packt Publishing, 2014.

[52] J. Yong and X. Zhou, *Stochastic Controls: Hamiltonian Systems and HJB Equations*, Stochastic Modelling and Applied Probability, Springer New York, 1999.

[53] D. Zabaljauregui and L. Campi, Optimal market making under partial information with general intensities, Applied Mathematical Finance, 27(1-2), pp. 1–45, 2019.

APPENDIX A

NUMERICAL SOLUTION OF THE OPTIMAL STOCHASTIC CONTROL PROBLEMS

A.1 Discretization of the Equation (3.14)

In this section, we proceed with the numerical discretizations of the time t and ν to obtain a solution for the verification equation (3.14). In order to solve the equations for u, we write the fully-explicit finite difference discretizations. Fully-implicit finite difference scheme can be also applied to solve the verification equations as done in [1]. To work with finite difference quotients, we discretize the domain of interest by dividing the corresponding intervals into M and N subintervals with constant step sizes

$$\Delta t = \frac{T-0}{M}, \quad \Delta\nu = \frac{\nu_{max}-\nu_{min}}{N},$$

respectively, such that $t_n = n\Delta\tau$ and $\nu_j = \nu_{min} + j\Delta\nu$, where $n = 0, 1, \ldots, M$ and $j = 0, 1, \ldots, N$. Let us denote the approximation value of $u(t, \nu; q)$ as $u^n_{j,q}$ for all grid points $(t_n, \nu_j; q)$. Thus, we have $u^n_{j,q} \approx u(n\Delta\tau, j\Delta\nu; q)$. The terms in equation (3.14) are replaced by the following terms:

$$\begin{aligned}
\partial_t u &= \frac{u^{n+1}_{j,q} - u^n_{j,q}}{\Delta\tau},\\
k(\theta-\nu)\partial_\nu u &= k(\theta-\nu_j)\left[\frac{u^{n+1}_{j+1,q} - u^{n+1}_{j,q}}{\Delta\nu}\mathbb{1}_{\theta>\nu_j} + \frac{u^{n+1}_{j,q} - u^{n+1}_{j-1,q}}{\Delta\nu}\mathbb{1}_{\theta<\nu_j}\right],\\
\partial_{\nu\nu} u &= \frac{u^{n+1}_{j+1,q} - 2u^{n+1}_{j,q} + u^{n+1}_{j-1,q}}{(\Delta\nu)^2}.
\end{aligned} \tag{A.1}$$

Here, we choose an upwind scheme for the term $k(\theta-\nu)\partial_\nu u$, as we should adapt the finite difference stencil numerically to simulate in the direction of the flow of the information, depending on whether $\theta > \nu_j$ or $\theta > \nu_j$. Inserting these terms into (3.14) provides us the discretized version of the equation:

$$u^n_{j,q} = u^{n+1}_{j,q} + \Delta\tau\Bigg(\mu q - \psi\nu_j q^2\sigma^2 + k(\theta-\nu_j)\Bigg(\frac{u^{n+1}_{j+1,q} - u^{n+1}_{j,q}}{\Delta\nu}\mathbb{1}_{\theta>\nu_j} + \frac{u^{n+1}_{j,q} - u^{n+1}_{j-1,q}}{\Delta\nu_j}\mathbb{1}_{\theta<\nu_j}\Bigg)$$
$$+ \frac{1}{2}\sigma^2\nu_j\frac{u^{n+1}_{j+1,q} - 2u^{n+1}_{j,q} + u^{n+1}_{j-1,q}}{(\Delta\nu)^2} + \lambda^+\left[q\varepsilon^+ + \frac{1}{\kappa^+}e^{-1-\kappa^+(\varepsilon^+ + \alpha(1-2q) - u^{n+1}_{j,q-1} + u^{n+1}_{j,q})}\right]$$
$$+ \lambda^-\left[-q\varepsilon^- + \frac{1}{\kappa^-}e^{-1-\kappa^-(\varepsilon^- + \alpha(1+2q) - u^{n+1}_{j,q+1} + u^{n+1}_{j,q})}\right]\Bigg) \quad \text{(A.2)}$$

with the final condition $u(T, \nu; q) = 0$. We use Neumann boundary conditions as follows:

$$u^n_{N,q} = 2u^n_{N-1,q} - u^n_{N-2,q}$$
$$u^n_{0,q} = 2u^n_{1,q} - u^n_{2,q}.$$

The stability of the numerical scheme (A.2) can be highlighted by showing that it satisfies the CFL condition which is introduced by Richard Courant, Kurt Friedrichs, and Hans Lewy in their original paper [17]. The CFL condition is given in the following definition.

Definition 10 ([43]). Any numerical scheme is convergent only if the dependency domain of it includes the related PDE's true dependency domain. This convergency condition should be fulfilled at least when Δt and Δx go to zero.

Our scheme (A.2) can numerically be shown to satisfy the CFL condition by the given parameters in Table 3.1 and taking sufficiently small Δt.

In order to summarize, we illustrate the solution in Algorithm 1, then use (3.12) to calculate $\delta^{\pm *}_t$.

A.2 Discretization of the Equation (3.41)

In this part, we only show the numerical discretizations of the time t, the variance ν and stock price S to solve the verification equation (3.41). In order to solve the equation, we apply a numerical method by writing the fully-explicit finite difference

Algorithm 1 Discretized solution of the verification equations

Given $T, M, N, \nu_{max}, \nu_{min}, \underline{q}, \overline{q}, \lambda^{\pm}, \epsilon^{\pm}, \kappa, \alpha, \psi, \mu, k, \theta, \sigma, \rho$.

Define $\Delta t = \frac{T}{M}$, $\Delta \nu = \frac{\nu_{max}-\nu_{min}}{N}$ and $Nq = -\underline{q} + \overline{q} + 1$.

for $i = M, M-1, \ldots, 0$ **do**
  for $j = 0, 1, \ldots, N$ **do**
    for $k = 0, 1, \ldots, Nq$ **do**
      use (A.2) as well as boundary and terminal data and calculate $u^{i}_{j,k}$.
    end for
  end for
end for

discretization and also linear interpolation and extrapolation methods. First, we discretize the domain of interest by dividing the corresponding intervals into M, N and K subintervals with constant step sizes

$$\Delta t = \frac{T-0}{M}, \quad \Delta \nu = \frac{\nu_{max} - \nu_{min}}{N}, \quad \Delta S = \frac{S_{max} - S_{min}}{N}$$

respectively, such that $t_n = n\Delta\tau$, $\nu_j = \nu_{min} + j\Delta\nu$ and $S_i = S_{min} + i\Delta S$, where $n = 0, 1, \ldots, M$, $j = 0, 1, \ldots, N$ and $i = 0, 1, \ldots, K$. Let us denote the approximation value of $u(t, \nu, S; q)$ as $u^n_{j,i;q}$ for all grid points $(t_n, \nu_j, S_i; q)$. Thus, we have $u^n_{j,i;q} \approx u(n\Delta\tau, j\Delta\nu, i\Delta S; q)$. Then, the terms in equation (3.41) should be replaced by the following terms including the mixed derivatives:

$$\begin{aligned}
\partial_t u &= \frac{u^{n+1}_{j,i;q} - u^{n}_{j,i;q}}{\Delta\tau}, \\
\beta(\mu - S)\partial_S u &= \beta(\mu - S_i)\left[\frac{u^{n+1}_{j,i+1;q} - u^{n+1}_{j,i;q}}{\Delta S}\mathbb{1}_{\mu > S_i} + \frac{u^{n+1}_{j,i;q} - u^{n+1}_{j,i-1;q}}{\Delta S}\mathbb{1}_{\mu < S_i}\right], \\
k(\theta - \nu)\partial_\nu u &= k(\theta - \nu_j)\left[\frac{u^{n+1}_{j+1,i;q} - u^{n+1}_{j,i;q}}{\Delta \nu}\mathbb{1}_{\theta > \nu_j} + \frac{u^{n+1}_{j,i;q} - u^{n+1}_{j-1,i;q}}{\Delta \nu}\mathbb{1}_{\theta < \nu_j}\right],
\end{aligned}$$

$$\begin{aligned}
\partial_{SS} u &= \frac{u^{n+1}_{j,i+1;q} - 2u^{n+1}_{j,i;q} + u^{n+1}_{j,i-1;q}}{(\Delta S)^2}, \\
\partial_{\nu\nu} u &= \frac{u^{n+1}_{j+1,i;q} - 2u^{n+1}_{j,i;q} + u^{n+1}_{j-1,i;q}}{(\Delta \nu)^2}, \\
\partial_{S\nu} u &= \frac{u^{n+1}_{j+1,i+1;q} - u^{n+1}_{j-1,i+1;q} - u^{n+1}_{j+1,i-1;q} + u^{n+1}_{j-1,i-1;q}}{4\Delta\nu\Delta S}.
\end{aligned}$$

We use the same boundary conditions given in Section A.1.

Then, placing these terms into the verification equation (3.41) and applying the linear interpolation and extrapolation methods for the terms $u(t, \nu, S + \epsilon^{+}; q)$ and $u(t, \nu, S - \epsilon^{-}; q)$ will provide the solution of the equation, that is $u(t, \nu, S; q)$.

The solution algorithm is almost the same as the one given in Section A.1 with the difference of adding the step size for S.

CURRICULUM VITAE

PERSONAL INFORMATION

Surname, Name: Aydoğan, Burcu
Nationality: Turkish (TC)
Marital Status: Single

EDUCATION

Degree	**Institution**	**Year of Graduation**
M.S.	Atılım University, Department of Mathematics	2014
B.S.	Atılım University, Department of Mathematics	2013
High School	Otakcilar High School	2007

PROFESSIONAL EXPERIENCE

Year	**Place**	**Enrollment**
2019 - Present	Atılım University	Research Assistant
2014 / Nov - Dec	Atılım University	Part-time Research Assistant

PUBLICATIONS

Aydogan B., Ugur, O. and Aksoy, U. "Optimal Limit Order Book Trading Strategies with Stochastic Volatility in the Underlying Asset". Computational Economics. (2020). (Under review)

Aydogan B., Aksoy, U. and Ugur, O. "On the Methods of Pricing American Options:

Case Study". Annals of Operations Research. 260, 79 - 94 (2018).